INFORMATION TO USERS

This manuscript has been reproduced from the microfilm master. UMI films the text directly from the original or copy submitted. Thus, some thesis and dissertation copies are in typewriter face, while others may be from any type of computer printer.

The quality of this reproduction is dependent upon the quality of the copy submitted. Broken or indistinct print, colored or poor quality illustrations and photographs, print bleedthrough, substandard margins, and improper alignment can adversely affect reproduction.

In the unlikely event that the author did not send UMI a complete manuscript and there are missing pages, these will be noted. Also, if unauthorized copyright material had to be removed, a note will indicate the deletion.

Oversize materials (e.g., maps, drawings, charts) are reproduced by sectioning the original, beginning at the upper left-hand corner and continuing from left to right in equal sections with small overlaps.

Photographs included in the original manuscript have been reproduced xerographically in this copy. Higher quality 6" x 9" black and white photographic prints are available for any photographs or illustrations appearing in this copy for an additional charge. Contact UMI directly to order.

UMI®

University of Alberta

Nanoliter Chemistry Combined with Microspot MALDI TOF MS
for Sensitive Protein and Peptide Characterization

by

Bernd Oskar Keller Ⓒ

A thesis submitted to the Faculty of Graduate Studies and Research in partial fulfillment of the requirements for the degree of Doctor of Philosophy

Department of Chemistry

Edmonton, Alberta

Spring 2001

The author has granted a non-exclusive licence allowing the National Library of Canada to reproduce, loan, distribute or sell copies of this thesis in microform, paper or electronic formats.

The author retains ownership of the copyright in this thesis. Neither the thesis nor substantial extracts from it may be printed or otherwise reproduced without the author's permission.

L'auteur a accordé une licence non exclusive permettant à la Bibliothèque nationale du Canada de reproduire, prêter, distribuer ou vendre des copies de cette thèse sous la forme de microfiche/film, de reproduction sur papier ou sur format électronique.

L'auteur conserve la propriété du droit d'auteur qui protège cette thèse. Ni la thèse ni des extraits substantiels de celle-ci ne doivent être imprimés ou autrement reproduits sans son autorisation.

0-612-60307-5

Canada

University of Alberta

Library Release Form

Name of Author: Bernd Oskar Keller

Title of Thesis: Nanoliter Chemistry Combined with Microspot MALDI TOF MS for Sensitive Protein and Peptide Characterization

Degree: Doctor of Philosophy

Year this Degree Granted: 2001

Permission is hereby granted to the University of Alberta Library to reproduce single copies of this thesis and to lend or sell such copies for private, scholarly or scientific research purposes only.

The author reserves all other publication and other rights in association with the copyright in the thesis, and except as herein before provided, neither the thesis nor any substantial portion thereof may be printed or otherwise reproduced in any material form whatever without the author's prior written permission.
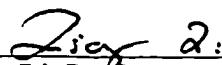
Bernd Keller
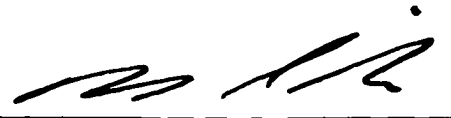
Oberdorfstrasse 8
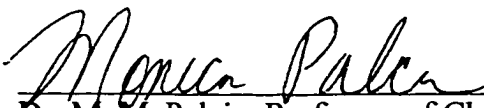D-78250 Tengen-Watterdingen
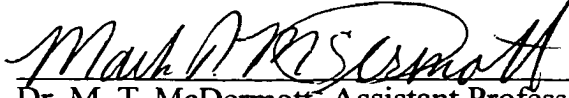Germany

December 6, 2000

University of Alberta
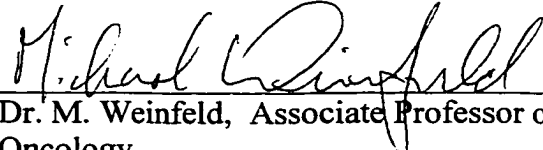
Faculty of Graduate Studies and Research

The undersigned certify that they have read, and recommend to the Faculty of Graduate Studies and Research for acceptance, a thesis entitled Nanoliter Chemistry Combined with Microspot MALDI TOF MS for Sensitive Protein and Peptide Characterization submitted by Bernd Oskar Keller in partial fulfillment of the requirements for the degree of Doctor of Philosophy.
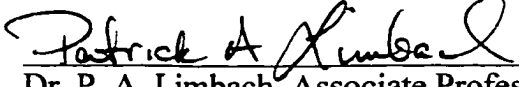
Dr. L. Li, Professor of Chemistry

Dr. N. J. Dovichi, Professor of Chemistry

Dr. M. M. Palcic, Professor of Chemistry

Dr. M. T. McDermott, Assistant Professor of Chemistry

Dr. M. Weinfeld, Associate Professor of Oncology

Dr. P. A. Limbach, Associate Professor of Chemistry

December 1, 2000

für meine Eltern

Elisabeth und Albert

Abstract

A combination of subnanoliter volume sample handling employing small-diameter capillaries and direct sample deposition onto very thin preformed matrix-layers makes matrix-assisted laser desorption/ ionization mass spectrometry (MALDI TOF MS) one of the most sensitive analytical methods currently available for protein and peptide detection. This research is focused on the technical development of this technique and demonstrates its applications in protein and peptide analysis. Employing microspot MALDI mass spectrometric analysis of peptides with a total sample loading of several tens of thousands of molecules (e.g. 25,000 molecules or 42 zeptomole of Substance P) is demonstrated. Several unique technical and fundamental issues in dealing with such a low level of analysis are discussed.

Extension of this technique's capabilities toward multiple chemical and/or enzymatic reactions within a nanoliter chemistry station allows for more detailed structural characterization of proteins. Required sample amounts of this technique are in the subfemtomole range, enabling, as an example, the distinction of hemoglobin variants from single red blood cells. Combined HPLC-fractionation and nanoliter chemistry is used to increase the number of identifiable proteins from bacteria extracts, thus contributing to the establishment of high quality databases for bacteria identification.

Application of this sensitive approach to high molecular weight proteins enables analysis of contaminated and dilute protein solutions in the low nanomolar range, however decreased resolution and formation of multiply-charged species have to be taken into account. The formation of multiply-charged species can be beneficial in reduction

studies of proteins consisting of disulfide-linked subunits for obtaining high-order structural information.

Employing a modified setup of the nanoliter chemistry station for solvent extraction with a nanoliter droplet of organic phase in microliter volumes of aqueous sample solutions enables the simultaneous detection of hydrophobic and hydrophilic analytes by MALDI TOF MS. Extension of this newly developed technique towards investigation of metal-peptide complexes is demonstrated.

Acknowledgements

I would like to thank my supervisor Dr. Liang Li for his support, advice and inspiration over the last four years. In our many discussions, I experienced his enthusiasm, thorough thinking, and dedication towards our research goals; and I felt well guided throughout my graduate studies.

I also thank the other members of my supervisory committee: Professor Norm J. Dovichi and Professor Monica M. Palcic and the other members of my examining committee: Professor Mark T. McDermott, Professor Michael Weinfeld, and Professor Patrick A. Limbach for their thorough review and suggestions regarding this thesis.

During the first 8 months in Dr. Li's laboratory I was fortunate to have had the opportunity to work together with Dr. Randy M. Whittal. His vast knowledge and technical expertise helped me build the solid foundations for the work presented in this thesis, for which I thank him. I also thank him for taking the time to proof read a major portion of this thesis.

I gratefully acknowledge the participation of other persons with whom I collaborated. I thank Professor M. M. Palcic for providing the facilities of her laboratory for handling the blood samples (Chapter 3) and the tetramethylrhodamine-labeled saccharides (Chapter 4). I also thank Dr. K. Sujino of Professor Palcic's lab and again Dr. R. M. Whittal for providing and analyzing those samples. I thank Dr. R. W. Purves, Dr. T. Yalcin, Dr. W. Gabryelski, Dr. D. C. Schriemer, and Dr. Y. Dai for their advice and help getting me settled into the lab. I thank Ms. Zhengping Wang for the HPLC-fractionation of the bacteria extracts (Chapter 5). I also thank all the other members of the group for helpful discussions and ideas.

I am especially indebted to Dr. D. Richards for her thorough proof reading of this thesis. With her help I eliminated many questionable grammatical endeavors into the English language and I thank her for that.

I thank the personnel in the general, purchasing, and post offices and the electronics and machine shops of the chemistry department, without whom this research work would not be possible.

I thank Professor Dietrich Frahne, Professor Rodney A. Badger, and Dr. Luis E. Sojo for their encouragement to pursue graduate school and their trust in me.

Table of Contents

List of Tables and Charts

List of Figures

withdrawn into the capillary ~1 mm from the capillary front end. After sample loading, the glass tube containing the sample is replaced with a matrix-covered MALDI target. The sample-filled capillary is then moved very close to the MALDI target and the sample is deposited by applying pressure to the capillary with the connected syringe. 16

List of Abbreviations

4-HCCA	α-cyano-4-hydroxycinnamic acid
α_2-M	α_2-macroglobulin
amu	atomic mass unit (= 1u)
CsA	cyclosporin A
Da	daltons, 1 Da = 1 u (atomic mass standard)
DHB	2,5-dihydroxy benzoic acid
Er:YAG	erbium: yttrium aluminium garnet
ESI	electrospray ionization
FTICR	fourier transform ion cyclotron resonance
FWHM	full width at half maximum
HABA	2'-(4-hydroxyphenylazo)benzoic acid
ID	internal diameter
IR	infrared
m/z	mass-to-charge ratio
μL	microliter (1 μL = 10^{-6} L)
μm	micrometer (1 μm = 10^{-6} m)
MALDI	matrix-assisted laser desorption/ionization
MCP	micro channel plate
Nd:YAG	neodymium: yttrium aluminium garnet
nL	nanoliter (1 nL = 10^{-9} L)
OD	outer diameter
pL	picoliter (1 pL = 10^{-12} L)
PSD	post source decay
SD	standard deviation
TMR	tetramethylrhodamine
TOF	time-of-flight
UV	ultraviolet
v/v	volume-to-volume ratio
w/w	weight-to-weight ratio

Chapter 1

Introduction:
Matrix-Assisted Laser Desorption/Ionization Time-of-Flight Mass Spectrometry and Its Application to Sensitive Protein Characterization

Protein identification and further characterization by matrix-assisted laser desorption/ionization time-of-flight mass spectrometry (MALDI-TOF-MS) has become a routine method in many laboratories. Due to intense development since the early 1990's, the availability of commercial MALDI mass spectrometers has boomed in the latter part of that decade. New applications and improved methods are continuously reported in the literature, however the MALDI instrument's capability in terms of sensitivity has not yet exhausted its full potential. Main reasons for this 'underuse' are the manifold difficulties encountered during handling and preparation of minute sample amounts as well as the challenge to transfer such small samples to the MALDI mass spectrometer in a suitable and effective manner. Subsequent sections give an overview on current MALDI-TOF technology and discuss several new approaches to circumvent the difficulties involved in low-abundant analyte detection by MALDI.

1.1 Introduction to MALDI TOF MS

1.1.1 The MALDI Process. In 1987, two groups independently reported the first use of matrix-assisted laser desorption. The method of Hillenkamp and Karas[1,2] employed solid matrix substances, whereas the method of Tanaka and coworkers[3,4] used glycerol and ultra-fine metal powder as matrix. Most of the more than 3000 reports listed in the Current Contents database (since 1995) utilizing the MALDI technique employ modified versions of the method of Hillenkamp and Karas, mainly due to its better sensitivity. Liquid matrices are still being investigated for specific applications.[5]

A simplified schematic of the MALDI process is given in Figure 1.1. Before introduction into the mass spectrometer, analyte and matrix are mixed, usually in a molar

1
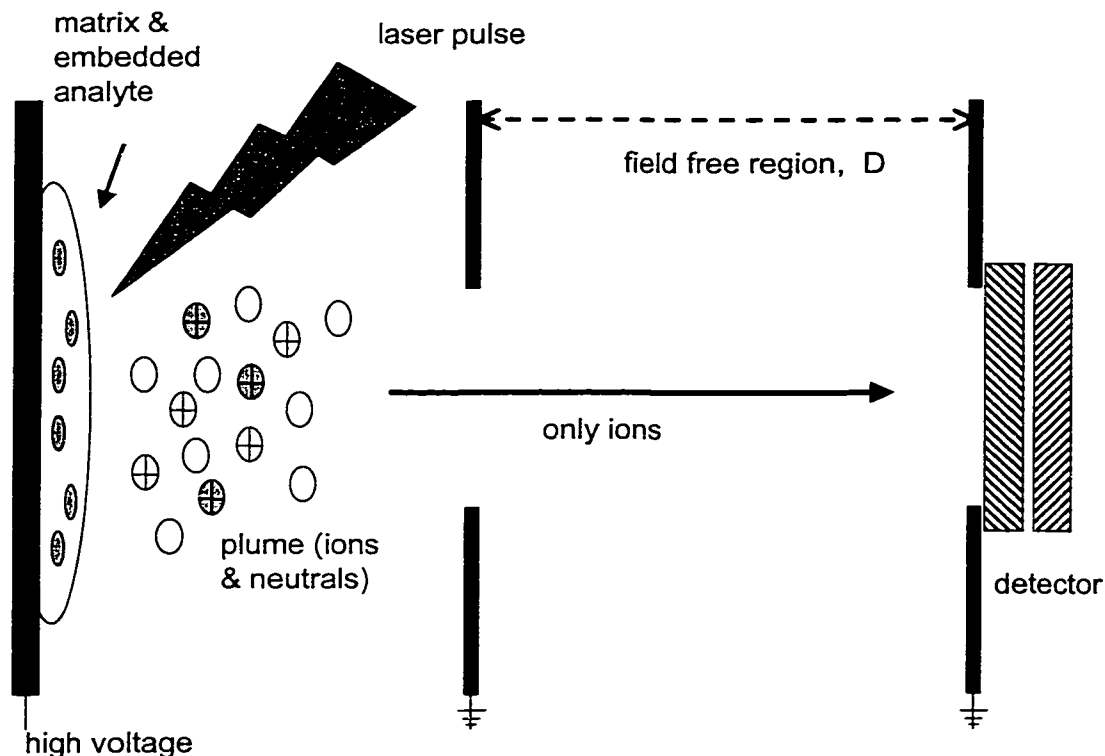
Figure 1.1   Schematic of the MALDI-TOF Mass Spectrometer (Linear Mode).

analyte to matrix ratio of 1:1000 up to 1:100000. In the case of a solid matrix substance, analyte molecules are embedded into the crystal structure during the drying process. The sample is then introduced into the high vacuum region ($\sim$10^{-8} Torr) of the mass spectrometer's ion source and desorption of matrix and analyte is achieved using a pulsed laser ($\sim$1-10 ns pulse). Lasers for UV-MALDI are generally nitrogen or Nd:YAG types; whereas for IR-MALDI, CO_2 or Er:YAG lasers are typically installed. Recently Laiko, Baldwin, and Burlingame demonstrated that MALDI ions can also be produced at atmospheric pressure.[6] The impact of the laser pulse forms a so called "MALDI plume" which can be described as a continuous phase transfer from the solid matrix/analyte crystals to the vacuum. This plume is characterized by a high density of neutral matrix molecules and a variety of ionic, radical, and electronically excited species. Subsequent reactions after the relaxation of the plume into the gas phase are under debate; several ionization processes and models have been proposed. It is believed that the direct

2

interaction of the laser pulse with the matrix molecules leads to primary ion formation due to processes like multiphoton ionization, energy pooling, proton transfer in excited states, disproportional reactions, desorption of preformed ions, or thermal ionization. These aforementioned processes lead then to further ionization processes in the MALDI plume, including gas phase proton transfers of matrix to matrix or matrix to analyte, gas phase cationization or electron transfer.[7]

The main function of the matrix is to absorb the laser energy. Since the matrix is in excess, the analyte molecules are protected from destruction. The matrix molecules become electronically excited by the laser energy absorption and thus provide the necessary energy to desorb the analyte molecules. The matrix also functions as a Brønsted acid or base, i.e. it donates or accepts protons from the analyte which leads to analyte ionization. The matrix also inhibits potential interactions between analyte molecules and between the analyte and target surface.[8]

1.1.2 The Time-of-Flight Analyzer. Ions produced by the MALDI process have been analyzed by a variety of mass spectrometers including magnetic sectors,[9] Fourier-transform ion cyclotron resonance,[10] and quadrupole ion trap instruments.[11] The most common analyzer for MALDI ions however, is the time-of-flight setup. Recently, promising combinations of time-of-flight/time-of-flight[12] and tandem quadrupole/time-of-flight instrument setups have been reported.[13]

The first well documented time-of-flight experiments where probably performed by Galileo Galilei. He simultaneously dropped two iron balls with different weights from the Leaning Tower in Pisa and both balls reached the ground at exactly the same time. Thus, he had disproven the statement of the great Greek philosopher Aristotle, which had been an unchallenged sacred dogma for centuries in the scientific world, "that falling bodies of unequal weight, if dropped from the same height at the same moment, will reach the ground at different periods".[14] In 1642, the same year Galileo died, another soon-to-be world famous scientist was born, Sir Isaac Newton. His universal theory of gravitation would explain Galileo's experimental findings.[15] The energy gained by two different masses falling from the same height is mass dependent, thus masses accelerated by a gravitational field can not be separated since they have the same velocity. A way to impart energy onto different masses in a mass-independent way is ion acceleration in an

3

electric field. Ions with equal charges will gain the same kinetic energy, but if they have different masses they will have different velocities and thus can be separated. Some of the early foundations for understanding the forces in electrical fields were laid by the French physicist and engineer Charles Augustin Coulomb during the eighteenth century.[16]

The concept of a linear time-of-flight mass spectrometer was first introduced by Stephens in 1946.[17,18] Two years later, Cameron and Eggers published the first design of a linear TOF instrument and the first mass spectra.[19] The first commercial instrument was based on the design reported by Wiley and McLaren in 1955,[20] and as already mentioned, the first MALDI-TOF applications were done in 1987.[1-4] In the time-of-flight analyzer source region the ions with mass m are accelerated by a voltage, V, according to

$$eV = \frac{1}{2} m v^2$$

where v is the ion's final velocity and e is the unit of elementary charge. All ions accelerated in the source obtain the same final kinetic energy assuming they have the same initial kinetic energy. Ions with different mass-to-charge ratios will thus have different velocities at the exit of the ion source and separate when passing through the field-free drift region before they reach the detector (see Fig. 1.1). The ion's final velocity, reached at the source exit, determines its flight time, t, through the field-free drift region, of length D, thus

$$t = \left(\frac{m}{2 \cdot e \cdot V} \right)^{1/2} \cdot D$$

For time-of-flight measurements an exact starting point has to be defined. In MALDI-TOF-MS a laser pulse induces the ion desorption and this pulse is therefore generally

4

used as the starting point. In theory, the mass of generated ions can now be calculated after their flight times have been measured. However, since the drift length, the applied voltage, and other instrument specific factors are usually not known with sufficient precision, calibration with known mass standards is necessary for accurate mass measurements.

Several characteristics of the time-of-flight analyzer are unique compared to other setups. There is no theoretical mass range limit, and MALDI-generated ions[21,22] as well as ions generated by electrospray[23] with masses greater than 1 MDa have been detected with time-of-flight analyzers. The time-of-flight analyzer is a non-scanning analyzer, thus all or most ions that are produced in the source region are detected. This property allows for very sensitive analysis, even of mixtures.

1.1.3 Improving Resolution. Resolution in mass spectrometers is defined as

$$R = m/m$$

where m is the ion mass and m the mass difference, i.e. in a time-of-flight instrument the temporal dispersion of the ions reaching the detector. Since ions in time-of-flight mass spectrometers are accelerated to constant energy,

$$m/m = t/(2t)$$

where t is usually measured as the full width at the half maximum (FWHM) of the respective signal. For optimal resolution in time-of-flight mass spectrometers, all ions with the same mass-to-charge ratio should arrive at the detector at exactly the same time. However, temporal, spatial, and initial kinetic energy distributions of the formed ions have an impact on the achievable resolution.[24] The use of very short laser pulses (typically 3 ns) creates ions in a very short time period and therefore the temporal distribution of MALDI ions is typically very small. Contributions to temporal distribution by limitations of ion-detection and time-recording devices have become

5

negligible, due to advancements in electronics and the introduction of GHz digital oscilloscopes. The MALDI process desorbs ions from a surface and all ions are directed away from the surface, thus the spatial distribution of MALDI ions is relatively small especially when the analytes are located in a very thin matrix layer (see Section 1.2.1). The most significant contribution to the resolution problem arises from the very broad initial energy distribution among the formed ions.[24,25] In instruments without compensation techniques (so called continuous extraction instruments), this kinetic energy distribution is carried all the way through to the detector and thus ions with the same m/z ratio arrive at slightly different times at the detector, creating a rather broad signal.

Several techniques have been reported for the compensation of the initial kinetic energy distribution. In-source techniques include impulse-field focusing [26] and time-lag focusing,[20] also called delayed extraction. Post-source methods are the ion mirror or reflectron,[27,28] velocity compaction,[29] dynamic field focusing,[30] and post-source pulse focusing.[31] Current state-of-the-art MALDI TOF instruments include generally a combination of time-lag focusing or delayed extraction and an ion mirror. These two techniques will be briefly introduced in the following two sections.

1.1.3.1 Ion mirror or reflectron. Figure 1.2 shows the simplified schematic of an ion mirror. The reflectron is a series of parallel plates. The applied potential on these plates increases gradually as shown in Figure 1.2. The potential of the last plate (V_R) usually matches the applied potential in the source (V_S). Note that if V_R is set to zero, the instrument can be used as a simple linear time-of-flight instrument (with detector 1). This linear mode is sometimes desirable for improving sensitivity (especially for high molecular weight species), since during the reflection process ions can be lost. The generated MALDI ions have a kinetic energy distribution (indicated by the different arrow lengths). Ions with the higher velocity or the higher kinetic energy will penetrate deeper into the reflectron region, and therefore spend more time in this area and reach the detector (detector 2) at the same time as the slower ions. Besides the resolution gain, there is another reason for coupling an ion mirror with a MALDI source. If MALDI ions undergo unimolecular decay in the field-free region, the fragments will have the same

6
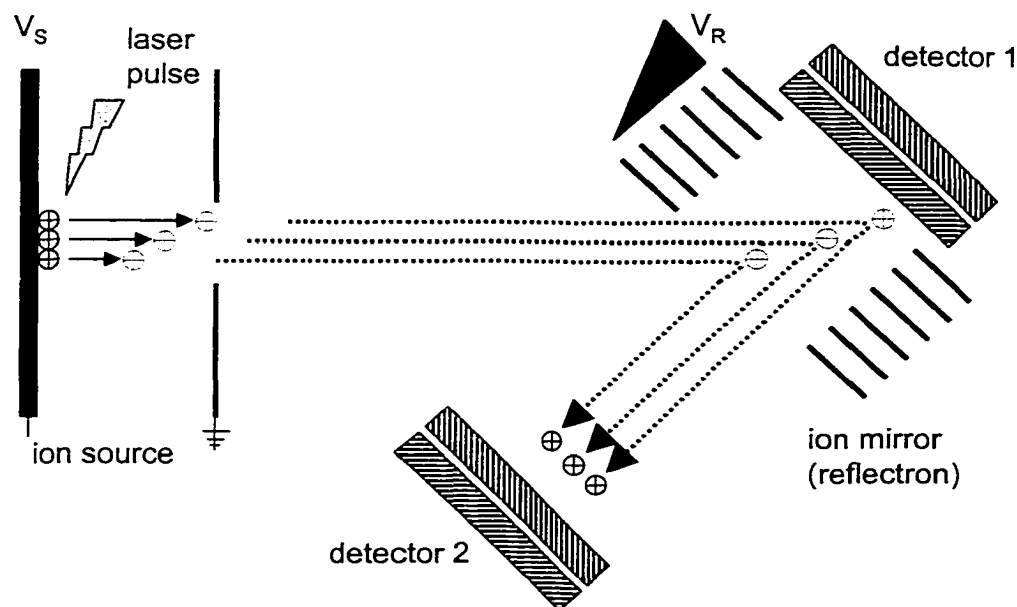
Figure 1.2 Schematic of an ion mirror or reflectron setup.

velocity as but a different kinetic energy than their parent ions. In a linear time-of-flight instrument, these fragment ions will thus be indistinguishable from the parent ions. Since the reflectron setup compensates for kinetic energy distributions at a post-source location, this setup can be used for so-called post-source decay analysis.[32,33] The ratio of the source to reflectron potential can be utilized to determine the masses of the fragment ions.[28]

1.1.3.2 Time-Lag Focusing or Delayed Extraction. Figure 1.3 shows the simplified schematic of a time-lag focusing instrument. For simplicity only ions moving towards the detector will be considered. This is a reasonable assumption to make since MALDI ions are desorbed from a surface and thus spatial distribution should be relatively small. Immediately after the laser pulse, the formed ions are allowed to expand into a field-free region of the source (Fig. 1.3A and B). High energy ions will move further away from

7
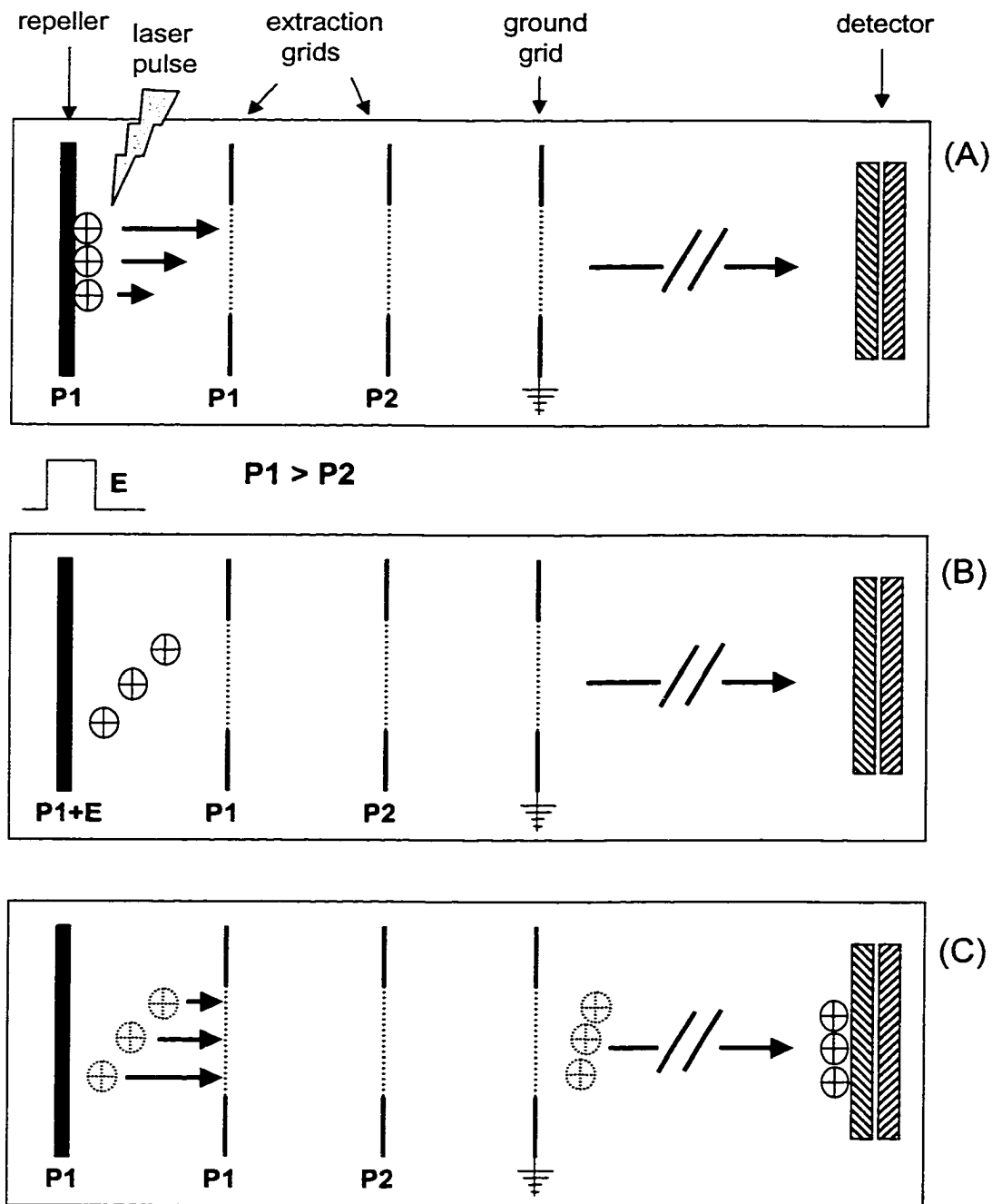
Figure 1.3 Schematic of time-lag focusing. (A) The ions are desorbed into a field-free region where they are separated according to their different initial kinetic energies. (B) Faster ions (high energy) move further away from the repeller. The high energy ions receive less energy from the extraction pulse than the low energy ions. (C) Due to this energy compensation, all ions reach the detector plane simultaneously.

8
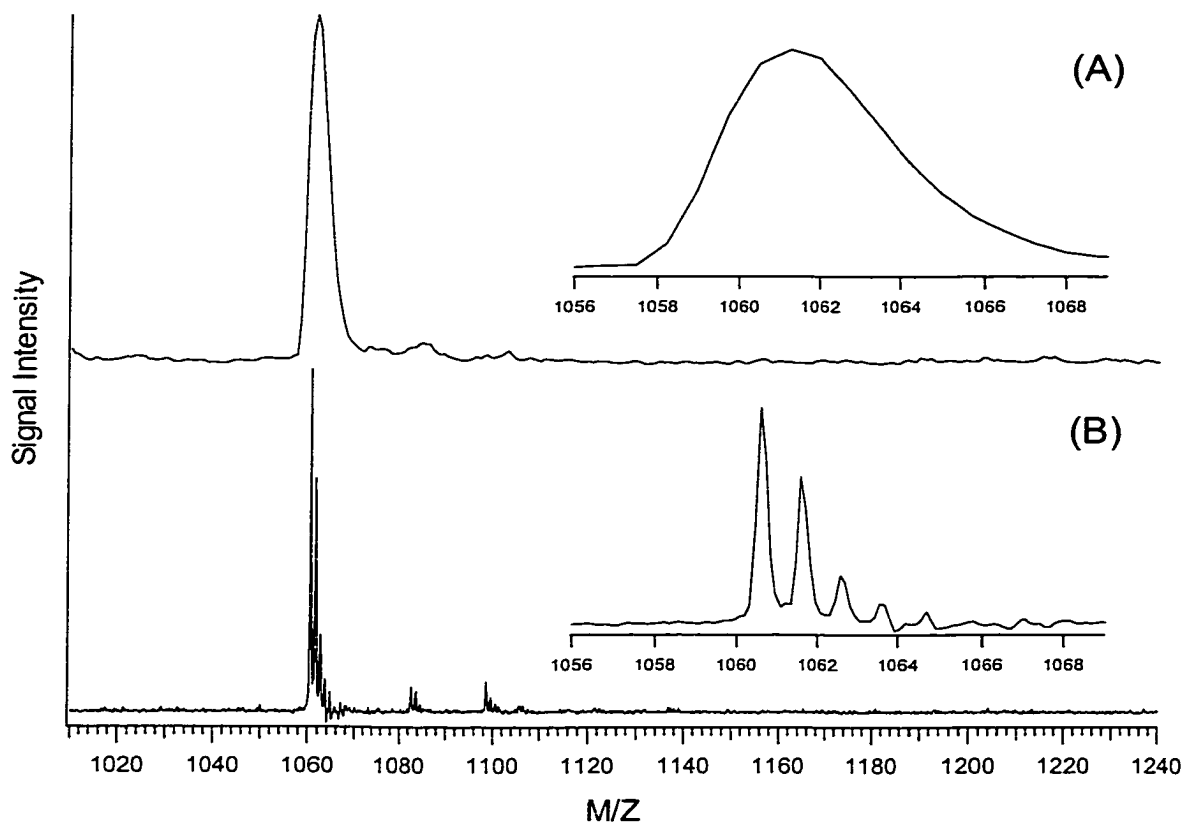
Figure 1.4   MALDI mass spectra of Bradykinin (M.W. 1060.2 Da, sequence RPPGFSPFR). (A) Spectrum obtained on a Hewlett-Packard G2025A LD-TOF system with continuous extraction. (B) Spectrum obtained on a home-built linear time-lag focusing TOF instrument.

the repeller than low energy ions (Fig. 1.3B). After a short time delay, an extraction pulse voltage (E) is applied to the repeller. This voltage pulse extracts the ions into the acceleration region of the source. Ions that are closer to the repeller (low energy ions) obtain more energy from this pulse than the ions further away (high energy ions). Thus, the initially less energetic ions catch up to the initially high energetic ions on their way to the detector (Fig. 1.3C). By careful optimization of the extraction pulse voltage and the delay time, very high resolution for many types of analytes can be achieved.[34] Figure 1.4 shows two MALDI mass spectra of the peptide bradykinin, employing a commercial continuous extraction instrument and a home-built linear time-lag focusing instrument.[34]

9

For the continuous extraction experiment a resolution of approximately 225 (FWHM) is achieved (Fig. 1.4A). In order to obtain a baseline resolved isotopic distribution of bradykinin a minimum resolution of ~2000 is required.[35] In Figure 1.4B the obtained resolution was ~3400 (FHWM). In this case all isotopic species are clearly separated.

It should be mentioned that in contrast to the ion mirror, time-lag focusing is mass dependent. Ions created during the laser pulse will have a similar velocity spread, thus ions with higher masses will have higher initial kinetic energy than lighter ions. When extracted into the accelerating region of the source, this higher initial kinetic energy will lead to decreased mass accuracy in the case of wide mass ranges, since the flight time of the heavier ions will be slightly shorter than required for the proper mass assignment. One possible compensation method would be to do a nonlinear curve fitting using several calibration points in a spectrum. However, a two-point calibration is preferable in MALDI, due to decreased signal suppression and the ability to do an internal calibration. Another approach for improved mass accuracy over wider mass ranges was demonstrated by Whittal, *et al.* by the introduction of functional wave time-lag focusing.[36] In this technique, the pulse applied to the repeller is modified so that it decreases in amplitude with time. Since ions of a higher mass spend more time in the source, higher mass ions receive less imparted kinetic energy from the pulse than ions of lower mass. This compensates for the difference in the ions initial kinetic energy and under optimized conditions the total kinetic energy remains constant leading to improved mass accuracy over wide mass ranges.

1.1.4 Typical Detector Setup. A crucial aspect of TOF instruments is their capability for precise flight time measurements. Among other factors, the timing accuracy of the detector is of significance. Multiple channel plate (MCP) detectors with time resolutions in the nanosecond range are thus considered to be the most suitable detectors for TOF instruments.[39] Gains greater than 10 million have been reported.[40] Figure 1.5 shows a schematic of an MCP and how it functions. All of this lab's instruments use two-stage MCP detectors, however, three-stage setups are also common.[38]

10
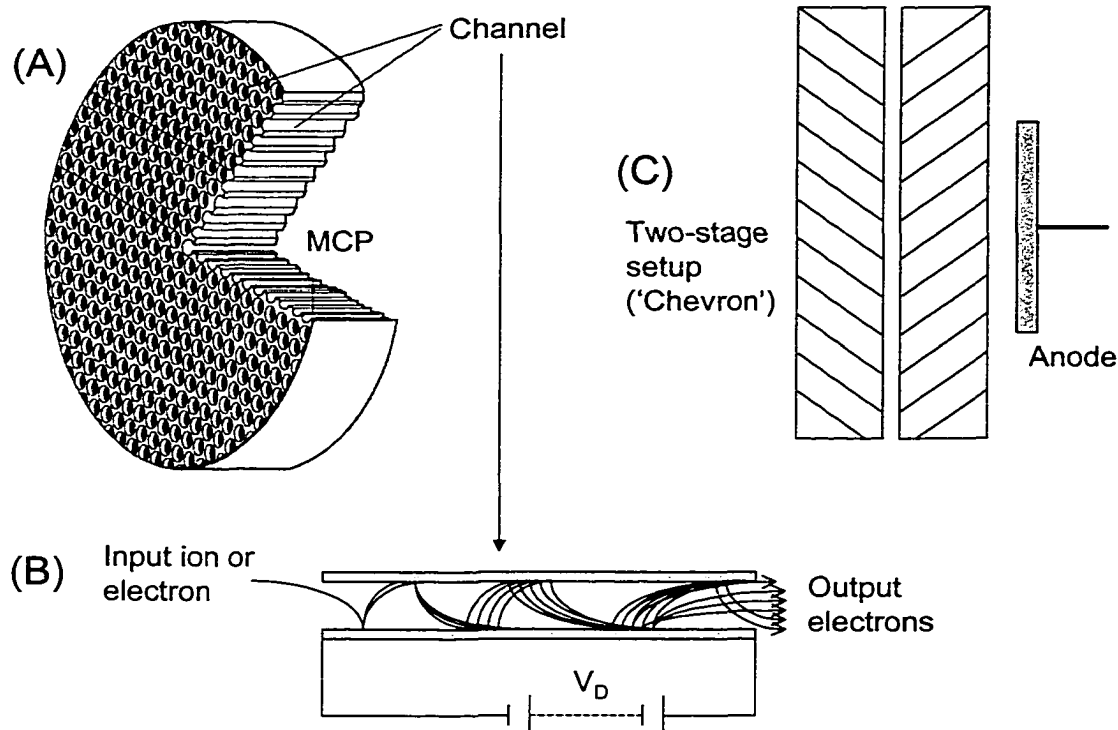
Figure 1.5 MCP detector setup and function. (A) The MCP is a thin disc (thickness: ~0.5 mm. diameter: ~18-25 mm) with millions of channels (diameter 5-12 μm) made of lead-doped glass using fiber optic technology.[37] The open area ratio, i.e. the ratio of the open area to the total effective area of the MCP is ~60%.[38] (B) Incoming ions or electrons cause a cascade of secondary electrons which are accelerated by the applied voltage and thus achieving an amplification.[38] (C) MCPs are typically stacked in a Chevron setup, to avoid positive ion breakthrough.[37]

1.2 Improving MALDI Sensitivity for Proteins and Peptides

For any analytical method, sensitivity improvement can generally be achieved by enhancing the technique's ability to either successfully analyze less concentrated samples or smaller sample volumes. Ideally the technique is capable of doing both. The motivation to find more sensitive methods for protein and peptide analysis by MALDI-TOF MS is based on the rapidly growing field of proteomics, i.e. characterization of all expressed proteins in a cell or a specific tissue.[41] As Kellner puts it, proteome analysis

11

tries "to give a snapshot of physiological processes at the molecular level".[42] Since protein abundances within a cell or a tissue can vary by several orders of magnitude,[41] analysis of low abundance proteins is a very challenging task. Another handicap for low abundant protein or peptide analysis is that there is no comparable technique available for amplification of sample as there is for DNA and RNA (i.e. in the case of DNA, Mullis's Nobel Prize winning polymerase chain reaction, or PCR).[43]

There are two general approaches in MALDI research to improve sensitivity. One deals with improvements in the matrix/sample preparation to enhance ionization efficiencies that allows for analysis of dilute samples. The other approach examines ways to decrease the necessary sample volume introduced into the mass spectrometer. The following sections present an overview of some recently published work in these areas.

1.2.1   Matrix/Sample Preparation Methods. Apart from good mass accuracy and reproducibility, high sensitivity is a characteristic of an optimal matrix/sample preparation method.   Since the introduction of MALDI, several protocols for matrix/sample preparation have been reported. Karas and Hillenkamp introduced the dried droplet method in 1988.[44] In this method, a mixture of matrix and analyte is simply air dried on a MALDI target. Although this method is not very sensitive, it is still commonly used. The wide-spread acceptance of this technique is mainly due to its simplicity, which also allows for its implementation into automated matrix/sample preparation. Other methods include vacuum drying,[45] crushed crystal,[46] slow crystal growing,[47] active film,[48,49] pneumatic spray,[50] electrospray,[51] fast solvent evaporation,[52] and the two-layer method.[53,54] The matrix/sample preparation methods most commonly used in this lab are the two-layer method and modifications of it. Figure 1.6 illustrates the two-layer method and compares the two-layer method with a modified version, the three-layer technique. The two-layer method was developed on the basis of the crunched crystal [46] and the fast evaporation method.[52] The main purpose of this method is to obtain thin matrix layers with evenly distributed analyte. It has been shown that the two-layer method provides high detection sensitivity and very good spot-to-spot reproducibility for peptides as well as proteins.[53,54]

12
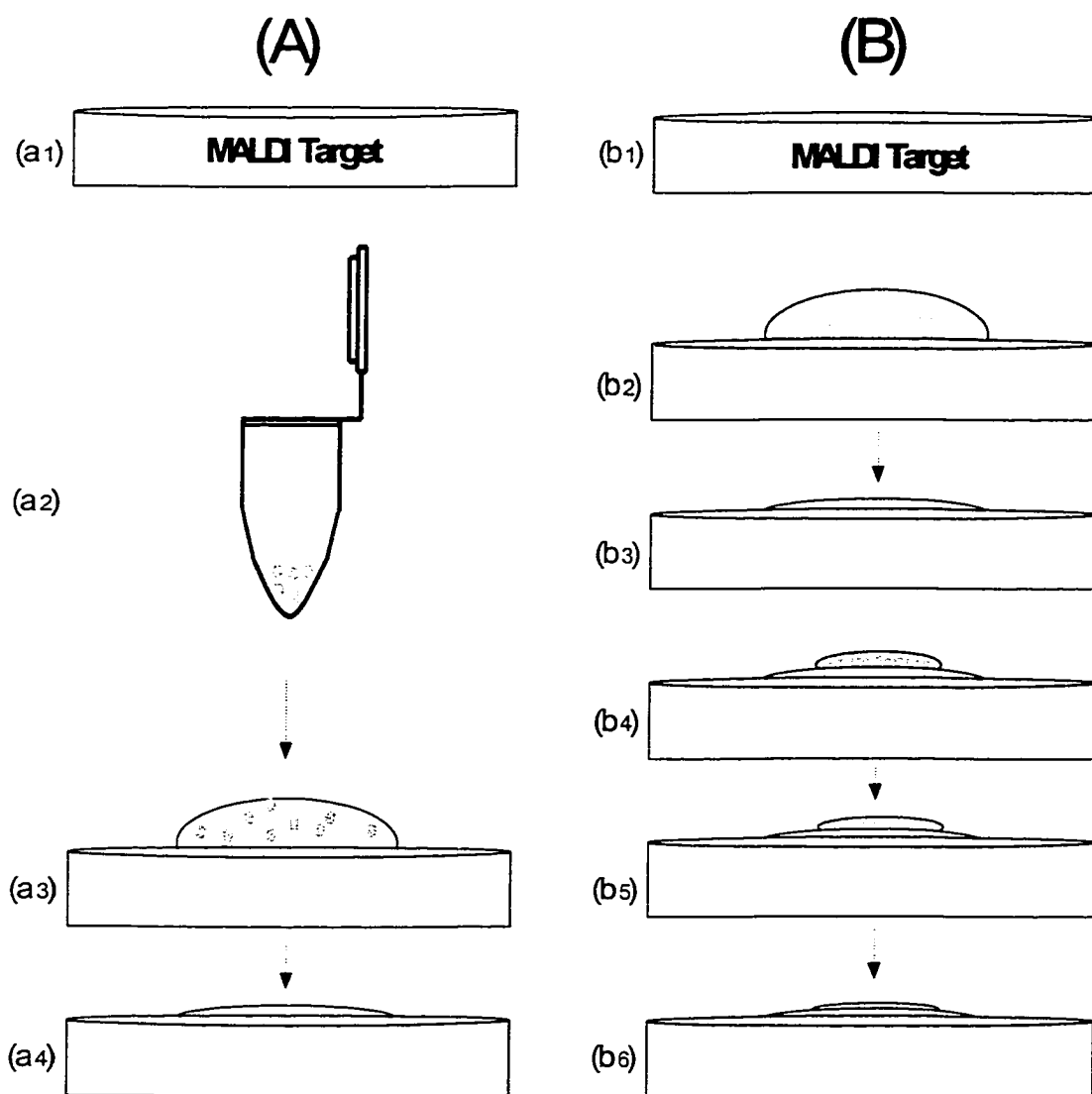
Figure 1.6   Comparison of double-layer (A) and three-layer (B) matrix/sample preparation. (A) [a1] Deposition of a first thin matrix layer (~1 µL; fast evaporation). [a2] Mixing of the sample with a saturated matrix solution (~2 µL). [a3] Deposition of the sample/matrix mixture onto the first matrix layer (~0.4 µL). [a4] Drying and crystallization of the second sample/matrix layer. (B) [b1] same as [a1]. [b2] Deposition of a saturated matrix solution on top of the first layer (~0.4 µL). [b3] Drying of the second layer. [b4] Direct deposition of the sample onto the second matrix layer (~0.2 µL). [b5] The sample solvent dissolves small amounts of matrix from the second layer and thus sample mixes with matrix. [b6] Drying of the sample/matrix mixture as a third layer.

13

Whittal, et al., used the two-layer technique without analyte in the second layer to provide base layers for direct analyte deposition with a nanoliter delivery system.[55] This will be discussed in more detail later. This three-layer technique is illustrated in Figure 1.6B. The direct deposition step of the three-layer technique is similar to the fast evaporation technique reported by Vorm and Roepstorff.[52] In the fast evaporation technique the analyte is directly deposited onto a very thin matrix layer. Very good sensitivity has been reported with this technique for standard peptides.[52] However this technique is not as rugged as the three-layer technique, since the thin layer can easily be destroyed, e.g. by washing steps or contaminated samples. It should be pointed out that the direct deposition of sample onto a matrix layer works only when the matrix solubility in the sample solvent is not too good but also not too weak. If the matrix is too soluble in the sample solvent the matrix layer will be destroyed, if the solubility is too weak, not enough matrix will dissolve or mix with the deposited analyte before recrystallization. Deposition of aqueous samples onto matrix layers prepared from α-cyano-4-hydroxycinnamic acid (4-HCCA) generally works very well, whereas the same is not true for sinapinic acid. This difference is most likely due to the insufficient solubility of sinapinic acid in water. To circumvent this problem, a fourth layer can be deposited onto the analyte, consisting of the same matrix solution as was used for the second layer.[55] Note that the ability to directly deposit sample onto matrix layers eliminates the need for premixing sample and matrix. This also helps to reduce the initially required sample volume as will be discussed below. Several applications for direct deposition of samples onto matrix layers have been reported, including deposition directly from capillary electrophoresis columns (CE),[56] piezoelectric microdispensers,[57-61] and combinations of CE and piezoelectric dispensing.[62]

1.2.2   Low Volume Deposition. Analyte loss due to wall adsorption can be a severe problem when dealing with very dilute solutions. Individual peptides have a concentration limit of 100 - 500 femtomole/μL (0.1 - 0.5 μM), i.e. below this concentration the peptides are irreversibly adsorbed to container walls over time.[63] Thus dilute solutions should be made from concentrated stocks and must be analyzed immediately. A more practical way to increase mass spectrometric sensitivity is therefore introducing small sample volumes with moderate concentrations into a mass

14

spectrometer. In the case of MALDI, low volume deposition is often coupled with direct deposition techniques. As already mentioned this is understandable since the direct deposition does not require premixing. Allmaier reported in 1997 the picoliter to nanoliter deposition of peptide and protein solutions employing a piezoelectric dispenser.[57] Between 150-250 femtomole of proteins and peptides were detected. Marko-Varga and coworkers have published a series of papers using piezoelectric microdispensers.[58-62] Protein amounts between 160-225 attomoles were detectable.[60] Piezoelectric micro dispensing is an attractive technique since it is amenable for automation and can be combined with microchip technology for protein chemistry.[61] However electrochemical effects on analytes, excessive sample loss due to wall adsorption, (from passing through long connecting tubing), reusability, and plugging problems need to be further addressed.

In 1994, Jespersen, et al. used pulled glass pipettes to deposit protein and peptide samples into 250 picoliter vials engraved into MALDI targets. Proteins and peptides were detected at low attomole levels.[64] Marshall and coworkers achieved low attomole sensitivity for peptides by deposition of volumes between 40-1000 nanoliters using microsyringes combined with MALDI-FT-ICR mass spectrometry in 1995.[65] More recently, Sweedler and coworkers have used pulled glass micropipettes with tip diameters of less than 1 μm for selecting individual cell organelles and positioning them on specially constructed glass MALDI targets for mass spectrometric analysis of peptides.[66]

There have been also several reports on peptide detection at the attomole level by electrospray ionization.[67] Caution must be exercised when reading the reported amounts as they are usually based on calculations of how many ions per scan are detected and not how much analyte has actually been introduced into the mass spectrometer. Comparison is therefore not possible with MALDI experiments, where sensitivity criteria are based on the total analyte amount introduced into the mass spectrometer.

This group has been involved in the development of a microspot MALDI delivery system since 1995.[68] The original system (see Figure 1.7) allows deposition of sample volumes down to ~20 pL. Substance P was detected with a total amount of 0.97 amol and this system was also used for analyzing lysates from single human erythrocytes.[55] Figure 1.8A-C shows microscope images of the microspot deposition technique.

15
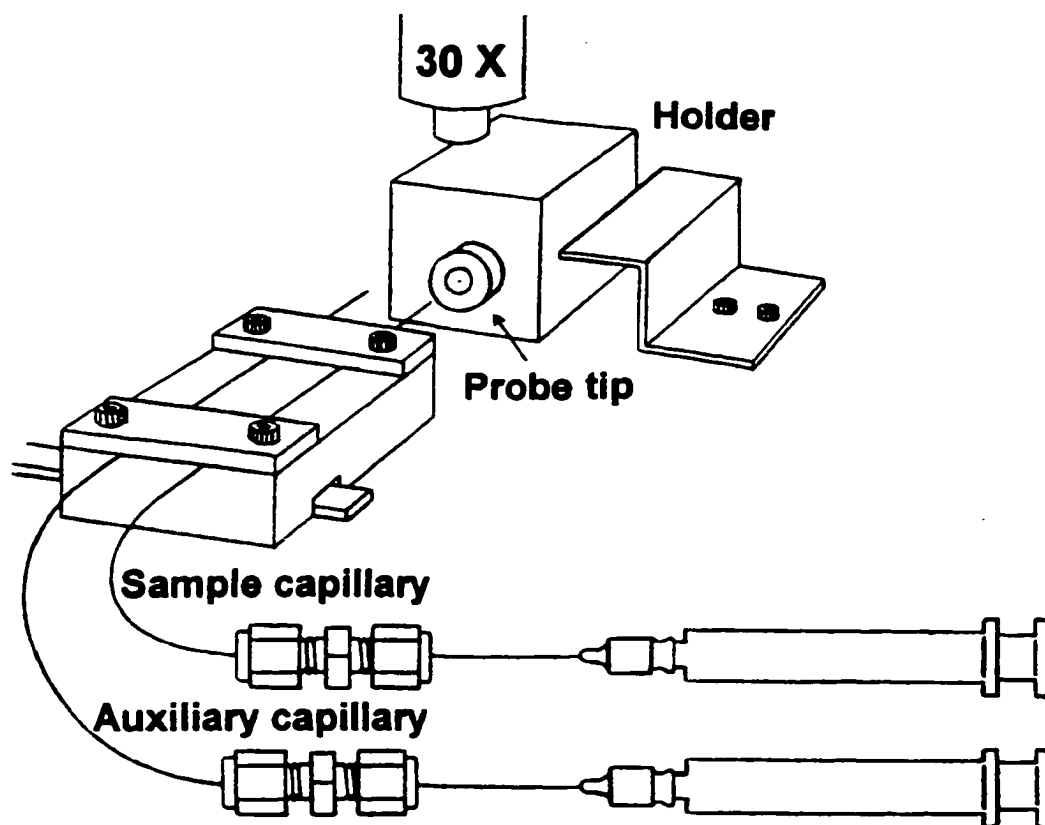
Figure 1.7 Original microspot delivery system designed by Rafael E. Golding. Two fused silica capillaries are attached to an x-y stage and connected to disposable syringes. For sample loading the x-y stage is moved so that the capillaries have contact to a sample solution that is presented in a horizontally mounted glass tube. Sample is then drawn into the capillary. The sample amount can be measured using a recticle and microscope above the x-y stage. To avoid excessive evaporation, the sample is withdrawn into the capillary ~1 mm from the capillary front end. After sample loading, the glass tube containing the sample is replaced with a matrix-covered MALDI target. The sample-filled capillary is then moved very close to the MALDI target and the sample is deposited by applying pressure to the capillary with the connected syringe.

The work presented in this thesis demonstrates further development of the microspot delivery system for improved detection sensitivity. The applications have been expanded to multiple chemical and enzymatic reactions inside the capillary in sub-nanoliter volumes. A modified setup has been devised for solvent extraction experiments into a nanoliter droplet of organic phase.

16

(A) A 20 μm i.d. fused-silica capillary, filled with a ~300 pL sample plug and positioned ~50 μm from the matrix-covered MALDI target surface, just before sample deposition.

(B) Immediately following sample deposition onto target. The resulting sample droplet on the target dries rapidly.

(C) The resulting microspot size depends on the deposited volume and on the deposition distance of the capillary. Typically spot size is between 80 to 200 μm. For better visualization, this microspot was created by deposition of ~300 pL of a concentrated $CuSO_4$ solution.

~150 μm
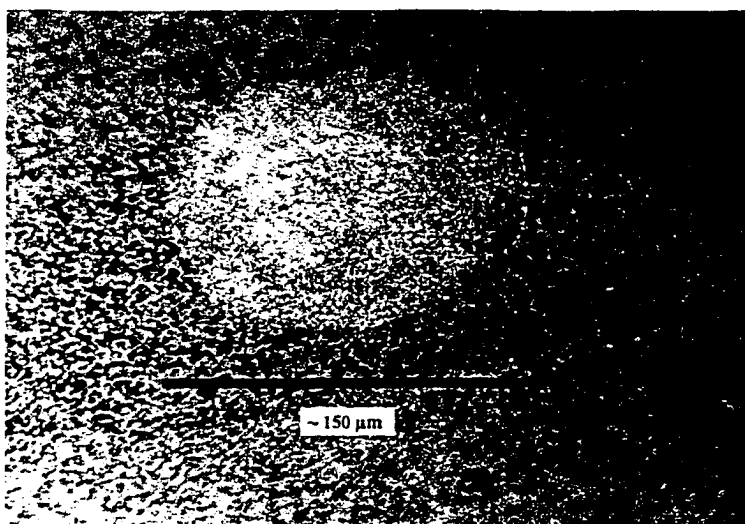
Figure 1.8   Microscope images of microspot deposition technique.

17

1.3 Literature Cited

(1)   Karas, M.; Bachmann, D.; Bahr, Y.; Hillenkamp, F. *Int. J. Mass Spectrom. Ion Processes* **1987**, *78*, 53-68.

(2)   Karas, M.; Hillenkamp, F. *Anal. Chem.* **1988**, *60*, 2299-2301.

(3)   Tanaka, K.; Ido, Y.; Akita, S. In *Proceedings of the Second Japan-China Joint Symposium on Mass Spectrometry*; Matsuda, H.; Liang, X.-T., Eds.; Bando Press: Osaka, Japan, 1987: pp 185-188.

(4)   Tanaka, K.; Waki, H.; Ido, Y.; Akita, S.; Yoshida, Y.; Yoshida, T. *Rapid Commun. Mass Spectrom.* **1988**, *2*, 151-153.

(5)   For example, see (a) Kolli, V. S. K.; Orlando, R. *Rapid Commun. Mass Spectrom.* **1996**, *10*, 923-926. (b) Zollner, P.; Schmid, E. R.; Allmaier, G. *Rapid Commun. Mass Spectrom.* **1996**, *10*, 1278-1282. (c) Fujita, T.; Itagaki, Y.; Hisaka, M.; Naoki, H.; Andriantsiferana, M. *Rapid Commun. Mass Spectrom.* **1997**, *11*, 1115-1119. (d) Whittal, R. M.; Russon, L. M.; Li, L. *J. Chrom. A* 1998, *794*, 367-375. (e) Sze, E. T. P.; Chan, T. W. D.; Wang, G. *J. Am. Soc. Mass Spectrom.* **1998**, *9*, 166-174. (f) Breuker, K., Knochenmuss, R., Zenobi, R. *Int. J. Mass Spectrom.* **1998**, *176*, 149-159. (g) Williams, T. L.; Fenselau, C. *Eur. Mass Spectrom.* **1998**, *4*, 379-383.

(6)   Laiko, V.V.; Baldwin, M.A.; Burlingame, A. L. *Anal. Chem.* **2000**, *72*, 652-657.

(7)   Zenobi, R.; Knochenmuss, R. *Mass Spectrom. Rev.* **1998**, *17*, 337-366.

(8)   Karas, M.; Glückmann, M.; Schäfer, J. *J. Mass Spectrom.* **2000**, *35*, 1-12.

(9)   Strobel, F. H.; Solouki, T.; White, M. A.; Russel, D. H. *J. Am. Soc. Mass Spectrom.* **1991**, *2*, 91-94.

(10)   For example see (a) Hettich, R. L.; Buchanan, M. V. *J. Am. Soc. Mass Spectrom.* **1991**, *2*, 22-28. (b) Castoro, J. A.; Wilkins, C. L. *Anal. Chem.* **1993**, *65*, 2621-2627.

18

(11)   For example, see (a) Chambers, D. M.; Goeringer, D. E.; McLuckey, S. A.; Glish, G. L. *Anal. Chem.* **1993**, *65*, 14-20. (b) Doroshenko, V. M.; Cotter, R. J. *Anal. Chem.* **1996**, *68*, 463-472. (c) Qin, J.; Steenvoorden, R. J. J. M.; Chait, B. T. *Anal. Chem.* **1996**, *68*, 1784-1791.

(12)   Medzihradszky, K. F.; Campbell, J. M.; Baldwin, M. A.; Falick, A. M.; Juhasz, P.; Vestal, M. L.; Burlingame, A. L. *Anal. Chem.* **2000**, *72*, 552-558.

(13)   Loboda, A. V., Krutchinsky, A. N., Bromirski, M.; Ens, W.; Standing, K. G. *Rapid Commun. Mass Spectrom.* **2000**, *14*, 1047-1057.

(14)   Levinger, E. E. *Galileo: First Observer of Marvelous Things*; Julian Messner, Inc.: New York, 1952.

(15)   Hall, A. R. *Isaac Newton: Adventurer in Thought*; Blackwell: Oxford, UK, 1992.

(16)   Gillmor, C. S. *Coulomb and the Evolution of Physics and Engineering in Eighteenth-Century France*; Princeton University Press: Princeton, NJ, 1971.

(17)   Stephens, W. *Phys. Rev.* **1946**, *69*, 691.[*]

(18)   Stephens, W. *Bull. Am. Phys. Soc.* **1946**, *21*, 22.[*]

(19)   Cameron, A. E.; Eggers, D. F. *Rev. Sci. Instrum.* **1948**, *19*, 605-607.[*]

(20)   Wiley, W. C.; McLaren, I. H.. *Rev. Sci. Instrum.* **1955**, 26, 1150-1157.

(21)   Nelson, R. W.; Dogruel, D.; Williams, P. *Rapid Commun. Mass Spectrom.* **1995**, *9*, 625.

(22)   Schriemer, D. C.; Li, L. *Anal. Chem.* **1996**, *68*, 2721-2725.

(23)   Van Berkel, W. J. H.; Van Den Heuvel, R. H. H.; Versluis, C.; Heck, A. J. R. *Protein Sci.* **2000**, *9*, 435-439.

(24)   Cotter, R.J. *Time-of-Flight Mass Spectrometry: Instrumentation and Applications in Biological Research;* American Chemical Society: Washington, DC, 1997.

---

[*] references were adopted from Gary Siuzdak's website "*A History of Mass Spectrometry*" at http://masspec.scripps.edu/hist.html

19

(25)   Beavis, R. C.; Chait, B. T. *Chem. Phys. Lett.* **1991**, *181*, 479-484.

(26)   Marable, N. L.; Sanzone, G. *Int. J. Mass Spectrom. Ion Phys.* **1974**, *13*, 185-194.

(27)   Mamyrin, B. A.; Karatev, V. I.; Schmikk, D. V.; Zagulin, V. A. *Zh. Eksp. Teor. Fiz.* **1973**, *64*, 82-89.

(28)   Tang, X.; Beavis, R.; Ens, W.; Lafortune, F.; Schueler, B.; Standing, K. G. *Int. J. Mass Spectrom. Ion Processes* **1988**, *85*, 43-67.

(29)   Muga, M. L. Anal. Instrum. **1987**, *16*, 31-50.

(30)   Yefchak, G. E.; Enke, C. G.; Holland, J. F. *Int. J. Mass Spectrom. Ion Processes* **1989**, *87*, 313-330.

(31)   Kinsel, G. R.; Johnston, M. V. *Int. J. Mass Spectrom. Ion Processes* **1989**, 91, 157-176.

(32)   Spengler, B.; Kirsch, D.; Kaufmann, R. J. *J. Phys. Chem.* **1992**, *96*, 9678-9684.

(33)   Spengler, B. *J. Mass Spectrom.* **1997**, *32*, 1019-1036.

(34)   Whittal, R. M.; Li, L. *Anal. Chem.* **1995**, *67*, 1950-1954.

(35)   Theoretical peak shapes for bradykinin at different resolutions were computed with Peptide Tools, Version A 01.01 (Hewlett-Packard, 1994).

(36)   Whittal, R. M.; Russon, L. M.; Weinberger, S. R.; Li, L. *Anal. Chem.* **1997**, *69*, 2147-2153.

(37)   Evans, S. In "*Methods in Enzymology: Mass Spectrometry*" McCloskey, J. A., Ed., Vol. 193, Academic Press: San Diego, CA, USA, 1990, pp. 61-86.

(38)   Technical Information on MCP Assembly, Hamamatsu Photonics, Shimokanzo, Japan, 1991.

(39)   Wurz, P.; Gubler, L. *Rev. Sci. Instrum.* **1996**, *67*, 1790-1793.

(40)   Laprade, B.; Fuchs, W.; Lincoln, B. In *Proceedings of the 41st ASMS Conference on Mass Spectrometry and Allied Topics*; Portland, OR, 1996, p. 81.

20

(41)   Wilkins, M. R.; Williams, K. L.; Appel, R. D.; Hochstrasser, D. F. *Proteome Research: New Frontiers in Functional Genomics*; Springer: Heidelberg, Germany, 1997.

(42)   Kellner, R. *Fresenius J. Anal. Chem.* **2000**, *366*, 517-524.

(43)   Mullis K. B; Faloona F. A., In "*Methods in Enzymology: Recombinant DNA*", Wu, R., Ed., Vol. 155, Academic Press: New York, USA, 1987, pp. 335-350.

(44)   Karas, M.; Hillenkamp, F. *Anal. Chem.* **1988**, *60*, 2299-2301.

(45)   Weinberger, S. R.; Boernsen, K. O.; Finchy, J. W.; Robertson, V.; Musselman, B. D. In *Proceedings of the 41st ASMS Conference on Mass Spectrometry and Allied Topics*; San Francisco, CA, May 31-June 4, **1993**, p. 775a.

(46)   Xiang, F.; Beavis, R. C. *Rapid Commun. Mass Spectrom.* **1994**, *8*, 199.

(47)   Xiang, F.; Beavis, R. C. *Org. Mass Spectrom.* **1993**, *28*, 1424.

(48)   Mock, K. K.; Sutton, C. W.; Cottrell, J. S. *Rapid Commun. Mass Spectrom.* **1992**, *6*, 233.

(49)   Bai, J.; Liu, Y. H.; Cain, T. C.; Lubman, D. M. *Anal. Chem.* **1994**, *66*, 3423-3430.

(50)   Köchling, H. J.; Biemann, K. In *Proceedings of the 43rd ASMS Conference on Mass Spectrometry and Allied Topics*; Atlanta, Georgia, May 21-26, **1995**, p. 1225.

(51)   Hensel, R. R.; King, R.; Owens, K. G. In *Proceedings of the 43rd ASMS Conference on Mass Spectrometry and Allied Topics*; Atlanta, Georgia, May 21-26, **1995**, p. 947.

(52)   Vorm, O.; Roepstorff, P.; Mann, M. *Anal. Chem.* **1994**, *66*, 3281-3287.

(53)   Dai, Y. Q.; Whittal, R. M.; Li, L. *Anal. Chem.* **1996**, *68*, 2494-2500.

(54)   Dai, Y.; Whittal, R. M.; Li, L. *Anal. Chem.* **1999**, *71*, 1087-1091.

(55)   Li, L.; Golding, R. E.; Whittal, R. M. *J. Am. Chem. Soc.* **1996**, *118*, 11662-11663.

(56)   Zhang, H.; Caprioli, R. M. *J. Mass. Spectrom.* **1996**, *31*, 1039-1046.

21

(57)   Allmaier, G. *Rapid Commun. Mass Spectrom.* **1997,** *11*, 1567-1569.

(58)   Önnerfjord, P.; Nilsson, J.; Wallmann, L.; Laurell, T.; Marko-Varga, G. *Anal. Chem.* **1998,** *70*, 4755-4760.

(59)   Önnerfjord, P.; Ekström, S.; Bergquist, J.; Nilsson, J.; Laurell, T.; Marko-Varga, G. *Rapid Commun. Mass Spectrom.* **1999,** *13*, 315-322.

(60)   Marko-Varga, G. *Chromatographia Suppl. I* **1999,** *49*, S-95-S99.

(61)   Ekström, S.; Önnerfjord, P.; Nilsson, J.; Bengtsson, M.; Laurell, T.; Marko-Varga, G. *Anal. Chem.* **2000,** *72*, 286-293.

(62)   Miliotis, T.; Kjellström, S.; Nilsson, J.; Laurell, T.; Edholm, L.-E.; Marko-Varga, G. *J. Mass Spectrom.* **2000,** *35*, 369-377.

(63)   Immler, D.; Mehl, E.; Lottspeich., F.; Meyer, H. E. In *Microcharacterization of Proteins*; Kellner, R.; Lottspeich, Meyer, H. E., Eds., Wiley-VCH: Weinheim, Germany, 1999, pp. 87-95.

(64)   Jespersen, S.; Niessen, W. M. A.; Tjaden, U. R.; Greef, v. d. J.; Litborn, E.; Lindberg, U.; Roeraade, J. *Rapid Commun. Mass Spectrom.* **1994,** *8*, 581-584.

(65)   Solouki, T.; Marto, J. A.; White, F. M.; Guan, S.; Marshall, A. G. *Anal. Chem.* **1995,** *67*, 4139-4144.

(66)   Rubakhin, S. S.; Garden, R. W.; Fuller, R. R.; Sweedler, J. V. *Nature Biotechnol.* **2000,** *18*, 172-175.

(67)   For example, see (a) Andren, P. E.; Emmett, M. R.; Caprioli, R. M. *J. Am. Soc. Mass Spectrom.* **1994,** *5*, 867-869, or (b) Lazar, I. M.; Ramsey, R. S.; Sundberg, S.; Ramsey, J. M. *Anal. Chem.* **1999,** *71*, 3627-3631.

(68)   Golding, R. E.; Whittal, R. M.; Li, L. In *Proceedings of the 43th ASMS Conference on Mass Spectrometry and Allied Topics;* Atlanta, GA, May 21-26, 1995; p. 1223.

Chapter 2

Detection of 25,000 Molecules of Substance P by MALDI-TOF Mass Spectrometry and Investigation of Issues Related to Ultrasensitive Mass Spectrometric Analysis of Peptides[a]

2.1 Introduction

With recent advances in ionization techniques and mass analyzers, mass spectrometry (MS) has become an exquisitely sensitive technique for peptide and protein analysis. While current mass spectrometric sensitivity is adequate for addressing a wide range of biological problems, there is a genuine need to further improve the detection sensitivity. For example, mapping the proteome of single cells requires ultrasensitive MS detection. The amount of peptides and proteins expressed in a single cell is usually less than 1 million copies per protein. Improving detection sensitivity is also critical in characterization of post-translational modifications of proteins. In this case, extensive sample workup necessary for unambiguous identification of modification sites and structural characterization of modifying groups often results in only trace amounts of peptides for final MS analysis.

At present analyzing very low abundance peptides by MS can still be a challenging task. However pushing beyond the current detection limits of MS methods is a realistic goal, considering that analyzing ions in a mass spectrometer can be an inherently very sensitive process. Using a proper sample introduction method and an efficient ionization technique, single atom analysis by mass spectrometry was

---

[a] A form of this chapter has been submitted for publication: B. O. Keller and L. Li *"Detection of 25,000 Molecules of Substance P by MALDI-TOF Mass Spectrometry and Investigation of Issues Related to Ultrasensitive Mass Spectrometric Analysis of Peptides"*

23

demonstrated almost two decades ago.[1] While single molecule analysis by MS has not yet been illustrated, there are no fundamental reasons that would exclude MS from being a method of single molecule detection. For the analysis of molecular species such as peptides, besides the ionization efficiency issue, another important issue deals with sample introduction.

There are a number of techniques reported recently in the literature on the improvement of detection sensitivity of mass spectrometry based on electrospray ionization[2-7] or matrix-assisted laser desorption/ionization (MALDI).[8-14] In our laboratory, we have been involved in developing a nanoliter chemistry (nanochem) station for peptide and protein analysis.[12-14] The key feature of this nanochem station is handling sub-nanoliter volumes of sample using a capillary tube.[14] The low sample volume is then presented to a MALDI mass spectrometer using a microspot sample deposition technique for MS analysis.[12,13]

Here we demonstrate the possibility of detecting peptides with a total sample loading of several tens of thousands of molecules (e.g., 25,000 molecules of Substance P). This state-of-the-art detection is achieved utilizing an optimized, three-layer sample preparation protocol in combination with microspot sample deposition.[13] Equally significant is that at this low level of detection, several fundamental issues related to ultrasensitive MS detection can be addressed. The issues discussed in this work include the minimum number of analyte molecules in a given area necessary to produce analyte signal, the minimum number of ions needed to produce a useful isotope pattern, and the overall detection efficiencies of MALDI-TOF for peptides. Based on these results, practical aspects related to further improvement in MALDI MS detection sensitivity are discussed.

2.2 Experimental

Substance P, Lys- [Ala^3]-bradykinin and alpha-cyano-4-hydroxycinnamic acid (4-HCCA) were from Sigma-Aldrich Canada (Oakville, Ontario, Canada). To purify 4-HCCA, about 10 g of 4-HCCA were first suspended in ~30 mL of cold ethanol, filtered through a class C glass filter, and the remaining residue was then recrystallized from

24

ethanol (95%) at 50° C. Stock solutions of peptides at 1 µg/µL were made up and diluted in 0.6 mL siliconized polypropylene vials (Rose Scientific, Edmonton, Alberta, Canada) using triply-distilled H_2O. Aliquots of stock solutions were stored at -20° C. Diluted sample solutions were made up directly before MS experiments.

Mass spectra of peptides were collected on a home-built linear time-lag focusing MALDI-TOF mass spectrometer, equipped with a nitrogen laser (337 nm wavelength, 3 ns pulse width, model VSL337ND, Laser Science Inc., Newton, MA, USA). This instrument has been described in detail elsewhere.[17] Specific details on data collection are given for each spectrum in the Results section. Spectra were acquired and processed with Hewlett-Packard supporting software and reprocessed with the Igor Pro software package (WaveMetrics, Inc., Lake Oswego, OR, USA).

MALDI targets made of stainless steel were thoroughly polished using micromesh cushioned abrasive sheets of different grades (Scientific Instrument Services, Ringoes, NJ, USA). As a final step, the targets were micropolished using a 1 µm and finally a 0.3 µm alumina slurry on a Buehler polishing cloth (Tech-Met Canada Ltd., Markham, Ontario, Canada). Targets were sonicated for 10 minutes in a 1:1 mixture of methanol and 10% formic acid then rinsed with methanol. Targets were wiped with a methanol-wetted paper towel directly before matrix deposition.

Prior to this work, microspot MALDI experiments were performed with three- and two-layer matrix/sample preparation methods.[13,15,16] For the sensitive detection demonstrated in this work, an optimized three-layer method was used and was found to be critical in lowering the detection limit. As a first layer ~1 µL of a 100 mM 4-HCCA solution in a methanol/acetone mixture (40%/60% by volume) was deposited into the center of the MALDI target. The droplet spread out over the whole cyclic target (4 mm diameter) and formed a very thin matrix crystal layer. As a second layer ~0.4 µL of a saturated 4-HCCA solution in a methanol/H_2O mixture (30%/70% by volume) was deposited into the center of the first layer. This second layer had a spot diameter of 1.5 to 2 mm. This layer was also very thin and smooth and consists of crystals of 2-3 µm in size. During matrix-layer formation, each layer was carefully checked with a portable mini-microscope (30 x magnification). Should any irregularities or cavities be observed in the crystal layer, the target was rinsed with water and methanol and the procedure was

25

repeated. Once the second layer had dried, 0.5 µL of triply dist. H_2O was deposited onto it and blown off with pressurized air after ~30 seconds. This washing step was then repeated. These procedures are effective steps to remove soluble salt contamination.

Deposition of picoliter samples was done using capillary tubes mounted in a nanoliter chemistry station. This sample-handling device is illustrated in Figure 2.1.
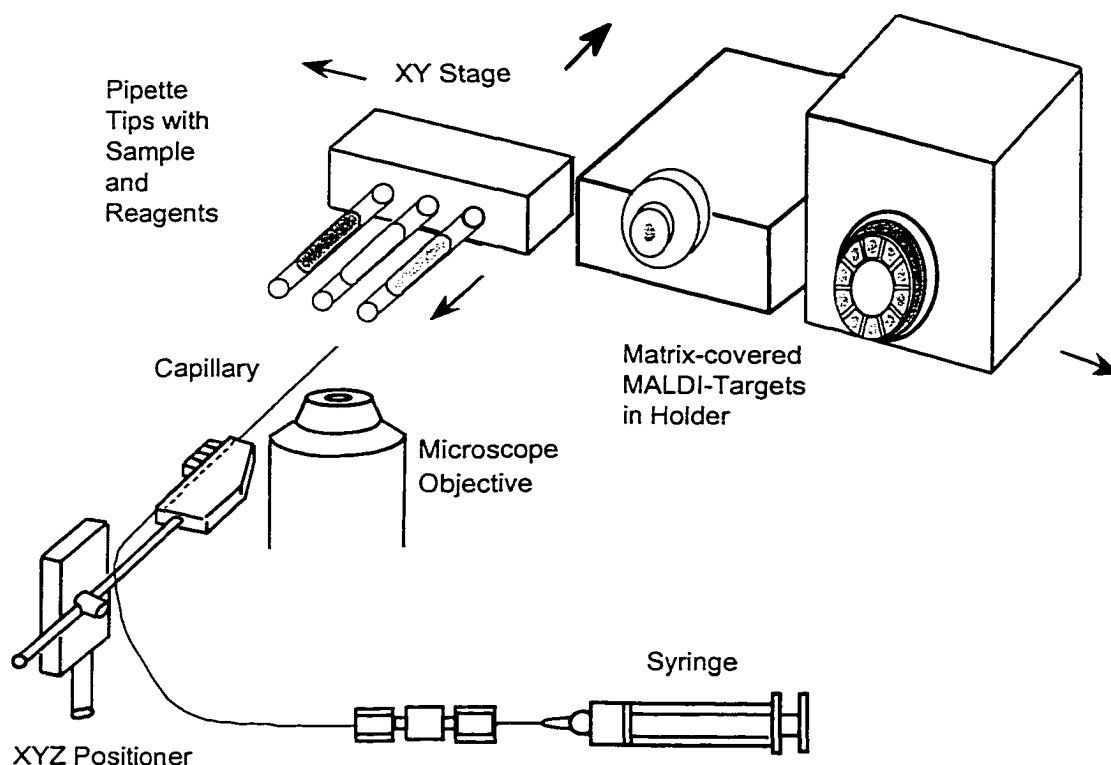
Figure 2.1 Nanoliter chemistry station. The original design (see Fig. 1.7 in Chapter one) was further developed and improved. This setup was situated on a 2D mounting stage of an inverted microscope system (Model IX 70, Olympus, Melville, New York , USA). Possible magnifications were as follows: 40x, 60x, 100x, 150x, 200x, 300x, 400x and 600x. For most applications a magnification of 40 or 60x was sufficient. Pipette tip holder and MALDI targets were sitting on the 2D stage whereas the 3D manipulator holding the capillary was mounted on a side bar that is independent of the 2D mounting stage. Two video cameras were employed to assist in observing the sample handling. One camera recorded through the objective and the second camera was connected to a customized telescope to give a magnified side view of the capillary. This second camera was a valuable tool during sample deposition since the view through the objective alone does not show the vertical position of the capillary during sample deposition onto the matrix-covered target.

26

A 10-μm-ID capillary tube was connected to a syringe as shown in Figure 2.1 and used to draw a sub-nanoliter volume of peptide sample from a horizontally mounted pipette tip. To minimize analyte loss due to adsorption onto the wall surface, the capillary was treated with a siliconizing agent before use (Glassclad-18, United Chemical Technologies, Bristol, PA, USA). The sample plug was observed under a microscope and its volume determined employing a calibrated recticle positioned in the eyepiece. The sample was then directly deposited from an approx. 0.1 mm distance onto the target into the center of the second matrix layer, yielding a sample spot with 80-150 μm in diameter, depending on the deposited volume. The target was then introduced into the mass spectrometer. During analysis the sample spot was scanned with the laser beam under video observation.

For comparison, analyte was also deposited applying a common macro technique with regular pipetters. Figure 2.2 shows a schematic comparison of the two techniques. Approximately 50 nL of sample solution were deposited directly into the center of the second matrix layer. The handling of less than a 100 nL volume with a Gilson P2 Pipetter (Mandel Scientific Ltd., Guelph, Ontario, Canada) was only achieved after the pipetter went through maintenance and recalibration.
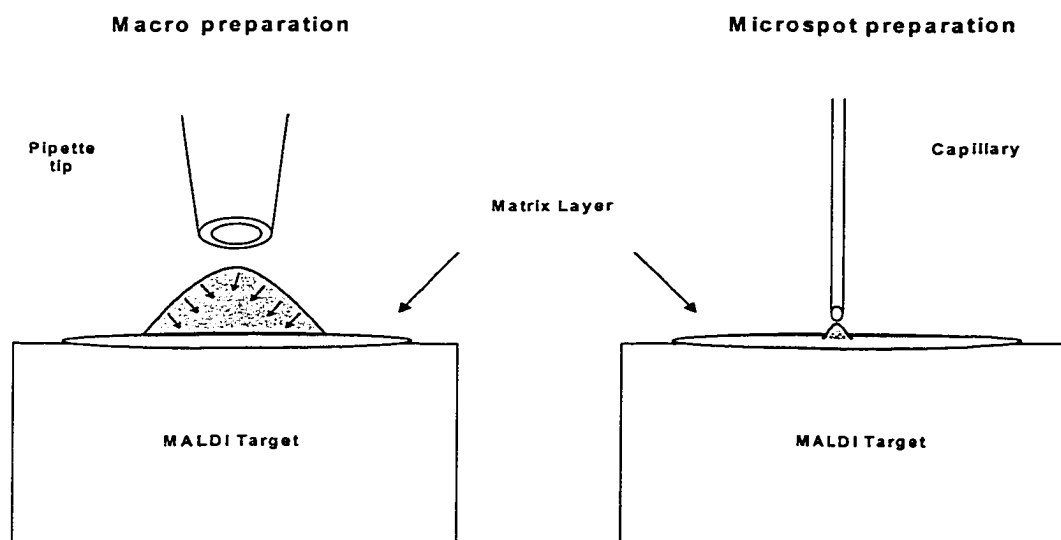
Figure 2.2   Schematic comparison of macro and microspot technique.

27

2.3 Results and Discussion

Figure 2.3 shows the mass spectra of the two analytes deposited from picomolar solutions with the macro sample preparation method employing pipetters (i.e., Fig. 2.2A). For the spectrum of Substance P, 64 single-shot spectra out of a total of 220, were summed and the signal to noise ratio is ~7:1. For Lys-[Ala^3]-bradykinin, 44 single shot spectra out of 140 were summed and the signal to noise ratio is ~6:1.
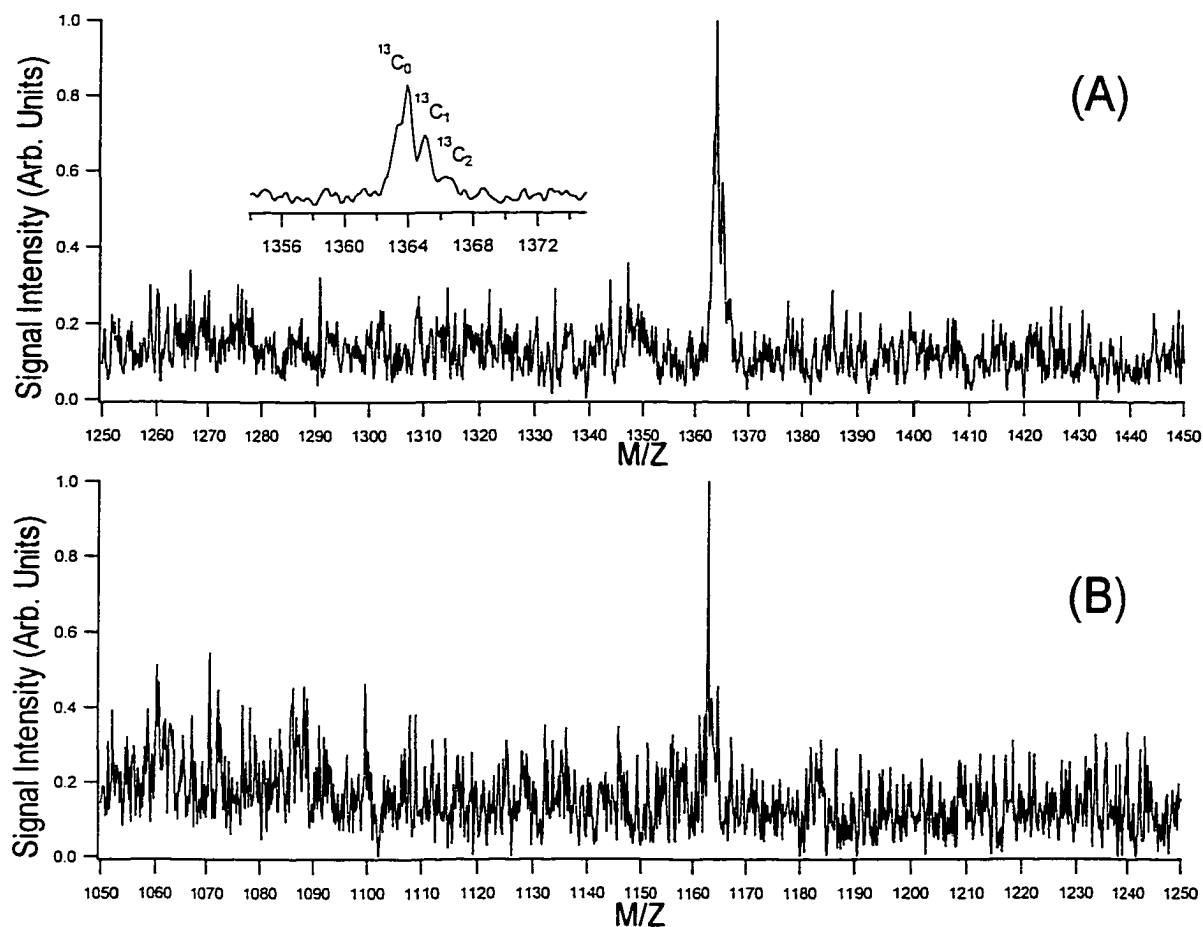
Figure 2.3   MALDI mass spectra of dilute peptides with the macro deposition technique as described in the text. (A) ~50 nL of 40 pM Substance P were deposited onto the 2nd layer of 4-HCCA (total amount: ~2 attomole) (B) ~50 nL of 70 pM Lys-[Ala^3]-bradykinin were deposited onto the 2nd layer of 4-HCCA (Total amount: ~3.5 attomole).

28

When we tried to use the microspot deposition technique for such low concentration analyte solutions, we could not obtain any useful signal. Only after increasing the analyte concentration by about 20 times, microspotted samples of Substance P could be detected. Figure 2.4 shows the microspot MALDI results.
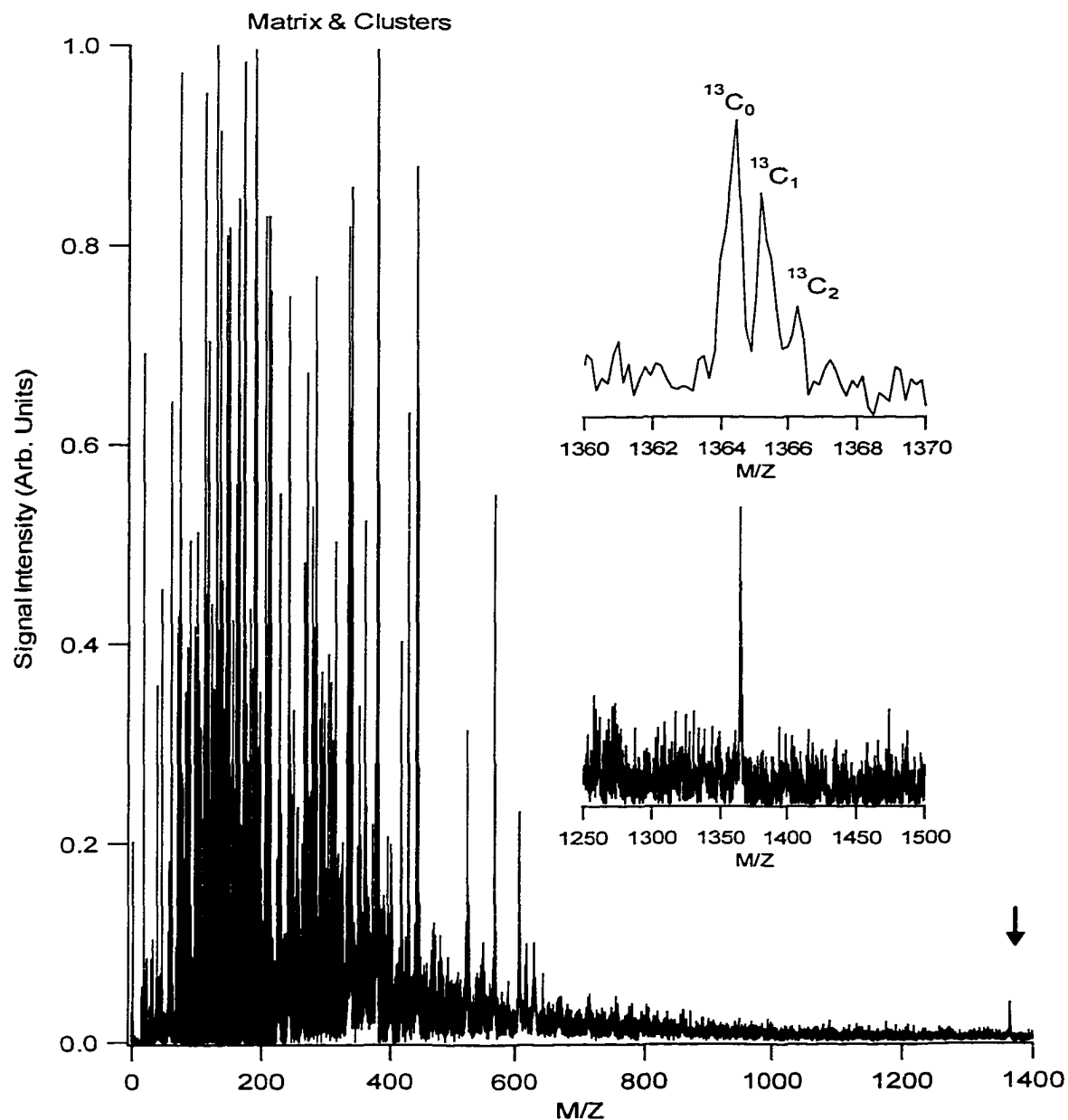
Figure 2.4 MALDI mass spectrum of Substance P using the microspot deposition technique as described in the text. ~50 pL of a 0.8 nM solution of Substance P were deposited onto the 2nd layer of 4-HCCA (Total amount: ~42 zeptomol or ~25,000 molecules).

For the spectrum of Substance P (Figure 2.4) 61 single-shot spectra, out of a total of 305, were summed and the signal to noise ratio is ~5:1. For all individual spectra a single shot spectrum was discarded if no signal was observed at all three m/z values of the $^{13}C_0$-, $^{13}C_1$- or $^{13}C_2$-isotopes in the molecular ion region. Several repetitive experiments were performed using new stock solutions, thoroughly cleaned targets, and new capillaries to ensure elimination of carry-over. Reproducible results were obtained for Substance P for total sample loadings of 40-80 zeptomole or 25,000 - 50,000 molecules.

The appearance of the typical isotopic pattern is good evidence that the observed signal is indeed from Substance P and not a "fabricated" signal due to the selection made when collecting the data. Since the intensities of the analyte signals shown in Figure 2.4 are very low, several control experiments were performed to ensure they are indeed from the ionization of peptide molecules. Experiments on matrix blanks were done to see if it was possible to "fabricate" signals with the restriction of adding a single-shot spectrum only when a signal was found at an arbitrarily selected m/z range. Figure 2.5 shows the spectra obtained from such experiments. For Figure 2.5A, 1000 laser shots were fired onto a matrix-covered target, on which triply distilled water was deposited instead of analyte solution. Only single-shot spectra, which produced at least one signal in the m/z range 1364-1367, (i.e., the same m/z range as for Substance P) were summed up. The result of 170-added single-shot spectra is a peak with a signal-to-noise ratio of approx. 2:1. Besides the low S/N ratio, the lack of the typical isotope pattern of an analyte in this mass range is further evidence for the authenticity of the signal obtained in Figure 2.4.

To be certain that the "fabricated" signal is indeed due to the arbitrary m/z range selection of the operator (and not a trace carryover from former experiments) we collected another spectra using the same target and matrix preparation. One thousand laser shots were fired at the target, but only single-shot spectra were added in which at least one signal in the m/z range of 1377-1380 appeared. Figure 2.5B shows the spectrum of this experiment and the obtained signal-to-noise ratio for the peak is comparable to the one shown in Figure 2.5A. Similar signals were obtained (data not shown) for other selected m/z ranges that did not contain possible matrix clusters.

30
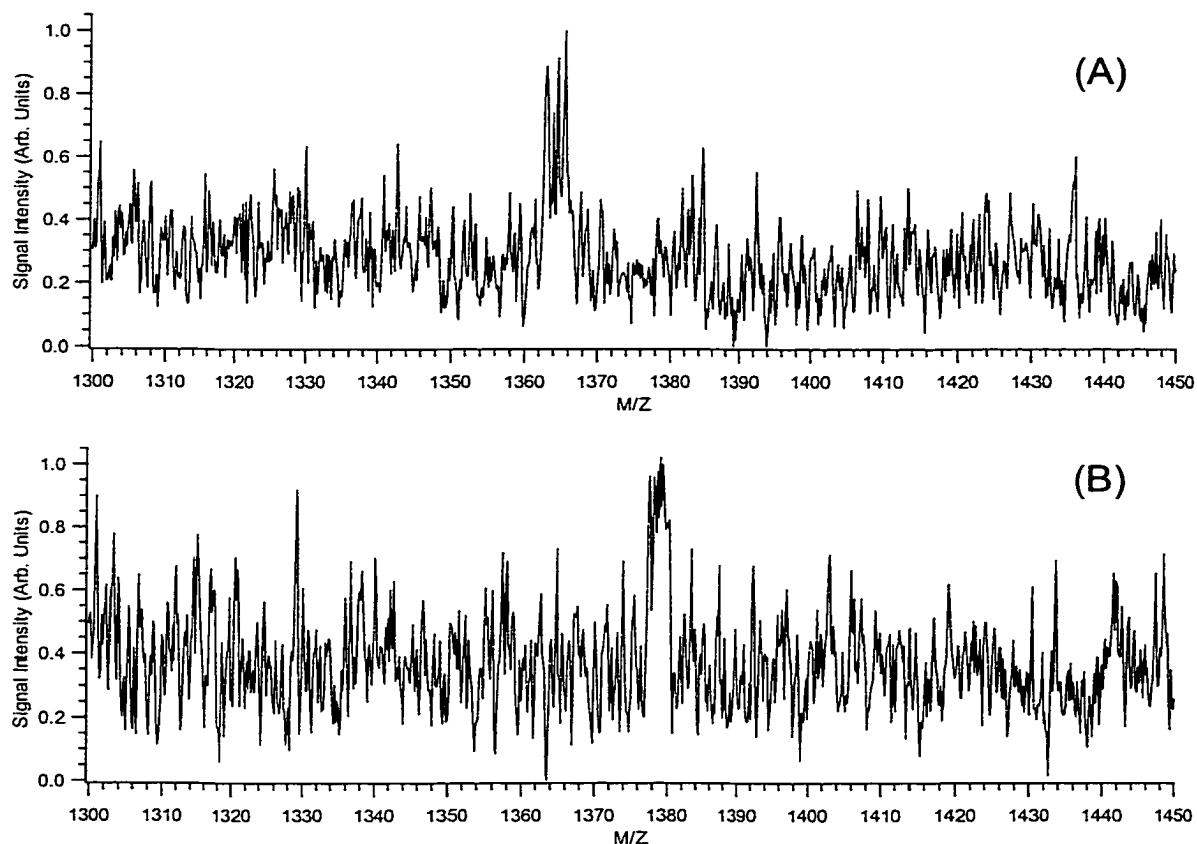
Figure 2.5   "Fabricated" signals from a matrix blank as described in the text. (A) 170 single-shot spectra out of 1000 trials were summed and averaged. (B) 190 single-shot spectra out of 1000 trials were summed and averaged.

While the S/N ratio is not high for the spectra shown in Figures 2.3A and 2.4, isotope pattern in the molecular ion region is clearly observed for Substance P in each case. For example, in Figure 2.4 the area ratio of the first three isotope peaks is 100:77:40 which is close to the anticipated result of 100:79:38 taking into account the natural abundance of the ^{13}C isotope.[20] For five repeated trials, loading between 25,000 and 50,000 molecules, the average isotope ratio was found to be $100:84\pm10:50\pm11$ for the $^{13}C_0$, $^{13}C_1$ and $^{13}C_2$ isotope peaks, respectively. This result indicates that by loading less than 50,000 molecules to the mass spectrometer, a sufficient number of ions are produced and detected that give rise to a useful isotope pattern. At this level of sample loading, we

31

need to consider the minimum number of ions required in order to produce an isotope pattern such as those shown in Figure 2.4.

We can use probability theory and statistics to estimate the number of analyte ions that must reach the detector in order to produce signals that give an isotopic pattern reflecting their natural abundances. We assume that introduction, ionization, and detection of analyte molecules are non-biased; i.e., all of the isotopes are selected randomly according to their natural abundance and create the same signal strength at the detector. This is a reasonable assumption in a linear time-of-flight mass spectrometer with a multi-channel plate detector where there should not be any transmission or detection bias in this narrow mass range. For the isotope pattern of Substance P, we limited ourselves to the three most abundant isotopic species, i.e., $^{13}C_0$, $^{13}C_1$, and $^{13}C_2$. The relative abundances for $^{13}C_0$, $^{13}C_1$, and $^{13}C_2$ are 0.421, 0.336, and 0.164, respectively.[20] The sum of these abundances or probabilities is 0.921 or 92.1%. Thus for any given number of ions reaching the detector, it is very likely that they are one of the three isotopes, i.e., $^{13}C_0$, $^{13}C_1$ or $^{13}C_2$. However, the probability that the ratio of these three isotopes resembles the natural isotope pattern will depend on the number of ions that reach the detector.

It is intuitive that a larger number of ions will more likely generate a pattern close to the natural abundance ratio. This is true for most conventional MS experiments where sample loading is sufficiently high. But for experiments with a limited number of ions reaching the detector, we can calculate the probabilities of obtaining an isotope pattern consisting of three isotope peaks with their abundance or ion counts falling into a certain range. For example, if 100 randomly selected analyte ions reach the detector and create a signal, the probability that 38 - 46 ions (i.e., ±10% range for $^{13}C_0$) are $^{13}C_0$ isotopes can be calculated as follows. First let's examine the probability for any number of ions being a $^{13}C_0$ isotope: [21]

32

$$P_n(m) = C^m \, p^m q^{n-m}$$

where

n	=	total number of ions (i.e., 100)	
m	=	number between 0 and n	
C^m	=	number of possibilities = n!/(m!(n-m)!)	
p	=	relative abundance of the isotope	
q	=	1 − p	

To calculate the probability that 38 - 46 ions are a $^{13}C_0$-isotope, the above formula for m = 38 to 46 where n = 100 and p = 0.421:

$$\sum_{m=38}^{m=46} P_n(m) = 0.64$$

This means that there is a 64 % chance of getting 38 - 46 ions of the $^{13}C_0$-isotope when 100 ions are detected. For the second isotope ($^{13}C_1$) there is a 60% chance of getting 30-37 ions, and for the third isotope ($^{13}C_2$) there is a 58% chance of getting 14-19 ions. The overall probability of getting an isotopic resemblance within a ±10 % range of the natural abundance for each of the three isotopes is the product of these three probabilities and is 0.22. Thus there is only a 22% chance to get such an isotopic resemblance if 100 ions reach the detector and create a signal. For larger numbers of ions the above formula has to be modified, since PCs can not readily calculate factorials for n > 170. We therefore use a proximity formula for calculating the probability $P_n(m)$ for larger numbers of n: [21]

$$P_n(m) \approx \frac{1}{\sqrt{2\pi n p}} \, e^{-\frac{1}{2}\left(\frac{m-np}{\sqrt{npq}}\right)^2}$$

33

Table 2.1 shows the results for an array of different ion numbers as well as for two different tolerance ranges. As can be seen from Table 2.1, if 10 ions are detected, there is only a ~4% chance of producing an isotope pattern with peak intensity variations of ±10%. The probability increases to 14% when the peak intensity variations are ±20%.

Table 2.1   Relationship between number of ions reaching the detector and probability of correct isotopic representation for Substance P.

Number of ions reaching the detector and creating a signal	Probability that the first three isotopic peak signals are re-presented each within ~±10 % of their natural abundance	Probability that first three isotopic peak signals are re-presented each within ~±20 % of their natural abundance
10	3.8 %	14.0 %
50	14.3 %	43.1 %
100	22.4 %	59.5%
200	32.9 %	77.7 %
500	59.9 %	95.8 %
800	77.8 %	98.9 %
1000	84.3 %	99.6 %
1200	93.3 %	99.8 %

Note that in the probability calculation, intensity variation is measured by the changes in absolute number of ions. In an actual MS experiment, relative intensity of peaks is measured. In this regard, ±5% absolute intensity variation can be translated into relative intensity changes of 100% for $^{13}C_0$, 73% to 88% for $^{13}C_1$ and 35% to 43% for $^{13}C_2$. In the microspot experiments, between 25,000 and 50,000 molecules were loaded to produce an isotope pattern that has an averaged relative intensity variation of about ±16% for $^{13}C_1$ and ±22% for $^{13}C_2$ from three trials, which puts this experiment into the

34

range of ±20% absolute intensity variation in probability calculation. Thus, from Table 2.1, we can conservatively estimate that with 80% probability at least 200 ions are actually detected by the mass spectrometer in order to produce an isotope pattern such as that shown in Figure 2.4. This estimation should allow us to establish the low boundary of ionization efficiency (LBIE) for Substance P by MALDI. In our mass spectrometer, three grids, each with 90% transmission, are used, giving an overall ion transmission of about 73%. We use two multi-channel plates (MCP) in a chevron setup as a detector (see Figure 1.5 in Chapter 1). Detection efficiency with this setup depends on the open area ratio (OAR) of the frontal MCP, since an approaching ion can only produce a signal when it enters a microchannel. The OAR is the ratio of the open area (channel holes) to the total area of the MCP. For the employed MCPs in our detector setup, the OAR is ~60%.[22] Another issue is the detection efficiency of the MCP itself, i.e. how probable is it that an ion entering a microchannel actually produces secondary electrons. Geno and Macfarlane dealt with this issue more than 10 years ago[23] and their model is considered an adequate tool to estimate conversion efficiencies.[24] For peptide ions with a velocity of more than 30,000 m/s the probability of an ion creating secondary electrons in an MCP is 1 or 100%. In our home-built instrument we use a 20 kV acceleration voltage and thus we can calculate the final velocity of the peptide ions employing the basic equations:

$$eV = 1/2 \ m \ v^2$$

thus
$$v = \sqrt{((2eV)/m)}$$

where e = single charge (= 1.6022×10^{-19} C), v = acceleration voltage (20 kV), m = ion mass (i.e. for Substance P; 1364 u = 2.265×10^{-24} kg) and v = velocity in m/s. Oxidized Substance P has an acceleration voltage velocity of about 53,000 m/s. This velocity is far above the necessary velocity of ~30,000 m/s to reach 100% probability of secondary electron emission. Thus all Substance P ions entering a microchannel should create a signal. However the manufacturer states that for ions in the energy range of 10-50 keV the MCP has a detection efficiency of ~75%.[22] This efficiency is attributed to unknown factors affecting the conversion of ion impact into secondary electrons. Assuming all ions generated in the source are focused to the detector and subsequently detected with

35

grid transmission loss and detector efficiency taken into account, a minimum number of about 600 ions must be produced according to following calculation:

$$\frac{200}{(73\% x60\% x75\%)} \approx 600$$

Since the sample loading is between 25,000 to 50,000 molecules, the LBIE for Substance P can now be calculated:

$$LBIE = \frac{600}{Number \quad of \quad deposited \quad molecules}$$

In our case the LBIE for Substance P is therefore 1-2 %.

From a practical application point of view, for accurate mass detection of an unknown peptide, we commonly compare the isotope pattern observed in an experiment with that calculated from natural abundance to determine the C_{12} peak. Due to the finite probability associated with the detection of certain isotope peaks, the number of ions necessary for mass measurement must be sufficiently high to ensure a useful pattern is generated. If isotope statistics become the limit for defining the C_{12} molecular ion peak (e.g., in the cases of detecting thousands of ions for peptides), one may use isotope depletion experiments to overcome this limitation. Isotope depletion combined with mass spectrometry has been demonstrated by Marshall and coworkers for other applications.[25] In the experiments, peptides and proteins are expressed in special cell growth media that allow the enrichment of certain types of isotopes, resulting in predominately single-isotope peak for the molecular ions. In theory, single ion detection with isotope-depleted samples can be used to define the molecular ion of a peptide.

Although a minimum of 200 analyte ions are believed to be detected, the signal to noise ratio for the analyte is very low as shown in Figure 2.4. This is probably partly due to the background noise associated with the MALDI process. The background level or baseline of the spectrum rises as laser desorption takes place from samples with or without analyte added. Considering the continuous nature of the baseline, the noise is not

36

from discrete matrix clusters, which bear a unique pattern that can be readily identified.[19] The background noise is likely from random detection events associated with ions and neutrals that reach the detector. In designing the ion source for our linear TOF[17], we noticed that if the grid size for the extraction plate was small (i.e., 0.5 cm in diameter; the current design is optimized at 1 cm) the baseline became severely elevated. We can use the following scenario to possibly explain the observed baseline elevation. After the ions are generated by MALDI, the plume of ions expands in the region between the repeller and extraction plate during the time-lag period. The fast moving ions such as matrix or matrix cluster ions migrate away from the center of the expansion axis due to radial velocity.[26] When the extraction voltage is applied, some of these ions will hit the extraction plate. The ions composed of the original impact ions, dissociated fragments, and secondary ions from the plate can reflect back to the extraction zone and be accelerated and possibly focused to the detector. But these ions will not have finite starting points and will be detected as continuous background. With the reduction in grid size, more ions will hit the extraction plate, hence the more elevated baseline. Another cause of elevated baseline is from the detection of neutral species. It is evident that when a high voltage is applied to the ion gate to deflect all ions away from reaching the detector, an elevated baseline is still observed. Ions during extraction and acceleration can convert into neutral species that maintain the same velocities as their corresponding ions.

The above discussion only suggests some possible sources of background noise that were observed. It is clear that to further improve detection sensitivity efforts on reduction of background noise are critically needed. In turn, this calls for a better understanding of the MALDI process and further optimization of the TOF instrumental design, particularly those related to source design and ion detection. Customized low noise detectors with open area ratios of up to 80% are available and might be one way to improve ion detection.[22] Alternatively one can explore the possibility of differentiating analyte ions from background ions by using techniques such as MS/MS. Tandem TOF/TOF has been recently demonstrated.[27]

Another area of potential improvement is in sample preparation. As mentioned above, the microspot technique worked only with the use of a relatively higher

37

concentration solution compared to the macro preparation. Since MALDI is essentially carried out from a "solid solution" where the analyte is dissolved in a host of matrix molecules, we need to consider the analyte concentration in matrix host or the molecule density of the analyte in the solid. The area of the microspot in relation to the deposited amount is much larger than in the macro preparation for equal sample concentrations. Table 2.2 compares the macro and microspot deposition technique for Substance P. It shows that a minimum concentration of ~5 molecules of analyte per μm^2 is necessary to obtain useful signals, assuming that all the analyte molecules are located close to the surface of the matrix layer. In another words, if a 40-pM solution is deposited by the microspot technique, the area concentration will be about 0.25 molecules per μm^2 or 25 molecules per 100 μm^2, which is apparently too low to generate any useful signals.

Table 2.2   Comparison of macro and microspot techniques for Substance P

	Macro preparation	Microspot preparation
Sample concentration	40 pM	800 pM
Volume deposited	~50 nL	~55 pL
Spot diameter	~0.55 mm	~80 μm
Spot area	~240,000 μm^2	~5000 μm^2
Total amount deposited	~2 attomole	~42 zeptomole
Area concentration	~5 molecules/μm^2	~5 molecules/μm^2

The data shown in Table 2.2 suggests that if the spot area can be further decreased while still meeting the concentration requirement of 5 analyte molecules per μm^2, the detection limit can be lowered further. Decreasing the microspot size can be done by using a smaller capillary for deposition. However handling of picoliter amounts in

38

smaller ID capillaries becomes increasingly more difficult, due to the larger surface to volume ratio, which leads to stronger tension forces inside the capillary. If smaller sample spots were attainable the laser spot size responsible for matrix and analyte desorption becomes an issue as well. A laser spot larger than the sample spot would introduce undesired background signals due to more matrix desorption than necessary for sufficient analyte desorption and ionization. Currently we are not able to determine the actual laser spot size at the low energies used for analysis. Extrapolation of spot size from current spot area data obtained by blasting a hole into a thin matrix layer using higher laser powers is not readily possible since the energy distribution in a laser plume is approx. Gaussian.[28] For lower laser energies a linear drop in spot size compared to the higher laser energies can not be expected. According to the manufacturer of our 337 nm nitrogen laser (Laser Science Inc., Newton, MA, USA) theoretically, a minimum spot size diameter of less than 1μm can be achieved when using an aberration corrected microscope objective. However this is experimentally very difficult for MALDI, since it would mean bringing the objective very close to the repeller in the source region.

One possible approach addressing the sample preparation issue is to utilize techniques commonly used in micro-fabrication to create matrix dots with small diameters, followed by deposition of analyte on top of the matrix dots. In this case the laser spot size would not matter since only matrix from the sample/matrix spot could be desorbed and problems due to enhanced background signals would be eliminated. The formation of small matrix-layer spots, however, experiences the same difficulties as the sample microspot formation.

2.4   Literature Cited.

(1)   (a) Hurst, G. S.; Nayfeh, M. H.; Young, J. P. *Appl. Phys. Lett.* **1977**, *30*, 229-234. (b) Chen, C.H.; Payne, M.G.; Hurst, G.S.; Kramer, S.D.; Allman, S.L.; Phillips, R.C. in *Lasers and Mass Spectrometry,* Lubman, D.M., Ed.; Oxford University Press: New York, 1990.

39

(2)   Wilm, M.; Shevchenko, A; Houthaeve-T; Breit, S.; Schweigerer, L.; Fotsis, T.; Mann, M. *Nature* **1996**, *379*, 466-469.

(3)   Valaskovic, G.A.; Kelleher, N.L.; McLafferty, F.W. *Science* **1996**, *273*, 1199-1200.

(4)   Hofstadler, S. A.; Severs, J.C.; Smith, R.D.; Swanek, F.D.; Ewing, A.G. *Rapid Commun. Mass Spectrom.* **1996**, *10*, 919-923.

(5)   Emmett, M.R.; Caprioli, R.M. *J. Am. Soc. Mass Spectrom.* **1994**, *5*, 605-613.

(6)   Andren, P.E.; Emmett, M.R.; Caprioli, R.M. *J. Am. Soc. Mass Spectrom.* **1994**, *5*, 867-869.

(7)   Lazar, I.M.; Ramsey, R.S.; Sundberg, S.; Ramsey, J.M. *Anal. Chem.* **1999**, *71*, 3627-3631.

(8)   Jespersen, S.; Niessen, W.M.A.; Tjaden, U.R.; van der Greef, J.; Litborn, E.; Lindberg, U.; Roeraade, J. *Rapid Commun. Mass Spectrom.* **1994**, *8*, 581-584.

(9)   Allmaier, G. *Rapid Commun. Mass Spectrom.* **1997**, *11*, 1567-1569.

(10)   Önnerfjord, P.; Nilsson, J.; Wallman, L.; Laurell, T.; Marko-Varga G. *Anal. Chem.* **1998**, *70*, 4755-4760.

(11)   Solouki, T.; Marto, J.A.; White, F.M.; Shengheng, G.; Marshall, A.G. *Anal. Chem.* **1995**, *67*, 4139-4144.

(12)   Golding, R.E.; Whitall, R.M., Li, L. *Proceedings of the 43th ASMS Conference on Mass Spectrometry and Allied Topics*; Atlanta, GA, May 21-26, 1995; p 1223.

(13)   Li, L.; Golding, R.E.; Whittal, R.M. *J. Am. Chem. Soc.* **1996**, *118*, 11662-11663.

(14)   Whittal, R. M.; Keller, B. O.; Li L. *Anal. Chem.* **1998**, *70*, 5344-5347.

(15)   Dai, Y. Q.; Whittal, R. M.; Li, L. *Anal. Chem.* **1999**, *71*, 1087-1091.

(16)   Dai, Y. Q.; Whittal, R. M.; Li, L. *Anal. Chem.* **1996**, *68*, 2721-2725.

(17)   Whittal, R. M.; Li, L. *Anal. Chem.* **1995**, *67*, 1950-1954.

(18)   Krause, E.; Wenschuh, H.; Jungblut, P.R. *Anal. Chem.* **1999**, *71*, 4160-4165.

(19)   Keller, B.O.; Li, L. *J. Am. Soc. Mass Spectrom.* **2000**, *11*, 88-93.

(20)   Relative abundances were calculated using MS-Isotope of the Prospector package at http://prospector.ucsf.edu.

(21)   Gnedenko, B. W. *Lehrbuch der Wahrscheinlichkeitsrechnung*; Verlag Harri Deutsch: Frankfurt am Main, 1978; Vol. 4.

(22)   Burle Electro-optics website at http://www.kore.co.uk/mcp-faq.htm.

(23)   Geno, P. W.; Macfarlane, R. D. *Int. J. Mass Spectrom. Ion Process.* **1989**, *92*, 195-210.

(24)   Personal communication, Dr. Scot Weinberger, Ciphergen, Fremont, CA, USA.

(25)   Marshall, A. G.; Senko, M. W.; Li, W.; Li, M.; Dillon, S.; Guan, S.; Logan, T. M. *J. Am. Chem. Soc.* **1997**, *119*, 433-434.

(26)   Cotter, R. J. *Time-of-Flight Mass Spectrometry: Instrumentation and Applications in Biological Research;* American Chemical Society: Washington, DC, 1997.

(27)   Medzihradszky, K. F.; Campbell, J. M.; Baldwin, M. A.; Falick, A. M.; Juhasz, P.; Vestal, M. L.; Burlingame, A. L. *Anal. Chem.* **2000**, *72*, 552-558.

(28)   Winburn, D. C. *Lasers*; Marcel Dekker Inc.: Cincinnati, Ohio, 1987; Vol. 22.

41

Chapter 3

Nanoliter Chemistry Combined with Microspot Matrix-Assisted Laser Desorption/Ionization Time-of-Flight Mass Spectrometry and Its Application to Peptide Mapping of Proteins from Single Cell Lysates[a]

3.1 Introduction

Chapter two describes the nanoliter chemistry station and its use for sensitive peptide analysis. As outlined in the introductory chapter, molecular weight determination is only a first step towards protein identification and further characterization. Several reaction steps are usually required for unambiguous identification or further protein characterization. Miniaturization and thus significant reduction of sample volume is desirable for a number of reasons. For example, in the early stage of a disease such as cancer, only a small population of normal cells undergoes transformation and a change in the proteome of these new tumor cells is expected.[1,2] In cell research, numerous cell lines derived from tumors in *in vitro* cell culture systems have been used as sources for a large number of cells. These cells are a uniform type and play an essential role in the process of investigating cell functions. However, because of differences in the cell growth environment conditions between the intact organism and the cell culture, great care must be taken in extrapolating the results of *in vitro* experiments to the reality of *in vivo*.[1,2] This is particularly true for proteins, whose identity, abundance and expression can vary greatly at different stages of cell development. Thus, analyzing the primary

---

[a] A form of this chapter is published as: R. M. Whittal, B. O. Keller, L. Li *"Nanoliter Chemistry Combined with Mass Spectrometry for Peptide Mapping of Proteins from Single Mammalian Cell Lysates" Anal. Chem.* **1998**, *70*, 5344-5347.

Dr. Randy Whittal collected the mass spectra of the standard proteins and the spectrum of the lysate digest from the normal single red blood cell.

42

cells isolated from a tissue, is the only way to provide a direct correlation in the change in protein content and identity with a biological event, such as the progression of a disease, without including potential cell culture artifacts. Such analysis requires very sensitive methods, because the number of tumor or other disease cells available for investigation from a tissue is often limited.

At present, several tracer techniques involving radiolabeling, immunoassay, and fluorescence tagging have been employed to provide information on the distribution of usually known proteins in a small number of cells or a single cell.[1,2] Miniaturized detection schemes based on electrochemical, laser-induced fluorescence detection and, more recently, mass spectrometry have shown great promise in analyzing cellular components, including peptides and proteins, in single cells.[3-12] However, unequivocal identification and characterization of trace amounts of unknown or modified proteins in very small volumes associated with tissues, single cells, subcellular compartments, and exocytosis still remain a formidable task. In this chapter, an analytical approach is described which combines three rapidly developing techniques to characterize attomole quantities of proteins from small-volume samples including single red blood cells: nanoliter or subnanoliter chemistry, matrix-assisted laser desorption /ionization time-of-flight mass spectrometry (MALDI-TOF MS), and protein database searching.

Over the past decade or so, rapid advances in mass spectrometry have made it a very sensitive tool for the detection of peptides and proteins. High sensitivity in MS is generally attained by reducing the sample presentation volume to improve the sampling efficiency. Low-volume electrospray ionization (ESI) [13,14] and microspot MALDI [9,15-17] have been shown to provide attomole detection of peptides and proteins. As demonstrated in proteome analysis by MS,[18] protein identification and characterization of posttranslational modifications often require a number of chemical and/or enzymatic reactions to be carried out on a protein of interest prior to mass spectrometric analysis. Carrying out protein reactions in very dilute solutions with concentrations of less than 10^{-8} M poses a number of difficulties; including severe autolysis in the case of enzyme digestion and adsorption loss onto the sample container. However these difficulties are largely overcome by using a moderate concentration of sample solution in a small volume so that the total amount of proteins required in the analysis is still small. Thus, the key to

43

success of characterizing trace amounts of proteins lies in the development of a low-volume sample presentation to a mass spectrometer.

Chemical reactions at nanoliter volumes can be performed either using microfabricated wells on a supporting substrate such as a chip[19] or using fused silica capillary tubes.[20] The latter offers the advantages of easy control of solvent composition (e.g. by varying the solvent evaporation rate) and readiness of transferring a fluid to other devices for detection.

3.2 Experimental

3.2.1 Materials. Bovine serum albumin, cytochrome c from horse heart, α-cyano-4-hydroxycinnamic acid (4-HCCA), n-octyl-β-D-glucopyranoside and trypsin (98%, L-1-Tosylamide-2-phenylethyl chloromethyl ketone (TPCK) treated for reduction of chymotrypsin activity) were from Sigma-Aldrich Canada (Oakville, Ontario). 4-HCCA was recrystallized from ethanol (95%) at 50°C. The normal blood sample was from Dr. Randy Whittal and the blood sample from a patient with sickle cell disease was a gift from Mr. T. Higgins of Dynacare-Kasper Medical Laboratories (Edmonton, Alberta, Canada). Glassclad 18, used to deactivate the fused-silica capillaries, was from United Chemical Technologies (Bristol, PA, USA).

3.2.2 In-Capillary Sample Preparation. The nanoliter chemistry station and its use for sample uptake and deposition onto a matrix-covered target has already been explicitly described in chapter two. For this work, we used a 20-μm-ID fused silica capillary, which had also been deactivated with the glassclad silylation fluid to reduce sample adsorption. As illustrated in Figure 3.1, a measured volume of a sample (usually 100-200 pL), determined by the sample plug length in the capillary using a calibrated recticle in the microscope, is withdrawn with the connected syringe under video microscopic observation. This subnanoliter sample resides inside the capillary and ~1 mm away from the capillary tip. The problem of in-capillary mixing of sample and reagent was overcome by initial sample solvent evaporation. The solvent in the sample is allowed to gradually evaporate (~3 min.) until a coaxial hole in the sample is formed. At this point, the syringe plunger can be withdrawn to take up 200-500 pL of an enzyme or chemical

44

(1) Sampling

Capillary

Sample

(2) Partial Drying

Solvent Vapor

(3) Reagent Loading

Enzyme
Solution

(4) Reaction (Digestion)

Holder

Parafilm

(5) Microspot Deposition

MALDI Probe

Matrix Film

Microscope Observation [40-60x]
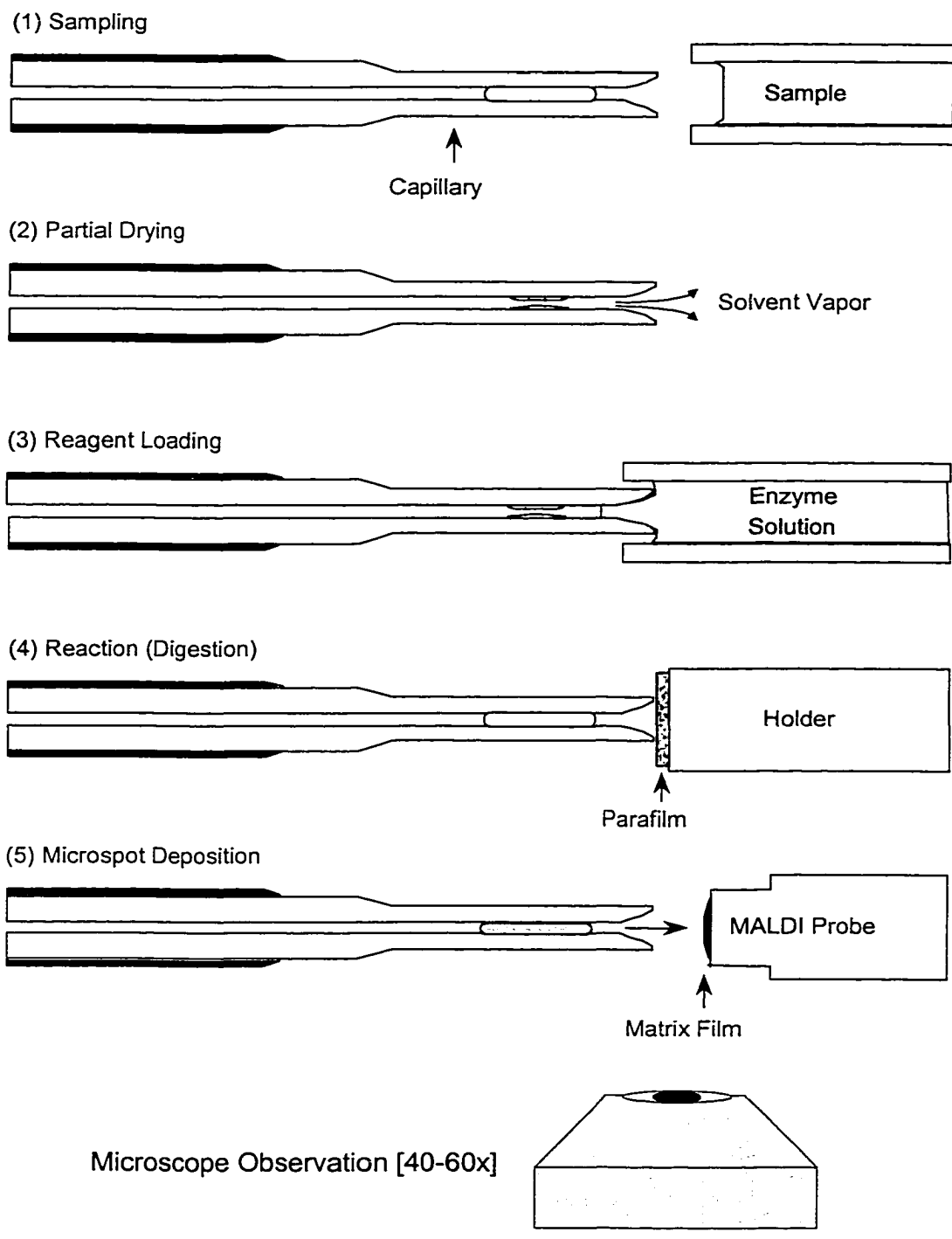
Figure 3.1   Sample preparation with the nanoliter-chemistry station.

45

reagent from a reagent vial. During the uptake of the reagent, the sample is not moved. Once the protein and the reagent are mixed, Parafilm, covering the capillary tip prevents solvent evaporation (solvent evaporation on the other end of the solution is minimal). The reactions can be allowed to proceed over several hours in the capillary, although 10-30 min of reaction time is adequate for most applications. If desired, the above reagent-loading procedures are repeated to carry out additional reactions using different chemical reagents, as is shown in subsequent chapters.

3.2.3 MALDI-TOF Analysis and Data Processing. After the final reaction step the sample digest is directly deposited onto a matrix-covered MALDI target. The matrix layer is prepared according to a previously reported two-layer method.[21] Prior to loading the sample and performing the reaction, ~0.5 nL of ethanol/water (1:1) is loaded into the capillary. This serves two purposes: first washing out the analyte species that may be adsorbed onto the capillary and, second, to wash the sample once it is delivered onto the matrix to reduce the intensity of the salt adduct ions in the mass spectra. After sample deposition from a close distance (~50 μm) the probe is inserted into a linear time-lag focusing MALDI-TOF mass spectrometer for analysis.[21] Data acquisition is done using Hewlett-Packard instrument software and a LeCroy 9350 M oscilloscope. Data is then further processed with the Igor Pro software package (Wavemetrics, Lake Oswego, OR, USA). Protein identification is performed with the MS-FIT program using the Swiss-Prot protein database (http://prospector.ucsf.edu).

3.3 Results and Discussion

The use of nanoliter chemistry as opposed to conventional microliter or larger reaction volumes, provides the opportunity to investigate trace amounts of proteins. For instance, with this system, we can routinely perform peptide mapping for the identification of proteins in a database with less than 500 attomoles of sample. This is generally about 2-3 orders of magnitude more sensitive than any other mass spectrometric techniques reported for protein identification by peptide mapping.[13,18] As an example, Figure 3.2 shows the MALDI mass spectra of the tryptic digests of

46
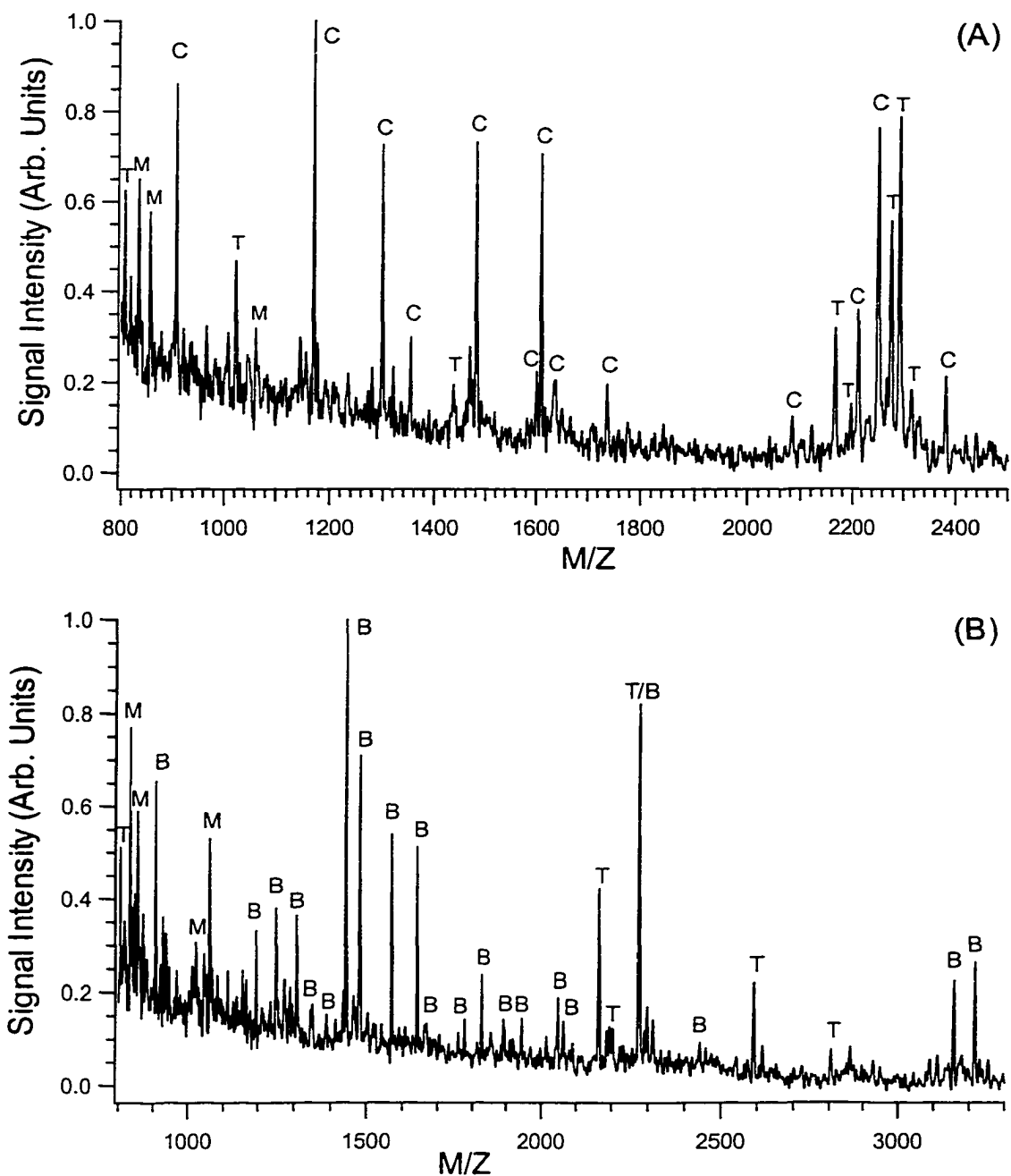
Figure 3.2 MALDI mass spectra of tryptic digests of (A) 80 amol of cytochrome c and (B) 450 amol of BSA. Specific peaks for matrix clusters, trypsin autolysis, cytochrome c, and BSA peptide fragments are labeled M, T, C, and B, respectively.

47

cytochrome c and bovine serum albumin (BSA). In this case, the cytochrome c was 0.4 μM and the BSA was 1.5 μM in 0.02 M NH_4HCO_3 buffer and 0.5 % n-octyl-β-D-glucopyranoside. The surfactant was added to make sample handling in the small i.d. capillaries easier due to reduced surface tension. A 2 μM trypsin solution was prepared in 0.04 M NH_4HCO_3 buffer and 0.5% n-octyl-β-D-glucopyranoside. After allowing the digestion to take place for ~10 min in the capillary, the sample digest was then deposited onto the matrix-coated target and analyzed. As Figure 3.2A shows, even with a sample loading of 80 amol, 12 peptide fragments were assigned to this protein and the detected peptides cover more than 80% of the primary amino acid sequence of cytochrome c. For the tryptic digest of 450 amol of BSA, 20 peptide fragments were assigned to this protein which cover 45% of the primary amino acid sequence. The current limit needed for peptide mapping appears to be mainly governed by enzyme autolysis. The use of immobilized enzymes on the capillary wall or in small particles suspended in a reagent may circumvent this problem.

The peptide fragments detected in both panels A and B of Figure 3.2 are sufficient for protein identification using a peptide mass database. Protein databases from different organisms and cell lines are being rapidly developed.[18] These databases combined with mass spectrometric analysis of enzyme digests of proteins should serve as an excellent tool for protein identification.

Nanoliter chemistry combined with MS can be used to interrogate small volume samples such as in single-cell analysis. This is illustrated in Figure 3.3 for the identification of hemoglobin variants in a single red blood cell. A red blood cell is typically 8 μm in diameter, 2 μm thick, has a total cellular volume of 87 femtoliters,[3] and contains ~450 amol of hemoglobin. There are over 600 human hemoglobin variants identified, with some causing serious illnesses.[23,25] Sickle cell disease is among the most common hemoglobin-based illnesses.[23] In normal hemoglobin, residue 6 in the β chain is glutamic acid. However in sickle cell disease, hemoglobin in the homozygous state has valine as residue 6 instead. Figure 3.3 shows the MALDI mass spectra of the tryptic digests of the single-cell contents from a normal red blood cell and a sickle cell Hb S.

Red blood cell sample preparation and single-cell loading have been described

48
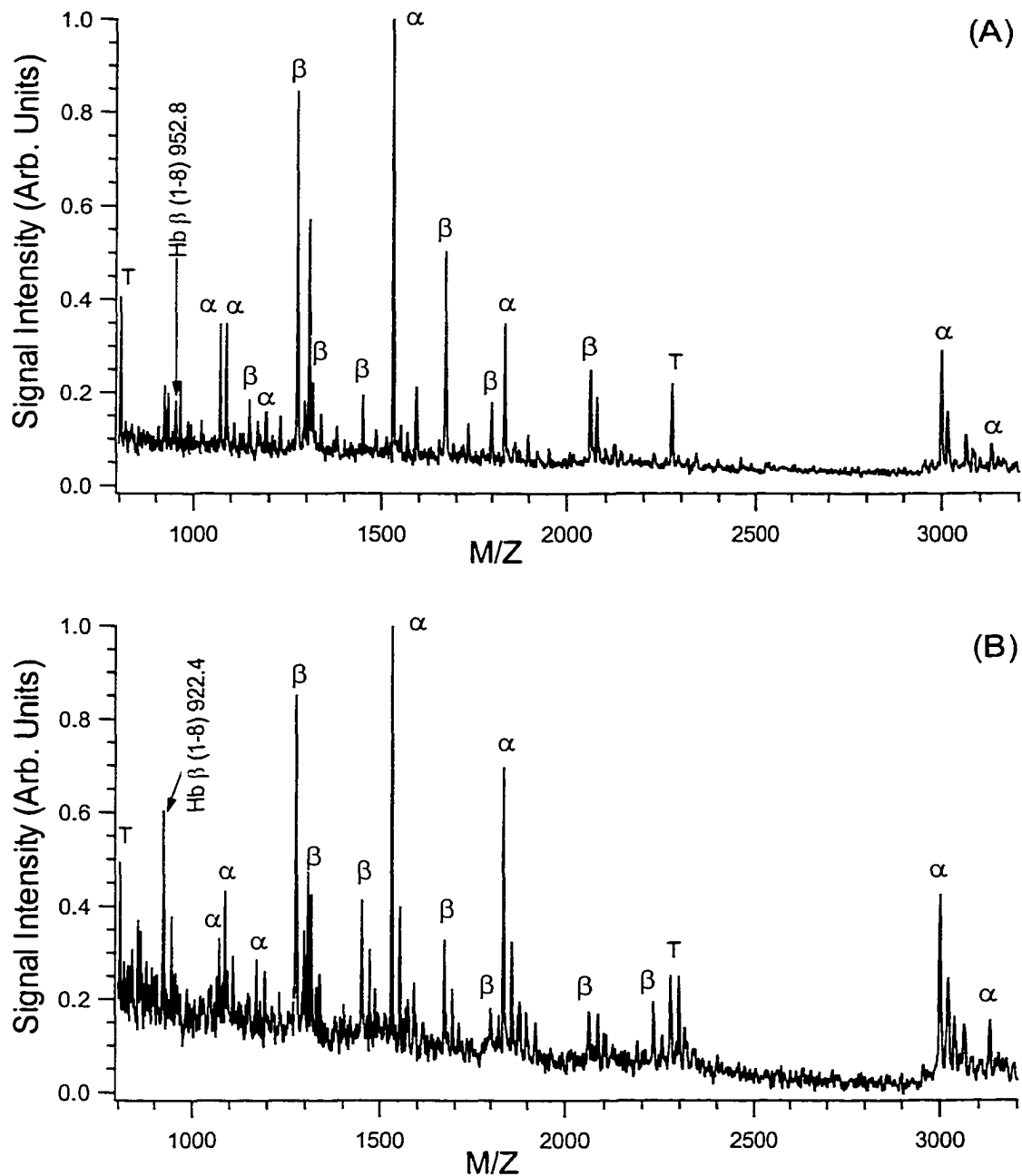
Figure 3.3   MALDI mass spectra of tryptic digests of single cell lysates from (A) a
normal red blood cell and (B) a red blood cell of a patient with sickle cell
disease. The substitution of only one amino acid is detected in the peptide
fragment, which refers to residues 1-8.   Peptide fragments from the
hemoglobin α or β chain are labeled α or β, respectively.

49

in more detail earlier.[9] In brief, red blood cells were obtained and stored in an isotonic saline solution, 0.85% NaCl by weight. A cell suspension with a concentration of 10-14 cells/nL was prepared. For single-cell loading onto the capillary, the suspension volume withdrawn was ~100 pL. The exact number of cells loaded was verified using a higher microscope magnification [200x]. The cell suspension inside the capillary was allowed to dry and a 2 μM trypsin solution was drawn into the capillary, and resulted in cell lysis and digestion of the cell contents. The digest was deposited onto the MALDI probe for mass analysis. As a control experiment, the sample-handling procedure was followed utilizing an aliquot of suspension with no cells present. No peptide peaks from hemoglobin were detected.

The mass spectra shown in Figure 3.3 display a number of peptide peaks from hemoglobin, covering over 60% of the amino acid sequences of the α or β chains. The peak at m/z 952.8 in Figure 3.3A is from the peptide fragment β 1-8. A similar fragment ion is also observed in Figure 3.3B from the sickle cell; but the mass is shifted 30 u lower, corresponding to the peptide fragment β 1-8 from the mutated hemoglobin S. The mass measurement accuracy is generally better than 50 ppm with external calibration (bradykinin and oxidized insulin chain B were used as the calibrants). No peaks in the mass spectra shown in Figure 3.3 can be assigned to peptides from the second most abundant protein in red blood cells, i.e., carbonic anhydrase (7 amol/cell). This is also the case for multicell experiments. However, if carbonic anhydrase is used as the only analyte, tryptic digestion can be readily carried out with the same protocol as that used for red blood cells. It appears that, in red blood cells containing hemoglobin and carbonic anhydrase with a concentration difference of ~64 times, only the most abundant protein undergoes efficient digestion. This is understandable from enzyme kinetics, which is governed by the substrate concentration. Any possible digestion products from carbonic anhydrase may fall below the detection limit of the current microspot MALDI system. It is clear that for studying more complex protein systems, a separation and concentration stage are required before carrying out nanoliter chemistry.

It should be noted that ~30 individual single-shot spectra were summed to produce the spectra shown in Figure 3.3. While MS/MS was not feasible with the linear TOF instrument used in this work, it should be entirely possible to generate fragment ion

50

spectra from postsource decay of selected peptide ions shown in Figure 3.3 with current reflectron MALDI-TOF technology.[25,26] The addition of MS/MS capability should be particularly useful for the characterization of posttranslational modifications.

As Figure 3.3 illustrates, it is possible to use above described approach for peptide mapping at the single-cell level. Apart from red blood cells, the detection sensitivity of the current method should be sufficient to analyze neuropeptides and proteins at different regions of neuron cells. To study low-abundance proteins in cells, cell sorting techniques can be used to isolate the individual type of cells from a tissue. The number of cells required to perform an analysis in nanoliter chemistry/MS should be significantly reduced. In addition, it should be feasible to adapt many strategies and methods currently used for handling larger volumes of samples to this combined nanoliter-chemistry/MS approach. In particular, the addition of a chemical separation stage such as 2D gel and capillary electrophoresis (CE) to the station will extend the application of this approach to more complicated protein mixtures. CE is well suited for the study of single cells or a few cells. [3-8,11] The separated protein components in CE can be collected in an array of small capillary tubes and subsequently loaded to the nanoliter-chemistry station for reaction and analysis. Since one analysis consumes less than 1 nL of the sample, multiple analyses, including protein molecular weight determination, peptide mapping using different enzymes, C-terminal or N-terminal ladder sequencing, and MS/MS of selected ions, can be potentially carried out from a total sample solution of several nanoliters with or without preconcentration. Automation and parallel processing of the sampling and reaction stages are also possible. This nanoliter-chemistry/MS approach should play an important role in the characterization of biological systems where the amount of the sample available is limited, such as studying protein variations and their functions *in vivo*.

3.4 Literature Cited

(1)   Alberts, B.; Bray, D.; Lewis, J.; Raff, M.; Roberts, K.; Watson, J. D. *Molecular Biology of the Cell*, 3rd ed.; Garland: New York, 1994.

(2)   Cooper, G. M. *Oncogenes*, 2nd ed.; Jones and Bartlett: Boston, 1995.

51

(3)   Yeung, E. S. *Acc. Chem. Res.* **1994**, *27*, 409.

(4)   Lilard, S. J.; Yeung, E. S.; Lautamo, R. M. A.; Mao, D. T. *J. Chromatogr.*, A **1995**, *718*, 397.

(5)   Kennedy, R. T.; Oates, M. D.; Cooper, B. R.; Nickerson, B.; Jorgenson, J. W. *Science* **1989**, *256*, 57.

(6)   Shear, J. B.; et al. *Science* **1994**, *267*, 74.

(7)   Ewing, A. G.; Mesaros, J. M.; Gavin, P. F. *Anal. Chem.* **1994**, *66*, 527A.

(8)   Kennedy, R. T.; Huang, L.; Aspinwall, C. A. *J. Am. Chem. Soc.* **1996**, *118*, 1795.

(9)   Li, L.; Golding, R. E.; Whittal, R. M. .*J. Am. Chem. Soc.* **1996**, *118*, 11662.

(10)   Hofstadler, S. A.; Severs, J. C.; Smith, R. D.; Swanek, F. D.; Ewing, A. G. *Rapid Commun. Mass Spectrom.* **1996**, *10*, 919.

(11)   Li, K. W.; et. al. *J. Biol. Chem.* **1994**, *269*, 30288.

(12)   van Strien, F. J. C.; et al. *FEBS Lett.* **1996**, *379*, 165.

(13)   Wilm, M.; et al. *Nature* **1996**, *379*, 466.

(14)   Valaskovic, G. A.; Kelleher, N. L.; McLafferty, F. W. *Science* **1996**, *273*, 1199.

(15)   Jespersen, S.; et al. *Rapid Commun. Mass Spectrom.* **1992**, 7, 142.

(16)   Solouki, T.; Marto, J. A.; White, F. M.; Guan, S. H.; Marshall, A. G. *Anal. Chem.* **1995**, *67*, 4139.

(17)   Zhang, H.; Caprioli, R. M. *J. Mass Spectrom.* **1996**, *31*, 690.

(18)   Wilkins, M. R.; et. Al. *Biotechnol. Genet. Eng. Rev.* **1995**, *13*, 19 and references therein.

(19)   Clark, R. A.; Ewing, A. G. *CHEMTECH* **1998**, *28*, 20.

(20)   Chang, H. T.; Yeung, E. S. *Anal. Chem.* **1993**, *65*, 2947.

(21)   Dai, Y.; Whittal, R.M.; Li, L. *Anal. Chem.* **1996**, *68*, 2721-2725.

(22)   Whittal, R. M.; Li, L. *Anal. Chem.* **1995**, *67*, 1950.

52

(23)   Bunn, H. F.; Forget, B. G. *Hemoglobin: Molecular, Genetic and Clinical Aspects*;
         W. B. Saunders: Philadelphia, 1986.

(24)   Shackleton, C. H. L.; Witkowska, H. E. *Anal. Chem.* **1996**, *68*, 29A.

(25)   Woods, A. S.; Little, D. P.; Cotter, R. J. *Proceedings of the 45th ASMS Con-
         ference on Mass Spectrometry and Allied Topics*, Palm Springs, CA, June 1-5,
         1997; p. 1323.

(26)   Fenselau, C. *Anal. Chem.* **1997**, *69*, 661A.

Chapter 4

Discerning Matrix-Cluster Peaks in MALDI-TOF Mass Spectra[a]

4.1 Introduction

As described in chapter three, peptide mass fingerprinting by MALDI-TOF mass spectrometry has become an important method for identification of proteins in a database. The quality of MALDI mass spectra has a direct influence on database searchability and the outcome of the data search.[1] It is desirable to obtain mass spectra that display a number of peptide peaks reflecting the specific digestion of a given enzyme. Aside from optimization of the enzyme digestion process to generate enzyme-specific peptide fragments, the sample/matrix preparation conditions for MALDI analysis of the resulting digest is also very critical to obtain useful mass spectra. This is particularly true in the case of dealing with a small amount of protein sample. Since the digestion process itself involves the use of relatively large amounts of salts and buffers, the protein digest, even from a purified protein, is often contaminated with salts. The introduction of a purification step prior to MALDI analysis is very useful to obtain high quality mass spectra of protein digests. However, when the amount of protein sample is low, such as in the case of low volume protein fractions collected from capillary electrophoresis and low abundance protein spots from a 2D-gel, a rigorous purification step may not always be applicable. This is especially true for highly sensitive techniques where the analyte

---

solution is directly deposited onto the matrix layer and thus most of the analyte resides in a very thin layer closer to the matrix surface. Several techniques using direct deposition have been reported in recent years.[2-8] The issue of sample loss vs. purification must be carefully weighed. Even with compatible purification, the salt content is higher for protein digests resulting from a small amount of proteins compared to those obtained from a large amount of proteins. Thus the analysis of protein digests from a small amount of proteins is prone to chemical background interference.

One of the major sources of background interference is from matrix-cluster formation. Many experimental factors can affect the extent of matrix-cluster formation, which include the type of matrix used, the salt content, pH, the relative amount of analyte, and the laser power. For the analysis of protein digests, α-cyano-4-hydroxycinnamic acid (4-HCCA) is widely used as the matrix because of its ability to generate mass spectra with high sensitivity and resolution.[9] For the analysis of a protein digest resulting from at least a picomole amount of proteins, mass spectra of the digest usually do not display strong matrix peaks with m/z above 550. Herein we show that matrix-clusters can cause interference in analyzing *dilute* peptide mixtures, i.e. typically in the medium to low nanomolar range, depending on the extent of contamination. The spectral pattern of cluster ions and their relative intensities cannot be readily predicted, causing difficulty in discerning these peaks from the actual peptide peaks. However, it is shown that these clusters are mainly from the combination of matrix, potassium, and sodium ions. Thus their masses can be calculated using a simple scheme. Knowing the masses of the possible cluster ions, the peaks from these ions can be discerned from the peptide peaks. Being able to discern matrix clusters from analyte is generally useful, not only for peptide mixtures. An example will be given for a routine sample submitted for MALDI analysis to the departmental mass spectrometry laboratory.

4.2 Experimental

4.2.1 Materials and MALDI Analysis. Bovine lactoferrin (M.W. ~80 kDa), dithiothreitol (DTT), iodoacetamide, 2,5 dihydroxybenzoic acid (DHB), α-cyano-4-hydroxycinnamic acid (4-HCCA) and trypsin (98%, L-1-Tosylamide-2-phenylethyl chloromethyl ketone (TPCK) treated for reduction of chymotrypsin activity) were from

55

Sigma-Aldrich Canada (Oakville, Ontario). 4-HCCA was recrystallized from ethanol (95%) at 50°C.

Mass spectra of protein digests and matrix clusters were collected on a home-built linear time-lag focusing MALDI-TOF mass spectrometer, equipped with a 337 nm laser having a 3 ns pulse width (model VSL 337ND, Laser Sciences Inc., Newton, MA, USA). This home-built instrument has been described in detail elsewhere.[10] In general 150-200 laser shots (3-5 μJ pulse energy) were averaged to produce a mass spectrum. Spectra were acquired and processed with Hewlett-Packard supporting software and reprocessed with the Igor Pro software package (WaveMetrics, Inc., Lake Oswego, OR). Each spectrum was normalized using the most intense signal.

4.2.2 Macro Digest Preparation. For the macro digest of lactoferrin, 13 μL of 1.4 μg/μL lactoferrin was pipetted into a 0.6 mL polypropylene sample vial (Rose Scientific, Edmonton, Alberta, Canada; siliconized type for reduced sample adsorption to container walls). 0.6 μL of 1 M NH_4HCO_3 and 0.6 μL of 250 mM DTT were added. After incubation for 25 minutes at 37°C, the vial was cooled down to room temperature and 0.6 μL of 400 mM iodoacetamide was added. After incubation in the dark for another 25 min at room temperature, 0.2 μL of a 3.5 μg/μL freshly prepared trypsin stock solution were added and the resulting 15 μM lactoferrin solution in 0.04 M digestion buffer was incubated overnight at 37°C. Dilution of the digest for analysis varied and is described in Figures 4.1 and 4.2. For on-target washing, distilled water at room temperature was used. Generally 0.5 μL of dist. water was deposited onto the sample spot and left for ~30 seconds before being blown off with pressurized air.

4.2.3 In-Capillary Digest and Microspotting. For in-capillary digestion, a nanoliter chemistry station was used.[11] The sample handling procedures and sample deposition onto the matrix-covered probe tip have been described in detail in chapter three. Briefly, a 20-μm-ID capillary tube connected to a syringe was used to draw a sub-nanoliter volume of a protein sample or reagents. Initially, a 200-300 pL volume of 45 mM DTT in 0.04 M NH_4HCO_3 was drawn into the capillary and allowed to dry close to the capillary entrance. Then a 100-200 pL volume of the protein sample was loaded and the capillary closed with a piece of Parafilm. After a reaction time of ~5 min the mixture was allowed to dry again close to the capillary entrance. A 200-300 pL volume of 100

56

mM iodoacetamide in 0.04 M NH_4HCO_3 was drawn into the capillary and the capillary entrance was closed again. After ~10 min reaction time, the mixture was allowed to dry and a 100-200 pL volume of freshly prepared 2 μM trypsin in 0.04 M NH_4HCO_3 was loaded. Sufficient digestion was usually achieved after 10-20 min. Before deposition of the final mixture onto the matrix-covered target, a 100-200 pL volume of saturated 4-HCCA in 40% methanol/water (v/v) was loaded into the capillary. The sample mixture and matrix solution were thereby separated by a small air gap. Both solutions were then simultaneously deposited onto a matrix-covered probe tip. Matrix layer formation was performed according to the two-layer matrix/sample preparation method.[4,12] To produce a very thin first layer, about 1 μL of a 5 mg/mL solution of 4-HCCA in 80% acetone/methanol (v/v) was deposited on the probe. After drying, a second layer of 0.4 μL of 4-HCCA saturated in 35% methanol/water (v/v) was deposited and allowed to dry. The sample/matrix mixture from the nanoliter sample preparation procedure was deposited on the probe as the third layer, with no further washing.

4.3 Results and Discussion

In routine MALDI-TOF analysis of tryptic digests of proteins using picomole amounts, interferences of matrix-cluster peaks from 4-HCCA can be eliminated by rigorous washing procedures in the two-layer matrix/sample preparation. This is demonstrated in Figure 4.1. An untreated digest, which is 100 times diluted in 150 mM saline solution, produces only matrix cluster peaks; specific lactoferrin peptide fragments are not identified. After the on-probe washing procedure, many specific lactoferrin peptide fragments are detectable and interference from matrix-clusters is almost eliminated. In this case the sample loss due to washing is largely compensated by the larger gain of the peptide signals. However, when dilute and/or heavily contaminated peptide mixtures are analyzed, matrix-cluster peaks can create a severe problem for accurate peptide identification. Figure 4.2 shows the MALDI spectra of the same tryptic digest as in Figure 4.1, however this time the digest was diluted 1200 fold with distilled water instead of 150 mM NaCl. For the unwashed preparation, matrix clusters interfere with peptide signals and the assignment of peaks to specific protein fragments becomes

57

very difficult. As is shown in the other two spectra, washing can decrease this interference, but signals from specific protein fragments can also be lost.

in 150 mM NaCl, no wash   (A)

after 3 washes   (B)
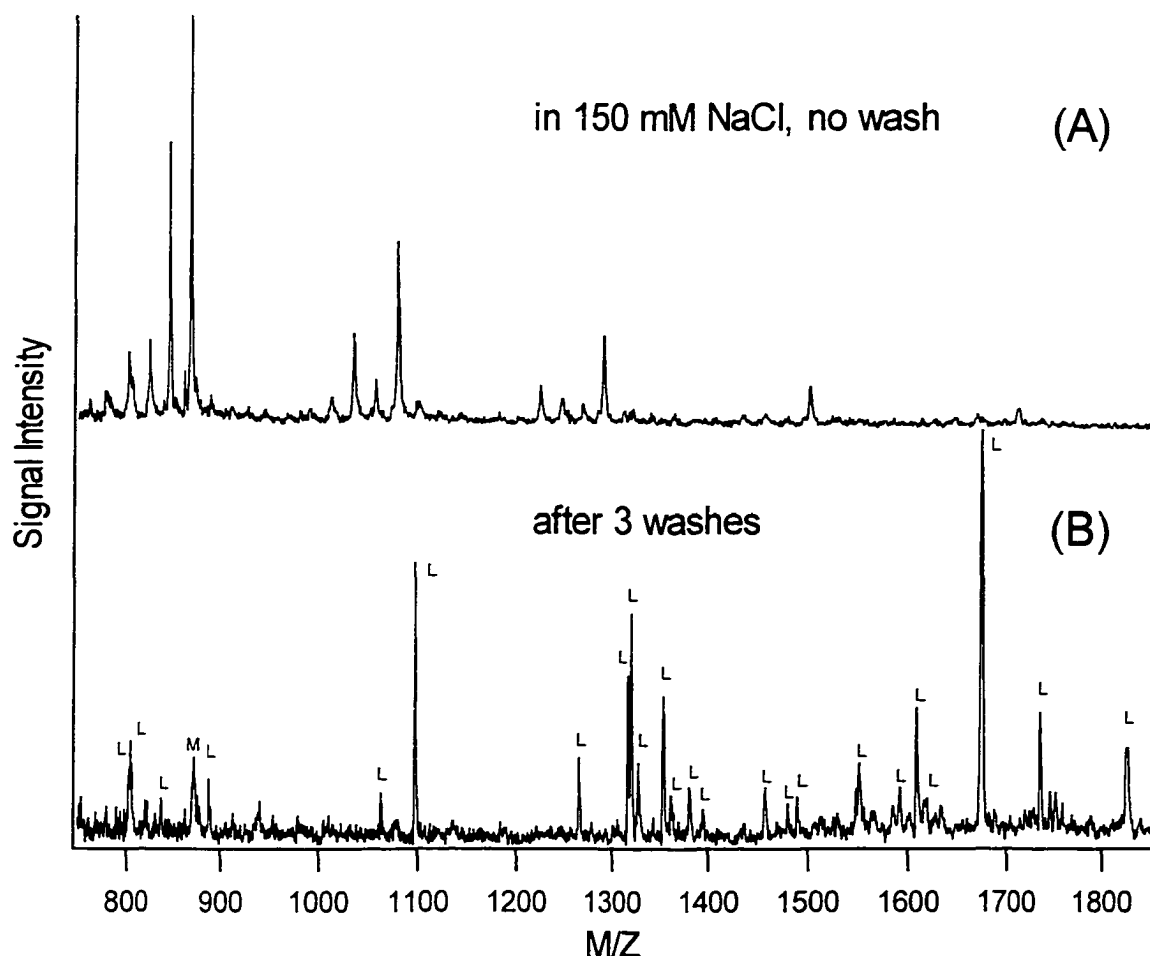
Figure 4.1 MALDI mass spectra of a tryptic digest of an aqueous 15 μM lactoferrin solution as described in the Experimental Section. Spectra of the digest with 100-fold dilution in 150 mM NaCl (physiological saline) (i.e., ~150 nM of digest peptides assuming 100% digestion). For both spectra 0.2 μL (30 fmol of total protein) of the diluted digest were directly deposited onto the 4-HCCA layer. (A) not washed (B) washed 3 times as described in the Experimental Section. Specific peaks from matrix clusters and lactoferrin peptide fragments are labeled M, and L, respectively.

Other than interference from trypsin autolysis, the matrix cluster peaks are not reproducible and their appearance and relative intensities in the spectra cannot be predicted. Note that in general the trypsin autolysis signals can be readily discerned from

58

the protein digest peptide peaks by perfroming a control experiment where all conditions are the same as in the actual protein digestion except no protein is added. In Figures 4.1 and 4.2 trypsin autolysis peaks are not detected, since the molar ratio of trypsin to protein is ~1:8 and thus autolysis peptides are not very abundant in the diluted digests. This is different in our microspot experiments where equal or excess amounts of trypsin compared to analyte are added. The most predominant autolytic peptides are the following fragments with masses (MH^+) 805.9, 907.1, 1112.3, 1154.3, 1434.7, 2164.3 and 2274.6. Nevertheless, since the course and extent of autolysis depends on experimental conditions, blank experiments remain a necessity.
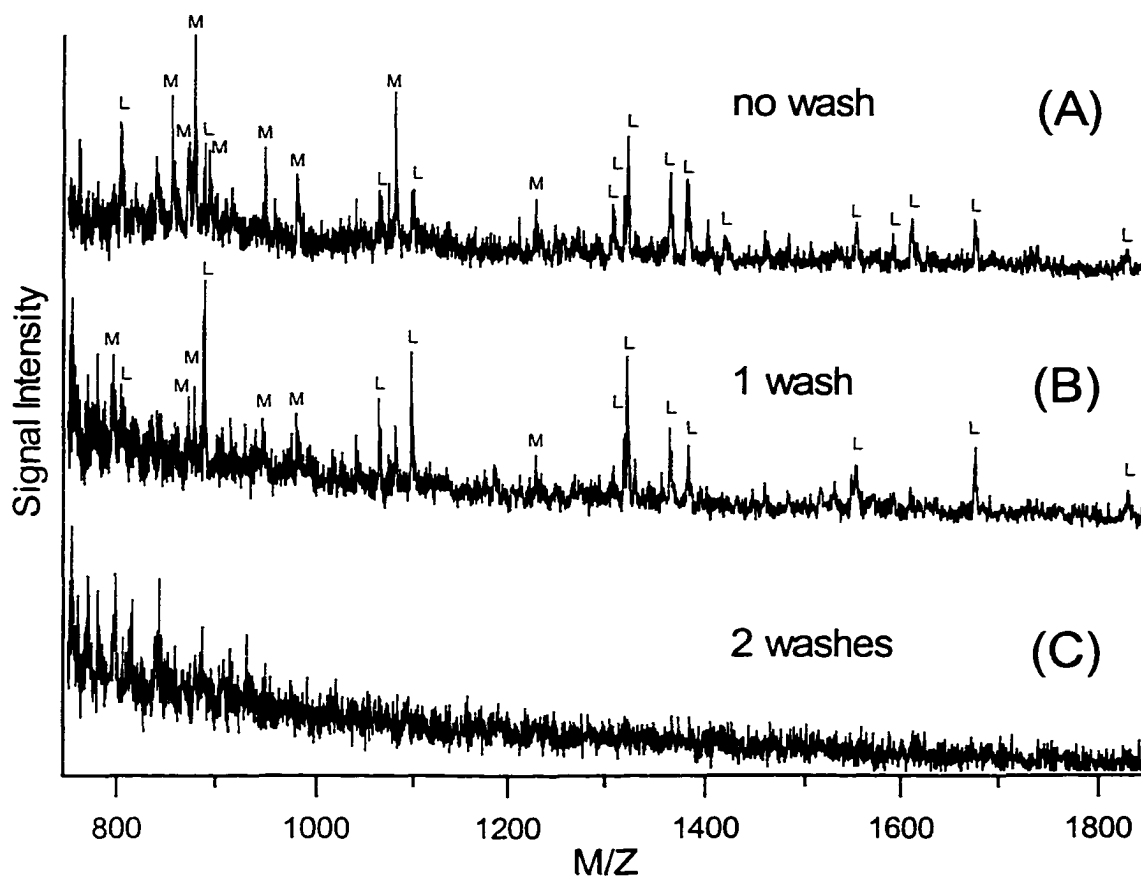
Figure 4.2   Spectra of the same digest as in Figure 4.1 with 1200-fold dilution in distilled water. For each of the three spectra, 0.2 μL of sample (2.5 fmol of total protein) were directly deposited onto the 4-HCCA layer. Specific peaks from matrix clusters and lactoferrin peptide fragments are labelled M and L, respectively. (A) not washed (B) once washed, and (C) twice.

59

We found that matrix cluster formation can be influenced by changing the sodium and potassium salt content in the matrix solution before the matrix is deposited for crystallization on the probe tip. Also, basic pH conditions lead to enhanced matrix cluster formation. Similar observations were reported for calcium adducts with dihydroxybenzoic acid (DHB) as matrix.[13] Sodium and potassium salts are common impurities found in 4-HCCA and many protein samples, it is therefore not surprising that these contaminants play an important role in matrix-cluster formation. Different matrix preparations with deliberately altered concentrations of these salts lead to different cluster peaks, but there are some salient features. Figure 4.3 shows three mass spectra of typical matrix-clusters from three different matrix preparations.
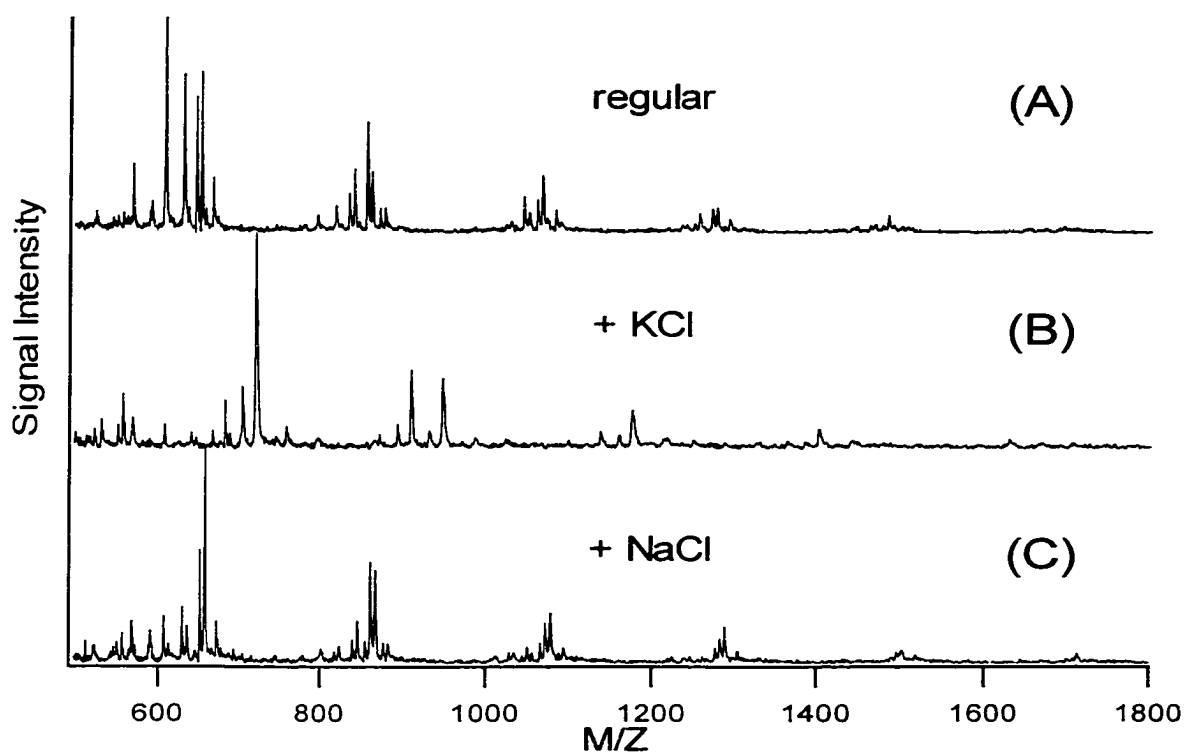
Figure 4.3   Mass spectra of 4-HCCA matrix clusters obtained under different matrix preparation conditions. (A) Untreated matrix from conventional two-layer preparation as described in the text. (B) 5 μL of second-layer 4-HCCA solution was first mixed with 5 μL 0.1 M NH$_4$HCO$_3$ then 5 μL of 1 % KCl was added. To neutralize the solution, 2 μL of a slurry of precipitated 4-HCCA were finally added and the solution centrifuged. As in the conventional preparation, 0.4 μL of this mixture was deposited onto a first-layer of 4-HCCA matrix. (C) Same preparation as in (B), except the 1% KCl solution was replaced with a 1% NaCl solution.

60

Cluster peaks always appear in assemblies of several members, with one or two members in the center having the highest intensity. Assemblies of cluster peaks are usually separated by 189 - 227 mass units, which represents the molecular weight range of the matrix 4-HCCA plus a proton, sodium, or a potassium ion. Generally the intensity of cluster peaks decreases with increasing mass. Interferences can appear in the mass region up to ~2000 u, which is unfortunately the region of interest for peptide mass mapping.

There are slight differences in the spectral patterns of Figure 4.1A and 4.3C, although both preparations were done with physiological saline solution. These differences are most likely due to the different methods of preparation. For Figure 4.1A the saline solution was deposited directly onto the second 4-HCCA layer, whereas for Figure 4.3C the saline solution was mixed in a basic environment (~pH 8.5) with the second matrix-solution, then acidified prior to deposition onto the first 4-HCCA layer. This further underlines the unpredictability of matrix cluster appearance. However, when looking at the observed masses for cluster peaks in different matrix preparations, we found that all theoretically possible cluster masses from combinations of intact 4-HCCA and potassium and/or sodium can be calculated with the following simple equations:

$$M_{Cluster} = nM - xH + yK + zNa$$

$$x = y + z - 1$$

$$y + z \leq n + 1 \qquad (thus\ x \leq n)$$

where $M_{Cluster}$ is the observed mass of the ionized cluster, $n = 0, 1, 2, 3, y$ or $z = 0, 1, 2, 3$, ... , and x is an integer meeting above conditions. M, K and Na stand for the molecular weights of 4-HCCA, potassium, and sodium, respectively.

Equipped with this knowledge, possible interferences from matrix-cluster peaks can now be easily detected and eliminated. This greatly facilitates the analysis of the digests of low amounts of proteins in conventional sample handling. As in Figure 4.2B, the matrix peaks can be discerned and these peaks will not be entered into the search program for database protein identification. Note that if a peptide peak has the same mass as one of the clusters, some judgment based on peak intensity is needed to ascertain the origin of the peak.

61

In addition we note that the above-described method of discerning matrix-cluster peaks for 4-HCCA should be applicable to other monoacidic matrix substances, when their specific characteristics (e.g., H_2O loss or other group losses, or different metal ions) are taken into account. For example, 2,5-dihydroxybenzoic acid (DHB) is another widely used matrix substance for peptide analysis. As is shown in Figure 4.4., it forms similar clusters in the presence of salts, although not to the same extent as 4-HCCA.
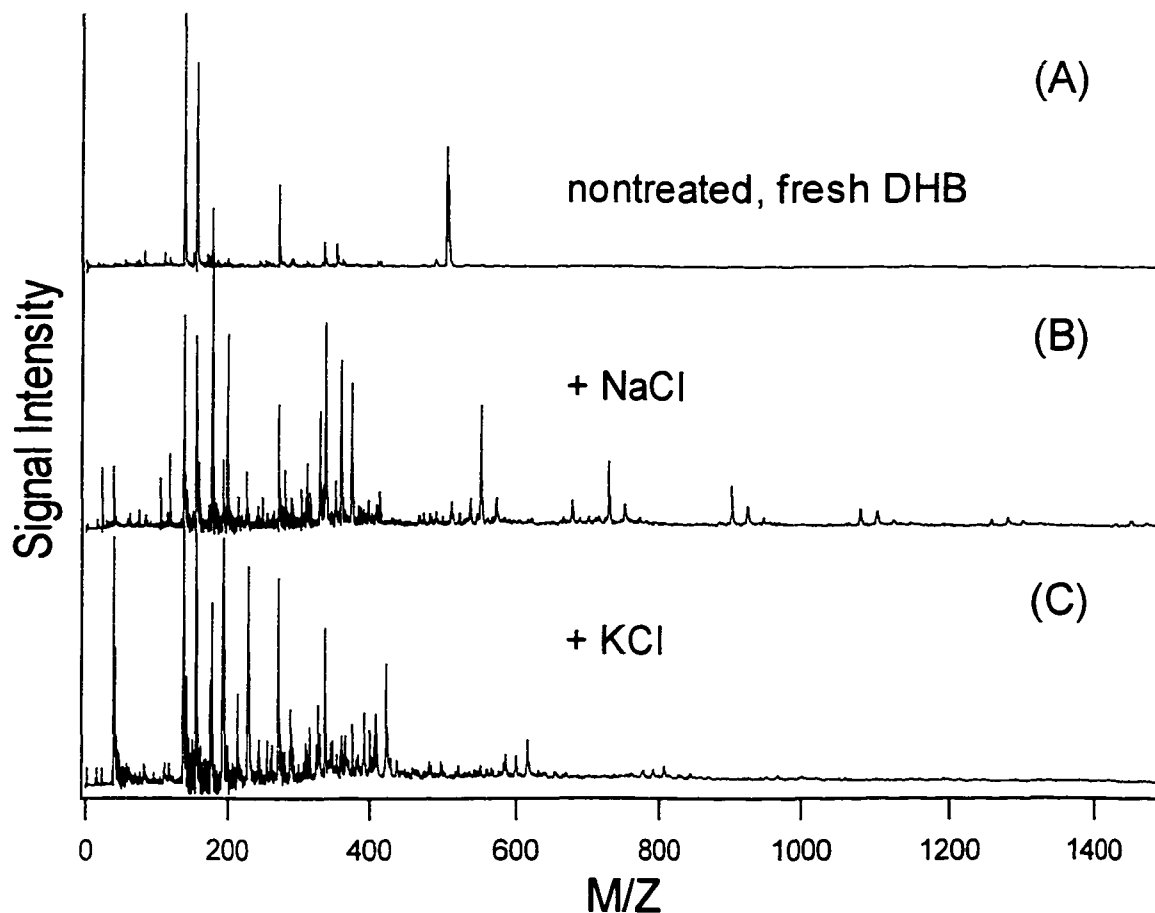
Figure 4.4 Mass spectra of DHB matrix clusters obtained under different matrix preparation conditions. (A) Untreated matrix from conventional dried-droplet matrix formation. 0.5 μL of 100 mM DHB in aqueous solution was deposited on a MALDI target, left to dry in air and analyzed. (B) 0.5 μL of a 100 mM DHB and 50 mM NaCl solution was deposited, dried in air and analysed. (C) 0.5 μL of a 100 mM DHB and 50 mM KCl solution was deposited, dried in air, and analyzed.

We find that the observed cluster masses for DHB can be calculated according to

$$M_{Cluster} = nM + p[M-H_2O] - xH + yK + zNa$$

$$x = y + z - 1$$

$$y + z \leq n + p + 1 \qquad (thus \ x \leq n + p)$$

where $M_{Cluster}$ is the observed mass of the ionized cluster, n or $p = 0, 1, 2, 3,..., n + p > 0$, y or $z = 0, 1, 2, 3,...,$ and x an integer meeting above conditions. M, $[M-H_2O]$, K and Na stand for the molecular weights of DHB, DHB – H_2O, potassium and sodium, respectively. The difference between the above equation and the equation used for 4-HCCA is the addition of the M – H_2O term for DHB. DHB loses H_2O much more readily than 4-HCCA. For 4-HCCA, cluster formations containing [M-H_2O] are usually not observed in the mass region above ~550 u.

Knowing the matrix cluster peaks is also crucial for microspot MALDI analysis of very low abundant proteins. This is illustrated in Figure 4.5 where MALDI spectra of tryptic digests of 0.5 fmol lactoferrin are shown. Note that 0.5 fmol is the actual amount of the starting protein used for the digestion. This amount is not the result of dilution of tryptic digests resulting from the use of a much higher amount of protein required in conventional protein sample handling with microliter volumes. In this case, when a single-shot spectrum is collected from inside the microspot and if it is unclear whether the peaks originate from peptides or matrix clusters, the spectrum is carefully checked for typical matrix cluster characteristics. If several cluster assemblies separated by ~189-227 u are detected, their intensity decreases with increasing mass and no significant signal of non-interfering peptides is detectable, then the single shot spectrum can be discarded.

Figure 4.5 also illustrates the importance of selecting the desorption sites on the MALDI probe. Sampling outside the microspot (see Figure 4.5A) only produces matrix cluster peaks at high laser power since of course no peptides are present. In the border region of the microspot (see Figure 4.5B), peptide concentrations might be very low and thus only weak signals of peptides are obtained and only at medium laser power. In this

63
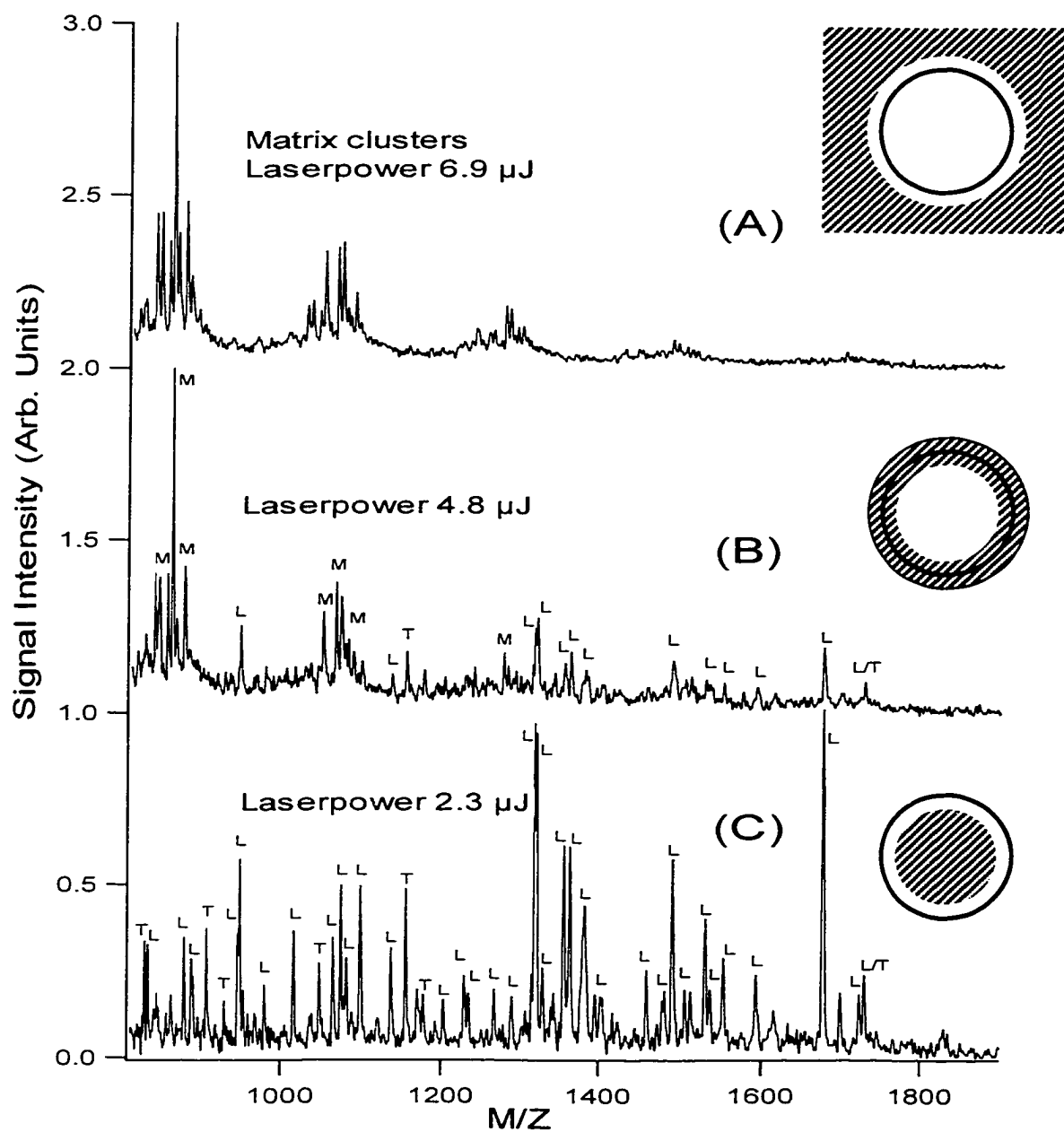
Figure 4.5 MALDI mass spectra of 390 pL of 0.1 µg/µL lactoferrin (0.5 fmol) after in-capillary reduction, carbamidomethylation, and tryptic digestion. (A) The laser beam is sampling outside the microspot (shadow areas in the picture), (B) laser is sampling in the border region of the microspot, and (C) laser is sampling inside the microspot. Specific peaks from matrix-clusters, trypsin autolysis, and lactoferrin peptide fragments are labelled M, T, and L, respectively.

64

case, significant interferences of matrix-clusters in the MALDI spectrum of a tryptic digest are observed. Only when sampling inside the microspot (see Figure 4.5C) strong peptide signals at low laser power are obtainable. In this case we discarded all spectra with any interfering cluster peaks (200 single-shot spectra out of 600 shots were summed).

It is certainly desirable to reduce the extent of matrix cluster formation whenever possible. Sample/matrix preparation should be carefully optimized. It is our experience that matrix purification using the simple ethanol recrystallization method can assist in reducing matrix cluster formation. The improvement in mass spectra upon recrystallization can be quite dramatic when a batch of 4-HCCA as received from the manufacturer contains much salt and impurities. For the microspot experiment, we find that by loading a small amount of matrix solution into the capillary after digestion and then depositing the digest *and* the matrix solution onto the matrix-covered probe tip, the spectral quality can be significantly improved, compared to direct deposition of the digest to the matrix layer. Specifically, it can help to neutralize the digestion buffer and thus avoid excessive matrix-cluster formation, and decrease the extent of salt adduct formation from tryptic peptides.

In the final example we demonstrate that the ability to discern matrix-cluster peaks from analyte signals is not only useful in the analysis of dilute peptide mixtures but is also generally a valuable tool in routine analysis. Figure 4.6 shows a MALDI mass spectrum of tetramethylrhodamine-labeled saccharides that were submitted for MALDI analysis to the departmental mass spectrometry laboratory. To deduce which mass peaks result from analytes and which result from matrix-clusters a QuickBasic program based on the above described algorithm for 4-HCCA matrix-cluster formation was employed. In the meantime this program has been transformed into JavaScript, extended to include H_2O and CN group losses and also the matrix substance DHB, and is now available at our group's Internet web page (http://www.chem.ualberta.ca/~liweb/MaClust.htm). The original program and the JavaScript code are listed in Appendix A. In this specific example, analyte peaks were expected at 791.4 Da and 953.4 Da. Most of the other peaks could be assigned to matrix-cluster peaks. Table 4.1 lists all peaks and their origins as

65
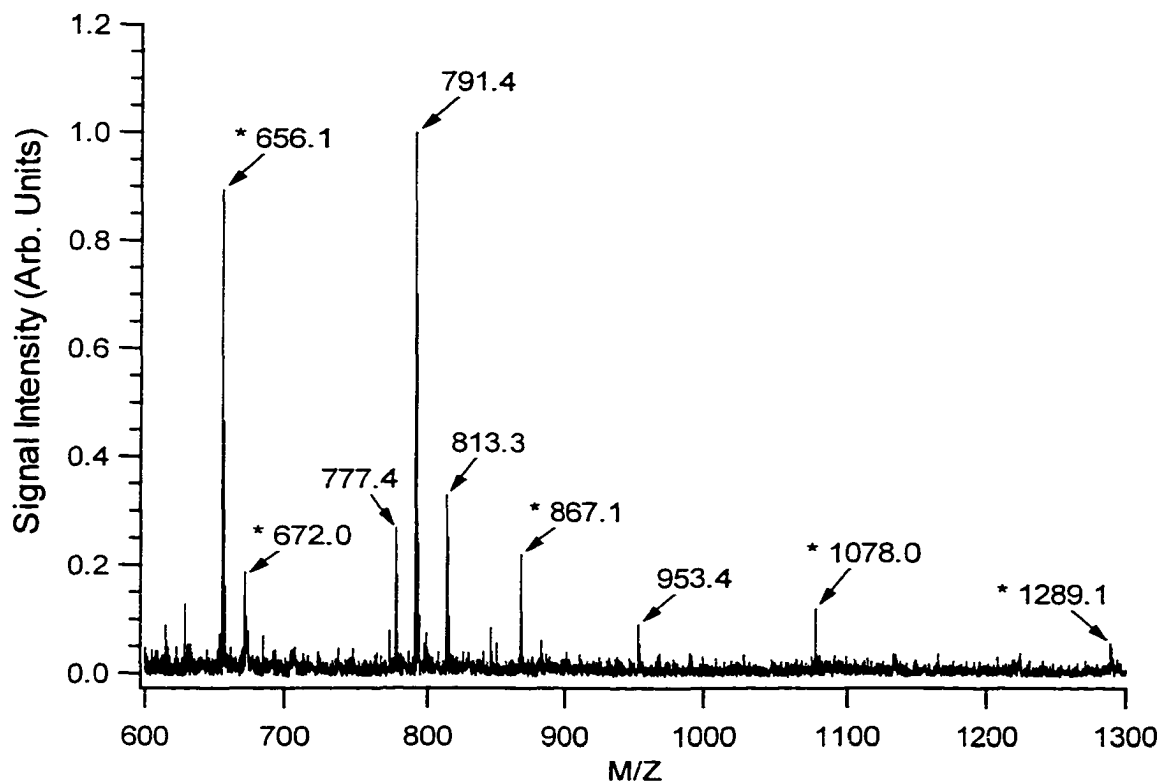
Figure 4.6 MALDI mass spectrum of tetramethylrhodamine-labeled saccharides. Identified matrix-clusters are labeled with '*'. This spectrum was obtained on a Voyager Elite MALDI-TOF mass spectrometer (Perseptive Biosystems, Framingham, MA, USA).

Table 4.1 Mass peaks of analytes and matrix clusters and their origin.

Mass (Da)	Origin (M= 4-HCCA)	Closest theoretical cluster (Da)
656.1	[3 M – 3H + 4Na]$^+$	-
672.0	[3 M – 3H + K + 3Na]$^+$	-
777.4	Possible artifact due to labeling compound with one less methyl group	779.2 $\rightarrow$ ([4 M+Na]$^+$)
791.4	[Glucose-β-TMR+H]$^+$	795.1 $\rightarrow$ ([4 M+ K]$^+$)
813.3	[Glucose-β-TMR + Na]$^+$	817.1 $\rightarrow$ ([4 M–H+K+Na]$^+$)
867.1	[4 M – 4H + 5Na]$^+$	-
953.4	[Mannose-α-1,6-glucose-β-TMR+H]$^+$	952.97 $\rightarrow$ ([4 M-H+4K+2Na]$^+$)
1078.0	[5 M – 5H + 6Na]$^+$	-
1289.1	[6 M – 6H + 7Na]$^+$	-

66

well as the theoretical matrix-clusters that are closest to the analyte peaks. The results confirm that the peaks at 791.4, 813.3 and 953.4 Da are due to analytes and not due to matrix-clusters. The closest theoretically possible matrix-clusters are sufficiently different in mass to be excluded. Only the peak at 953.4 Da is less than half a Da different from a theoretically possible matrix-cluster, yet this difference ensures that this peak is not a matrix-cluster signal since the instrument's mass accuracy at this mass range is sufficient to distinguish these two masses. Nonetheless, there is additional information that indicates that this signal does not originate from a matrix-cluster. All identified matrix-clusters contain mostly sodium as salt contaminant, whereas the theoretically possible matrix-cluster at 953.0 Da contains mostly potassium. The appearance of a predominantly potassium-containing matrix-cluster in a spectra dominated by mostly sodium-containing matrix-clusters is highly unlikely. This example emphasizes the need for sound judgment when evaluating mass spectra. From the above results it also becomes clear that the mass peak found at 777.4 is not due to a matrix cluster ((possibly an artifact due to the labeling compound containing one less methyl group).

At present, discerning matrix peaks is performed manually. Nevertheless, it should be possible to perform this task using software control included in the mass spectrometer's data acquisition package. Such an implementation could also become a valuable quality control tool for routine and especially for automated high-throughput techniques.

4.4 Literature Cited

(1)   See for examples, (a) *Proteome Research: New Frontiers in Functional Genomics*; Wilkins, M.R.; Williams, K.L.; Appel, R.D.; Hochstrasser, D.F., Eds.; Springer: Berlin, 1997; (b) Quadroni, M.; James, P. *Electrophoresis* **1999**, *20*, 664-677; (c) Jungblut, P.; Thiede, B. *Mass Spectrom. Rev.* **1997**, *16*, 145-162.

(2)   Vorm, O.; Roepstorff, P.; Mann, M. *Anal. Chem.* **1994**, *66*, 3281-3287.

(3)   Zhang, H.; Caprioli, R.M. *J. Mass Spectrom.* **1996**, *31*, 1039-1046.

(4)   Dai, Y.; Whittal, R.M.; Li, L. *Anal. Chem.* **1996**, *68*, 2721-2725.

(5)   Li, L.; Golding, R.E.; Whittal, R.M. *J. Am. Chem. Soc.* **1996**, *118*, 11662-11663.

(6)   Allmaier, G. *Rapid Commun. Mass Spectrom.* **1997**, *11*, 1567-1569.

(7)   Kussmann, M.; Nordhoff, E.; Rahbek-Nielsen, H.; Haebel, S.; Rossel-Larson, M.; Jakobsen, L.; Gobom, J.; Mirgorodskays, E.; Kroll-Kristensen, A.; Palm, L.; Roepstorff, P. *J. Mass Spectrom.* **1997**, *32*, 593-601.

(8)   Murray, K.K. *Mass Spectrom. Rev.* **1997**, *16*, 283-299.

(9)   Beavis, R.C.; Chaudhary, T.; Chait, B.T. *Org. Mass Spectrom.* **1992**, *27*, 156-158.

(10)   Whittal, R.M.; Li, L. *Anal. Chem.* **1995**, *67*, 1950-1954.

(11)   Whittal, R.M.; Keller, B.O.; Li, L. *Anal. Chem.* **1998**, *70*, 5344-5347.

(12)   Dai, Y.Q.; Whittal, R.M.; Li, L. *Anal. Chem.* **1999**, *71*, 1087-1091.

(13)   Dubois, F.; Knochenmuss, R.; Steenvoorden, R.J.J.M.; Breuker, K.; Zenobi, R. *Eur. Mass Spectrom.* **1996**, *2*, 167-172.

68

Chapter 5

Bacterial Protein Identification by HPLC Fractionation, Nanoliter Digestion, and Microspot MALDI Analysis[a]

5.1 Introduction

Reliable identification of bacterial species or strains is an urgent requirement in many areas including clinical and environmental monitoring applications, in-field hazard assessment, and food processing.[1,2] Since proteins may constitute up to 65% of the dried cell weight of bacteria, they are ideal biomarkers for unambiguous bacteria identification.[3] In order to determine unique protein biomarkers for a specific microorganism preferably all its proteins should be identified first. Mass spectrometry is an important tool in the ongoing investigations towards finding suitable protein biomarkers for microorganisms.[1] MALDI TOF MS represents an ideal technique for protein characterization, due to its sensitivity and its ability to directly analyse moderately complex peptide or protein mixtures without a separation step.[4] It has been shown that direct analysis of bacteria extracts with MALDI TOF MS gives reproducible spectral patterns in inter-laboratory studies when special care is taken during sample preparation.[5] Nevertheless, ion suppression effects in MALDI analysis of mixtures cannot be ignored, especially since protein abundance variations within the same bacteria, for example due to different growth conditions, can affect the spectral pattern.[5] The introduction of a separation step can help to avoid this problem. For example, the number of detectable

---

[a] A form of this chapter is in preparation for publication: B. O. Keller, Z. Wang, L. Li *"Bacterial Protein Identification by HPLC Fractionation, Nanoliter Digestion and Microspot MALDI Analysis"*. Ms. Zhengping Wang prepared the *E.coli* bacteria extracts, collected the HPLC-UV-chromatogram, and did the HPLC-fractionation.

69

proteins increased greatly when bacteria extracts were submitted to HPLC separation before mass spectrometric analysis.[6,7] Another important issue is that for unambiguous protein identification, molecular weight determination alone is not sufficient. Peptide mapping by enzymatic digestion or further sequencing of preferably isolated proteins is typically required. HPLC fractionation, protein digestion, and offline MALDI TOF MS has been shown to be a reliable combination for such a task.[6] However, due to the great variance in abundance of proteins within bacteria, low abundant proteins might not always be detectable. One approach to solve this problem is to use preparative HPLC columns that allow increased sample loading. The disadvantage of this approach is of course the need for large amounts of starting material. The potential of MALDI mass spectrometers in terms of sensitive protein and peptide analysis has been demonstrated in the previous chapters. This considered, the use of preparative HPLC columns and large sample amounts may seem redundant. In addition, it is often difficult to acquire such large amounts of starting material. These issues provided the motivation to develop a new method that separates bacteria extracts on a conventional analytical HPLC column and is combined with offline protein digestion and MALDI-TOF analysis. As shown in Chapter three, our lab's in-capillary approach using the nanoliter chemistry station can be used for sub-femtomole protein digestion.[8] In the present chapter, we expand the capabilities of our method to include pre-concentration and cleanup of protein samples originating from analytical HPLC column fractionation of *E.coli* extracts. In addition, we demonstrate the ability to perform multiple chemical and enzymatic reactions on pre-concentrated samples before microspot MALDI analysis.

5.2 Experimental

5.2.1 Chemicals and Materials.

E.coli bacteria samples were a gift from Dr. S. R. Long, Edgewood RDE Center, Aberdeen Proving Ground, MD, USA. Dithiothreitol (DTT), iodoacetamide, α-cyano-4-hydroxycinnamic acid (4-HCCA) and trypsin (98%, L-1-Tosylamide-2-phenylethyl chloromethyl ketone (TPCK) treated for reduction of chymotrypsin activity), horse cytochrome c, leucine aminopeptidase (LAP), and trifluoro-acetic acid (TFA) were from Sigma-Aldrich-Fluka (Oakville, Ontario, Canada). 4-HCCA was recrystallized from ethanol (95%) at 50C before use.

70

5.2.2 Extraction of Bacteria Samples. The *E.coli* 9637 extract was prepared by solvent suspension methods.[5,7] Briefly, about 25 mg lyophilized *E.coli* was suspended in 500 μL 0.1% TFA, the suspension was vortexed for 3-5 minutes and centrifuged, and the supernatant was removed. This suspension procedure was repeated until no apparent protein signals were detected from the supernatant by MALDI. The supernatants were pooled, filtered with a Microcon-3 (i.e. a 3000 Da molecular weight cut-off membrane (Amicon, Inc., Beverly, MA, USA), and then concentrated to 150 μL by a high-speed vacuum centrifuge.

5.2.3 HPLC-Fractionation. Separation of *E.coli* 9637 extract was performed on a HP1100 HPLC (Hewlett-Packard, Palo Alto, USA) using a 4.6×250 mm C_8 column. The mobile phases were nanopure water (A) and acetonitrile (B) with 0.05% TFA in both phases, the solvent gradient was 2-20% B over 10 minutes, 20-40% B over 40 minutes, and then 40-55% B over 10 minutes, the flow rate was 0.5 mL/min. Fractions were collected each minute during the run. For every separation, 30 μL *E.coli* extract were injected into the C_8 column. The fractions were concentrated to about 10 μL by a high-speed vacuum centrifuge.

5.2.4 In-capillary Sample Preparation. All experiments were done using a nanoliter chemistry station, which has been described in more detail in Chapters two and three.[8] 20-μm-ID fused silica capillaries were purchased from Polymicro Technologies (Phoenix, Arizona, USA). The capillary tube was connected to a syringe and used to draw sub-nanoliter volumes of protein sample from a horizontally mounted pipette tip. To minimize analyte loss due to irreversible adsorption onto the wall surface, the capillary was treated with a siliconizing agent before use (Glassclad-18, United Chemical Technologies, Bristol, PA, USA). The sample plug was observed under a microscope and its volume determined using a calibrated recticle that was positioned in the eyepiece. As illustrated in Figure 5.1, for concentration of samples, an ~500 pL sample plug was dried inside the capillary close to the capillary entrance. This step was repeated up to 20 times to achieve sufficient sample concentration inside the capillary. As a washing step a plug of ~1 nL of triply distilled water was drawn into the capillary and pushed out after ~20 seconds. Such a washing step was usually included after 2 or 3 sample concentration

71
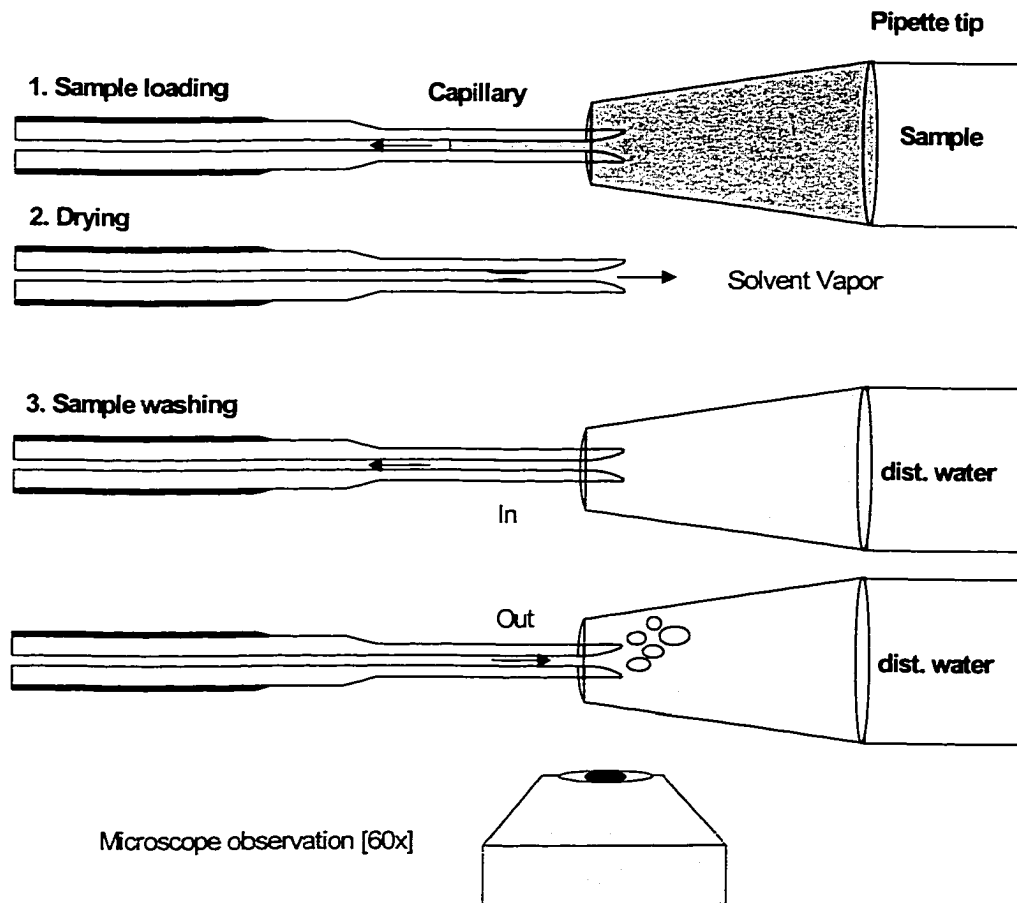
Figure 5.1   Schematic drawing of sample concentration and first washing step.

steps and as a final step. It was found that the drying step inside the capillary could be accelerated by providing an orthogonal airstream at the open capillary end. For this purpose a flat-end syringe needle was positioned into a 3-D manipulator and hooked up to pressurized air or a nitrogen tank and positioned perpendicularly to the capillary end. This setup is illustrated in Figure 5.2. Using this airstream, the drying steps were performed approximately 10 times faster than previously. After the final washing step, enzyme or other chemical solutions were drawn into the capillary. The capillary was then pushed against a piece of Parafilm to close the entrance and thus stop any further evaporation. After sufficient reaction time the sample/enzyme or sample/chemical
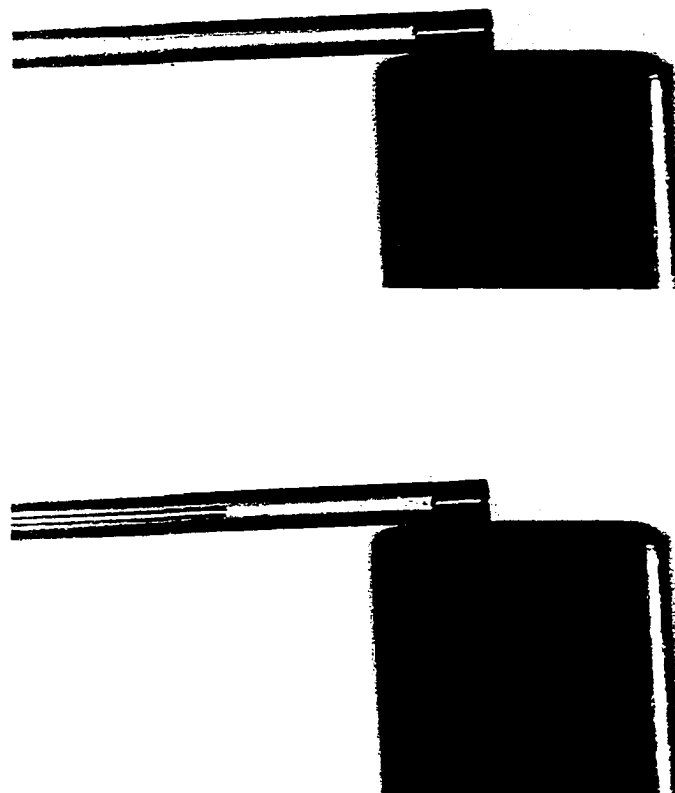
Figure 5.2 Microscope images (40x) of capillary with sample plug and needle. This setup for provides an orthogonal airflow for faster drying of the sample plug inside the capillary.

mixture was dried up again inside the capillary and further chemical or enzymatic reactions were performed by introducing different chemical/enzyme solutions in an additional step. When all desired reaction steps had been performed an ~500 pL plug of sat. matrix solution was drawn into the capillary. The sample and matrix solution were separated by a small air gap. Both plugs were then simultaneously deposited onto a matrix-covered MALDI target. The matrix-covered target was prepared using a modified

version of the two-layer method.[7,9] In brief, as a very thin first layer, about 1 μL of a 5 mg/mL solution of 4-HCCA in 80% acetone/methanol (v/v) were first deposited on the clean probe. After drying, a second layer of 0.4 μL of 4-HCCA saturated in 35% methanol/water (v/v) was deposited and allowed to dry. Matrix-loading and deposition are illustrated in Figure 5.3.

Parafilm on a target

1. Last reaction step finished

capillary

Pipette tip

2. Loading of matrix solution

air gap

matrix solution

3. Deposition of sample & matrix solution

air gap

Matrix-covered MALDI target

Microscope observation [60x]
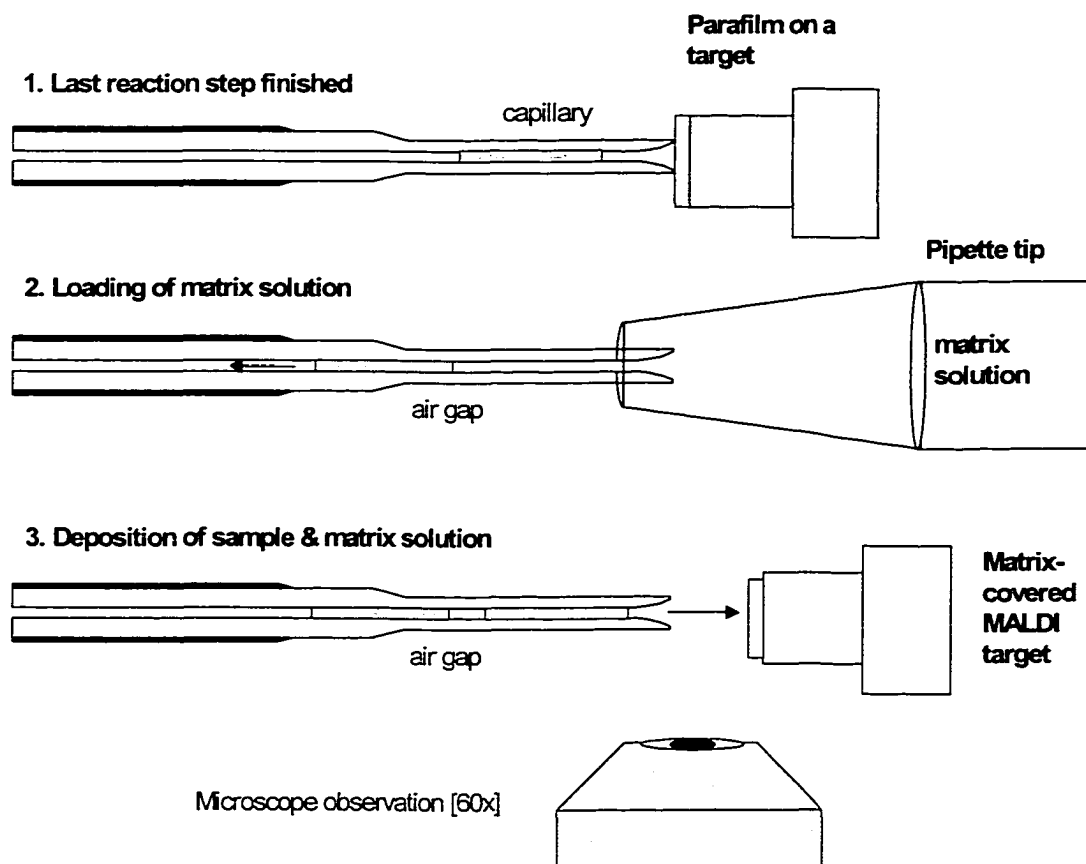
Figure 5.3   Schematic drawing of matrix loading as second washing step and deposition onto matrix-covered MALDI target.

5.2.5. MALDI Analysis. Mass spectra of proteins and their digests were collected on a home-built linear time-lag focusing MALDI-TOF mass spectrometer, equipped with a 337 nm laser having a 3 ns pulse width (model VSL 337ND, Laser Sciences Inc.,

74

Newton, MA, USA). This home-built instrument has been described in detail elsewhere.[10] In general, 150-200 laser shots (3-5 µJ pulse energy) were averaged to produce a mass spectrum. Spectra were acquired and processed with Hewlett-Packard supporting software and reprocessed with the Igor Pro software package (Wavemetrics, Inc., Lake Oswego, OR). Each spectrum was normalized using the most intense signal.

5.3. Results and Discussion

5.3.1 Effect of Washing Steps. During initial experiments, it quickly became apparent that for many fractions the in-capillary concentration step (Figure 5.1.) was necessary to accumulate enough protein inside the capillary to ensure efficient enzymatic digestion. However, since the vacuum centrifugation had already concentrated the fraction extensively, salt contaminants became a major problem during the in-capillary concentration step and resulted in the capillary being plugged. The washing step using distilled water solved this plugging problem. Although some protein may have been lost it appeared that the bulk of the protein sample remained inside the capillary, thus only contaminants were washed out. Minimal loss of protein during the wash can be explained by protein adsorption to the C_{18}-coated capillary wall or other nonspecific wall interactions. Contaminants that do not interact with the capillary wall are washed out with the distilled water. This concentration and washing step is somewhat comparable to other, larger scale protein cleanup procedures, for example C_{18}-coated microbeads in pipette tips (e.g. ZipTips).[11,12] In these cleanup procedures, protein solutions are drawn through a microbead bed situated at the beginning of a pipette tip. The proteins adsorb onto the beads, salt contaminants are washed out using distilled water, and the proteins are later eluted with organic solvent/acidified water mixtures. The difference in our case is that the protein sample was dried up inside the capillary. This ensures complete transfer of the proteins to the capillary wall and potential wall binding sites.

To demonstrate the effects of the two employed washing steps (as shown in Figures 5.1 and 5.3) we performed three experiments using cytochrome c in a highly salt-contaminated solution (Figure 5.4). For each experiment, the same amount of sample

75
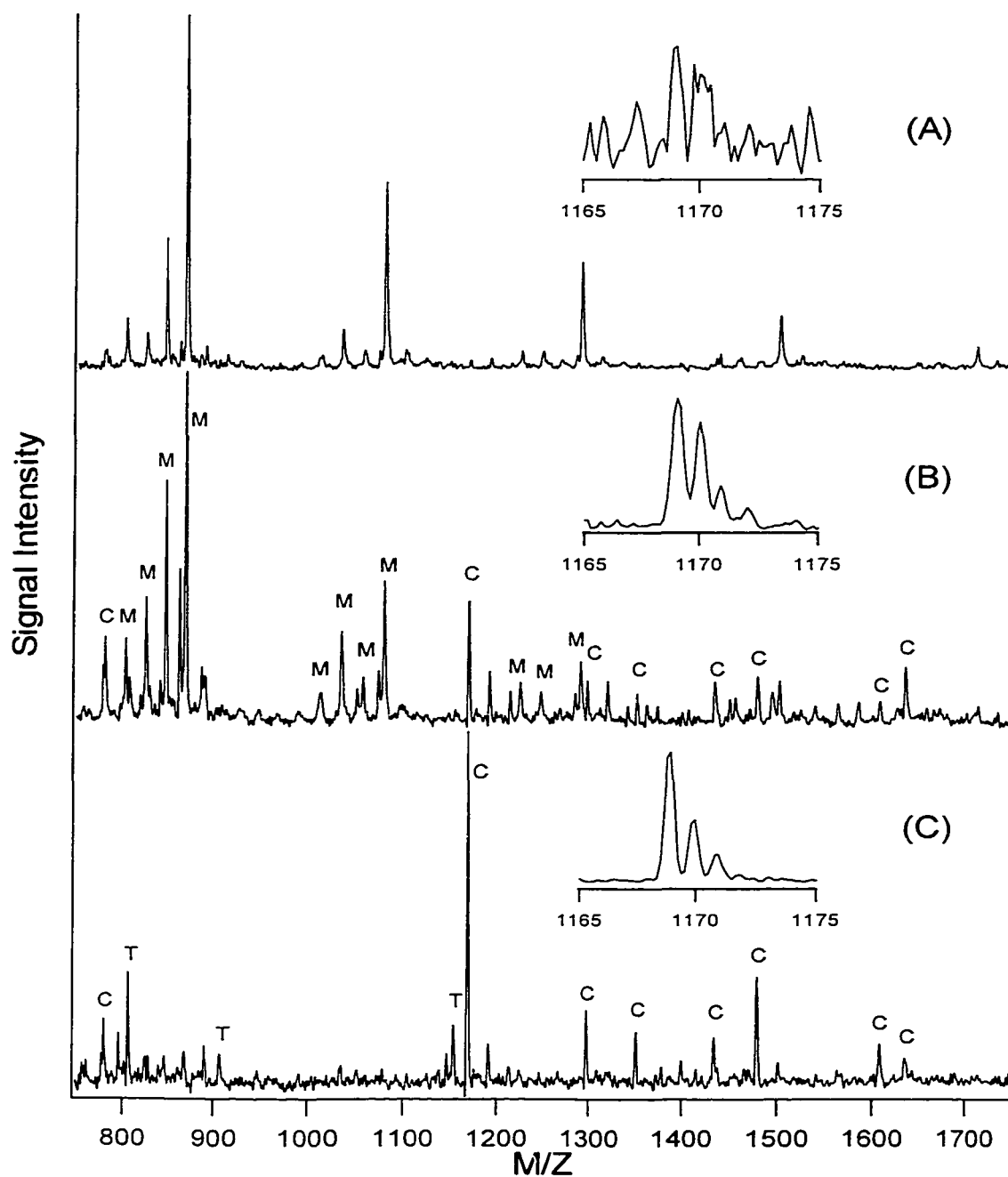
Figure 5.4 MALDI mass spectra of in-capillary tryptic digests of a 4 μM cytochrome c solution in 40 mM NaCl and 20 mM NH₄HCO₃ buffer. (A) Direct deposition of digest mixture onto MALDI target without any washing step. (B) Simultaneous deposition of contaminated digest mixture and a matrix solution plug onto target. (C) Simultaneous deposition of digest mixture of washed protein and matrix solution onto target. The inserts show the mass region of the most intense tryptic peptide of cytochrome c with amino acid sequence TGPNLHGLFGR.

76

was loaded into the capillary and treated as described in the Experimental section. The spectrum of the untreated digest mixture (Figure 5.4A) shows mainly matrix-cluster peaks, which is a common observation at such a high salt content (see Chapter 4).[13] The second spectrum (Figure 5.4B) shows matrix clusters, however, eight tryptic peptides of cytochrome c are discernable from the matrix clusters. This proves that the simultaneous deposition of digest mixture and matrix solution is already quite an effective washing step. This also confirms that tryptic digestion is not inhibited in solutions containing large amounts of salt. Note that the digestion was done at a relatively low concentration of digestion buffer (only 20 mM NH_4HCO_3). Generally, higher concentrations of up to 100 mM NH_4HCO_3 are used because the enzyme's optimal activity is at a higher pH. Direct deposition of digest mixtures (Figure 5.4A) with such a high basic buffer content however are usually not feasible, since the matrix cover on the target would be immediately dissolved and thus the experiment ruined. This demonstrates again the benefits of loading matrix solution before deposition (see Chapter 4).[13] During the simultaneous deposition of digest and matrix, the buffer is neutralized and the pre-deposited matrix-layer on the target remains intact. Thus, even digest mixtures with high buffer content are feasible for microspot deposition. The best cleanup effect is achieved when the protein in the capillary is washed with distilled water before digestion in the capillary and the digest mixture simultaneously deposited with matrix onto the matrix-covered target. This is demonstrated in Figure 5.4C. All matrix cluster interferences are eliminated and a low abundance of autolysis peaks of trypsin appears in the spectrum. This is not disadvantageous, since autolytic peptides are well known and they can easily be discerned from other peptides. These peaks can also be utilized for internal calibration and thus improve the mass accuracy for the tryptic peptides under investigation.

5.3.2. Analysis of HPLC Fractions. Figure 5.5 shows the HPLC chromatogram of the *E.coli* extract obtained with UV detection. Based on a first chromatogram run at a fast gradient of 2-90% acetonitrile, the separation was optimized in the following manner. The very strong peaks at the very beginning of the chromatogram are the low mass components in the extract that are not very useful for this study. Thus, a very fast gradient was kept in this range. To improve the resolution of the higher molecular weight protein band, the gradient rate was lowered for this time range.

77
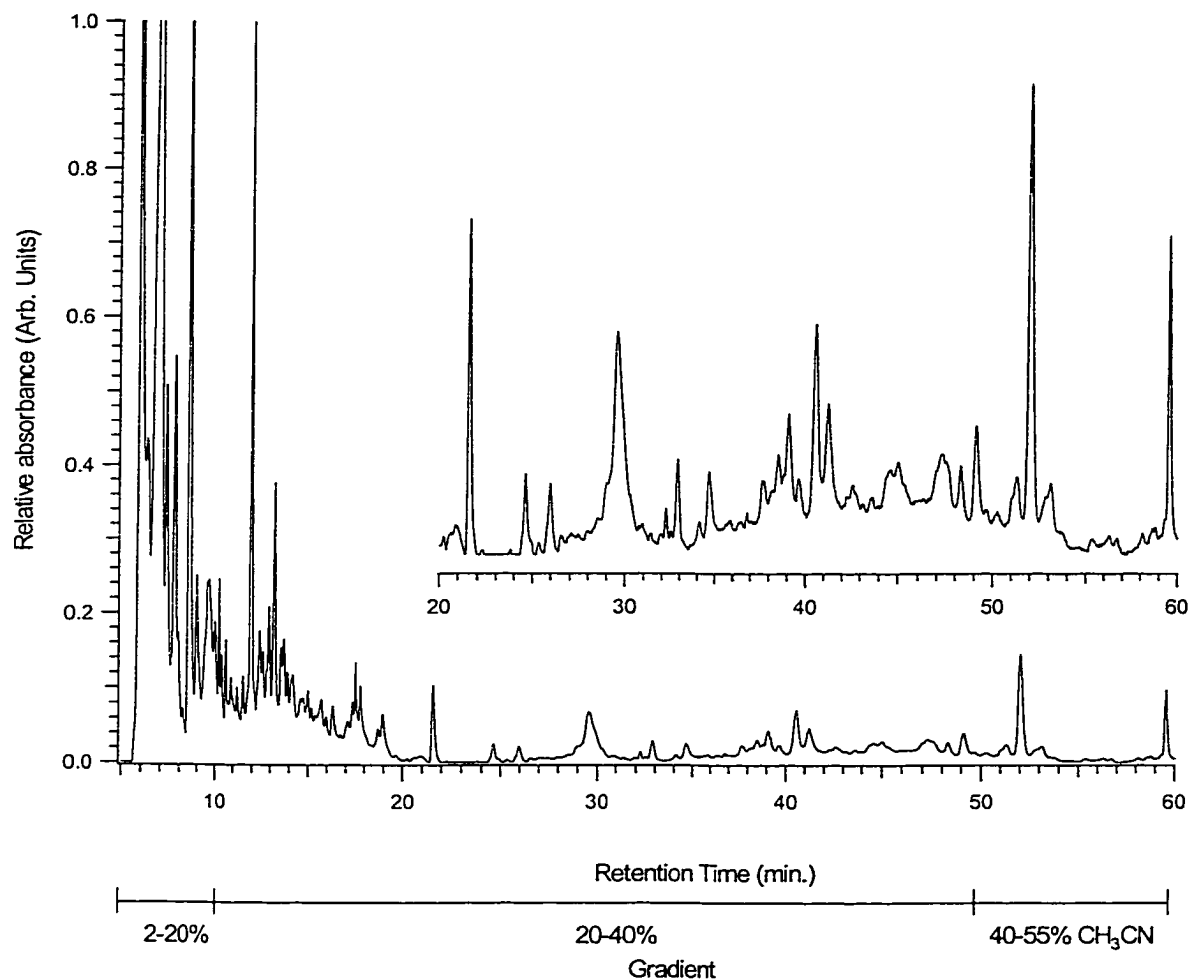
Figure 5.5 HPLC-UV-Chromatogram of an *E.coli* extract (analytical C₈-column).

Using nanoliter chemistry, only a small portion of the sample fraction is used for each experiment. In our lab, we always first take a few nanoliters of sample for molecular weight analysis. As an example, Figure 5.6 shows a mass spectrum of a fraction containing a protein that was identified as DNA-Binding Protein HU-Alpha (see section 5.3.2.2 below). Molecular weight determination is followed by trypsin digestion for peptide mapping. The remaining fraction is stored in the freezer at $-20°$ C. If peptide mapping along with the molecular weight information cannot unambiguously identify the protein in the database, several nanoliters from the remaining fraction are taken for further experiments until we confidently identify the protein or determine that identification is not possible with our current techniques and database. The following sections will demonstrate the capabilities of the nanoliter chemistry techniques.

78
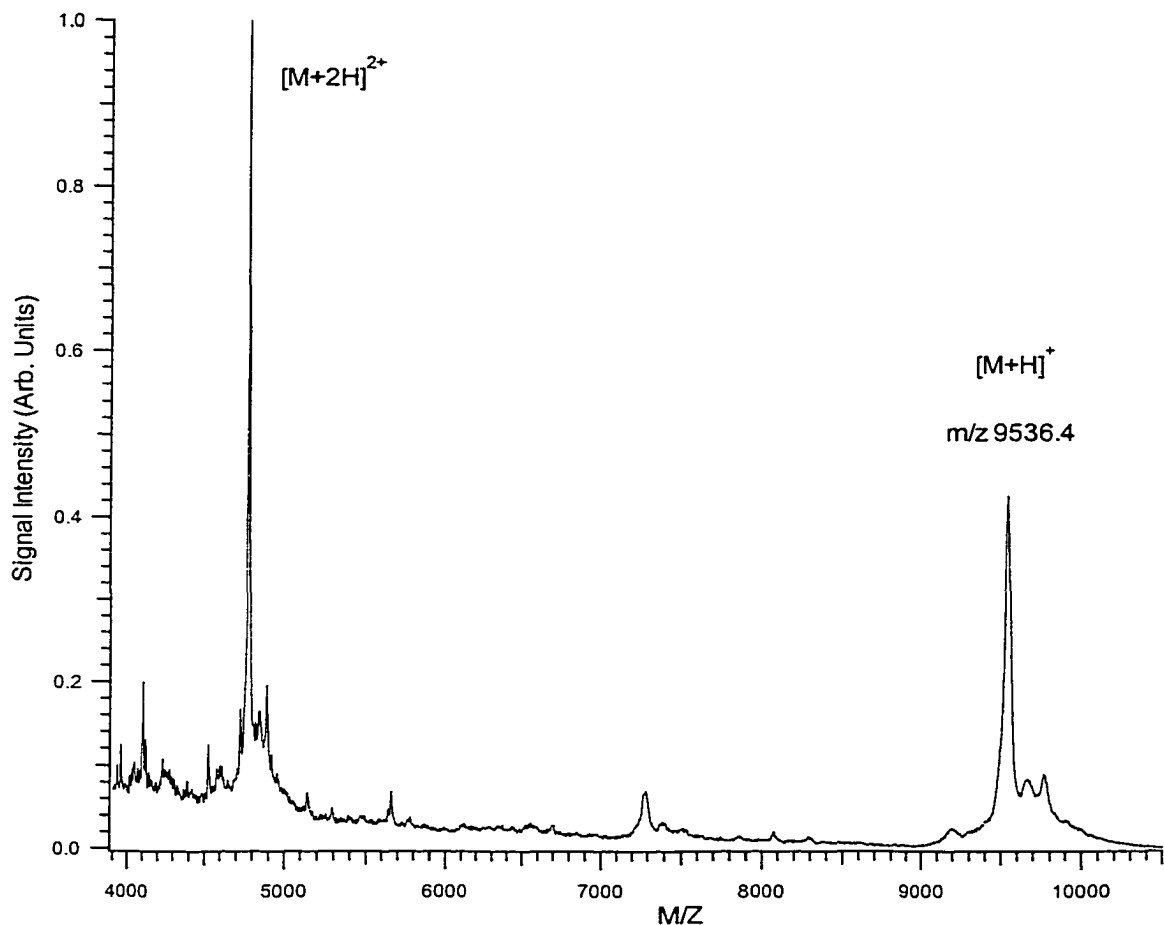
Figure 5.6   MALDI mass spectrum of a fraction containing DNA-Binding Protein HU-Alpha.   A total volume of ~2 nL in ~500 pL portions was concentrated inside the capillary before deposition onto the MALDI target.

5.3.2.1   Comparison of Tryptic Digests Obtained with and without Protein Reduction and Alkylation.   Cysteine residues in proteins often form disulfide bonds with each other.   These bonds determine the protein's secondary structure.   For effective cleavage of these bonds, the digestion enzyme must have access to the cleavage sites. Often sequences containing cysteines with disulfide bridges are digested only partially or not at all since the secondary structure does not allow the enzyme enough access to the sites.   The most common reduction and alkylation step in digestions utilize dithiothreitol (DTT) and iodoacetamide, respectively.[14]   Treatment with DTT leads to reduction of the disulfide bonds, yielding one free sulfhydryl group for every cysteine residue.   Since

79

reaction with ambient oxygen can easily reverse this reaction, the free sulfhydryl group must be protected; a common reagent for this purpose is iodoacetamide. Iodoacetamide reacts with free sulfhydryl groups to form very stable carbamidomethylated sulfides. Note that iodoacetamide is applied in excess compared to DTT and also functions as a DTT-deactivator. This excess of iodoacetamide is necessary since otherwise the leftover DTT would reduce disulfide linkages in the subsequently employed enzymes. Such a reduction would denature the secondary structure of the enzyme and thus lead to its inactivity. For every carbamidomethylated cysteine a mass shift of +57 Da (+58 Da for cysteines involved in disulfide bonds) has to be taken into account when performing peptide mass searches in databases.

Figure 5.7 shows the mass spectra of trypsin digests of a *E.coli* bacteria extract fraction containing a protein with mass 7868.3 Da (mass spectrum not shown). Peptide mapping using the data from Figure 5.7B with the molecular weight data identified a top candidate of 50S Ribosomal Protein L31. However, a number of peptide peaks did not match with this protein. To increase our confidence in the protein assignment, we examined the digestion data carefully with the assistance of protein structure information contained in the proteome database. 50S Ribosomal Protein L31 consists of 70 amino acid residues (cysteines and potential cleavage sites, K and R, are in bold):

1	9		23 25		39
MKKDIHPKYE	EITAS**C**S**C**GN		VM**K**I**R**STVGH		DLNLDV**C**S**K**C

47		70
HPFFTG**K**QRD	VATGGRVDRF	NKRFNIPGSK

Without prior chemical treatment to the protein (Figure 5.7A), the sequence fragment from positions 9-47 was not digested further by trypsin. Apparently, trypsin access was blocked effectively by the existing disulfide bridges to possible cleavage sites at positions 23 (K), 25 (R), and 39 (K). The actual positions of the disulfide bridges is unknown. After reduction and alkylation, two more peptides are detectable covering the sequence from positions 26-39 and 40-47. It is clear that while peptide mass data from Figure 5.7B

80
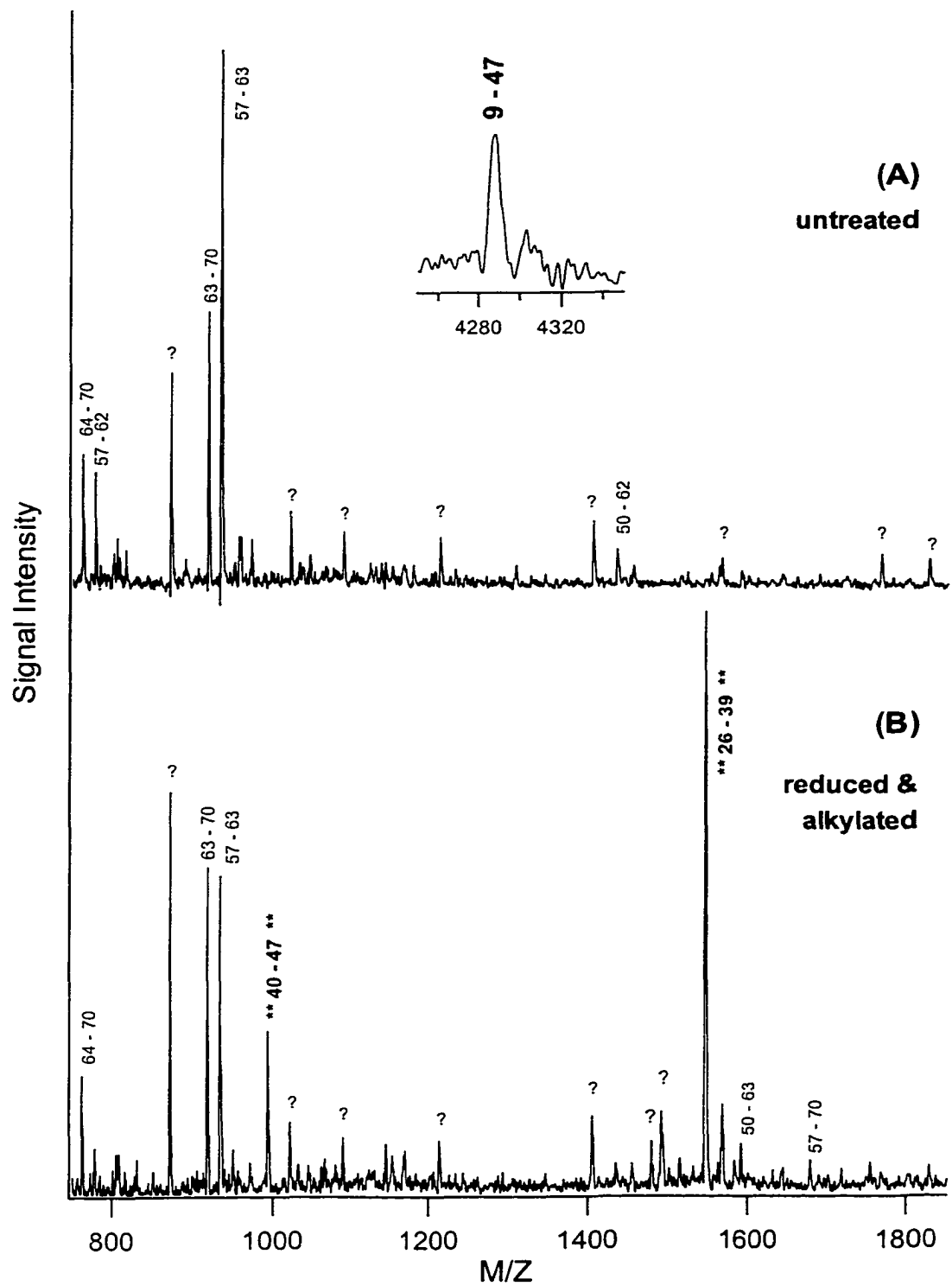
Figure 5.7 MALDI mass spectra of in-capillary tryptic digests of fraction containing 50S Ribosomal Protein L31.

81

helped to find the top candidate, data from Figure 5.7A can be used as another piece of structural information for confirming the protein identity.

The above results illustrate that the multiple reactions or experiments enhance our confidence in protein identification. This example also demonstrates that the analysed fraction does contain more than one protein or is contaminated with tryptic peptides from other proteins (signals marked with a '?'). In this particular case, we were not able to identify the spurious signals.

5.3.2.2 Sequential Enzymatic Digestions. There are cases where not enough specific peptides for unambiguous protein identification are detected. This could either be due to lack of sufficient starting material or due to contamination with other peptides, which obscure the database search results. It has been shown by different groups that additional sequence information of only one or two tryptic peptides is often enough for confident protein identification.[15,16] A common technique for obtaining sequence information is MS/MS fragmentation of isolated peptides. MS/MS fragmentation is achieved either by using collision-induced dissociation (CID) in any type of tandem mass spectrometer[17,18] or post-source decay MALDI (PSD) using a reflectron TOF instrument.[19] Although the fragmentation process of a single peptide can be a very sensitive process, the introduction of a tryptic peptide into the mass spectrometer requires usually at least a starting amount of protein in the high femtomole range (see discussion in the introduction chapter).

A different way of obtaining additional sequence information is the application of exoproteolytic enzymes directly on tryptic digest mixtures. James and coworkers have successfully applied exopeptidase digestions to obtain sequence information both at the N- and C-termini of tryptic peptides.[20,21] Figure 5.8 shows mass spectra of in-capillary digests of cytochrome c. Leucine Aminopeptidase M (LAP), an enzyme with molecular weight of ~280,000 Da, cleaves subsequently single amino acids from the N-terminus of peptides.[22] Several research groups including ours have successfully used this enzyme to create N-terminal peptide ladders.[23-25] Figure 5.8A shows a spectrum of a tryptic digest of horse cytochrome c. Total sample loading was 1.2 femtomoles or 15 picograms of protein. Figure 5.8B shows another tryptic digest after exposure to LAP for 2 minutes. In

82
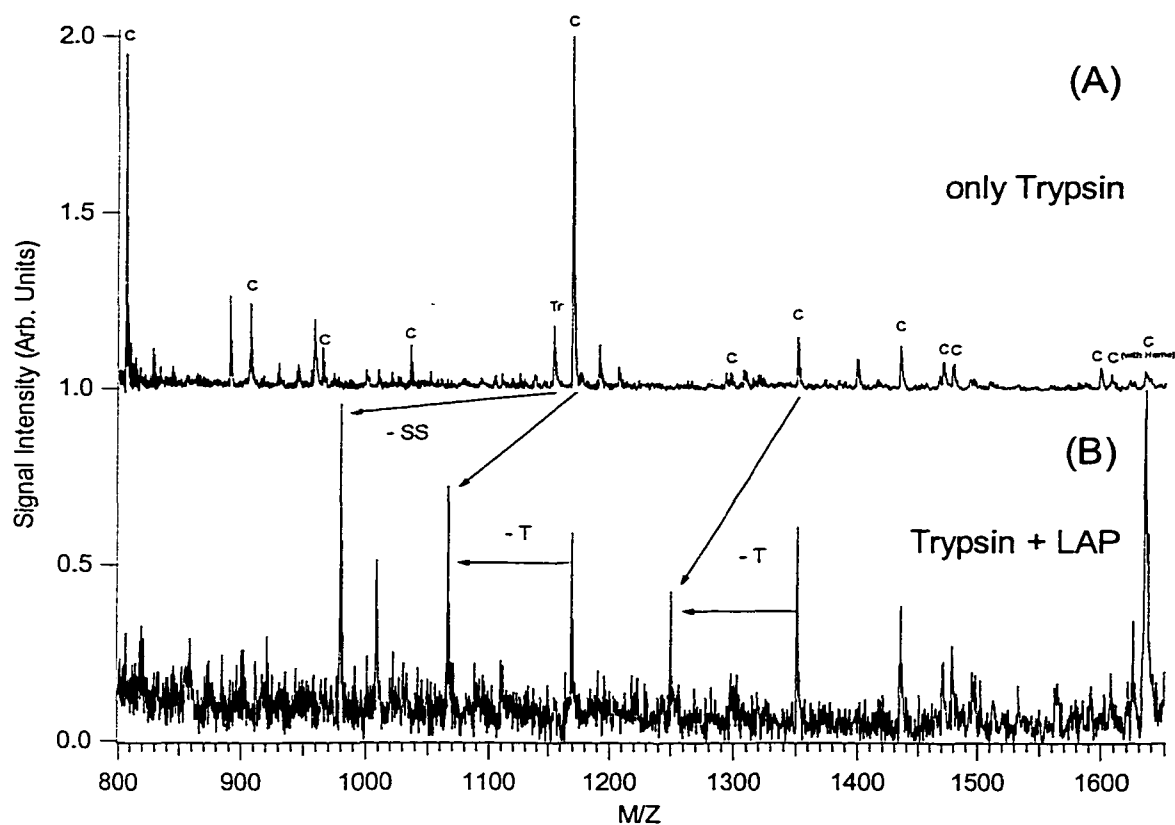
Figure 5.8   MALDI mass spectra of in-capillary digests of cytochrome c.

this case total sample loading was 1.4 femtomoles or 17 picograms. Two of the tryptic peptides originating from cytochrome c undergo N-terminal exoproteolytic digestion by LAP. The peptide with average mass 1351.5 Da and sequence TEREDLIAYLK as well as the peptide with average mass 1169.3 Da and sequence TGPNLHGLFGR each lose threonine at their N-terminus, yielding peptides with masses at 1250.4 and 1068.2 Da, respectively. Since the in-capillary technique employs usually equal or excess amounts of trypsin (compared to protein) to speed up the digestion, it is clear that autolytic peptides can be present in high enough amounts to undergo exoproteolytic digestion as well. This is also observable in Figure 5.8. The autolytic peptide with average mass 1154.3 Da and sequence SSGTSYPDVLK loses two serines at the N-terminus, yielding a peptide with mass 979.5 Da. These results demonstrate that additional sequence information is obtainable at the low femtomole or picogram level. The nanoliter

technique is therefore an interesting alternative to MS/MS fragmentation techniques in cases where not enough analyte material is available. Another advantage of the sequential enzymatic digestion is the relative simplicity of the obtained mass spectra compared to MS/MS spectra. Fragmentation spectra can often be very difficult to interpret in cases where the CID process produces too many or not enough fragments of a specific analyte. However, it has to be pointed out, that exoproteolytic digestion has its difficulties too, and does not work for all proteins.[26] We were not able to do in-capillary N-terminal exoproteolytic digestion of whole proteins larger than ~6000 Da and in all in-capillary tryptic digestions we were never able to get a signal from the N-terminal tryptic peptide of the digested protein. The reason for this phenomena is unknown. However one possible explanation is that the protein's N-terminus adsorbs so strongly to the capillary wall surface that access for the exoproteolytic enzyme is blocked. Note that already the existence of a methyl group at the N-terminus effectively blocks LAP.[22] This would also explain why no N-terminal fragments in tryptic digestions are observed; these fragments might not be eluted.

In the final example, we show a time study of sequential enzymatic digestion performed on an HPLC fraction containing DNA Binding Protein HU Alpha (microspot MALDI spectrum of untreated fraction is shown in Figure 5.6). Figure 5.9 shows sections of mass spectra from three in-capillary digests of this fraction. For each experiment a total volume of ~5 nL was concentrated in ~500 pL portions inside the capillary as described in the Experimental section. From the tryptic peptides and from the molecular weight information the protein was identified tentatively. In the shown mass range, two peptides underwent exoproteolytic digestion by LAP. The peptide with monoisotopic mass 958.51 Da and sequence TGRNPQTGK lost the N-terminal threonine and yielded a new peptide with mass 857.47 Da. In the chosen timeframe, this peptide did not undergo further digestion by LAP. The peptide with mass 1244.71 and sequence IAAANVPAFVSGK however, underwent several N-terminal amino acid losses during the course of treatment with LAP. The exoproteolytic digestion stopped at the V-P bond, since LAP is not capable of cleaving X-P bonds.[22] Thus, the signal from the remaining peptide with mass 804.47 and sequence VPAFVSGK increased in strength, whereas all the intermediate signals from the N-terminal ladder decreased in strength as seen in

84
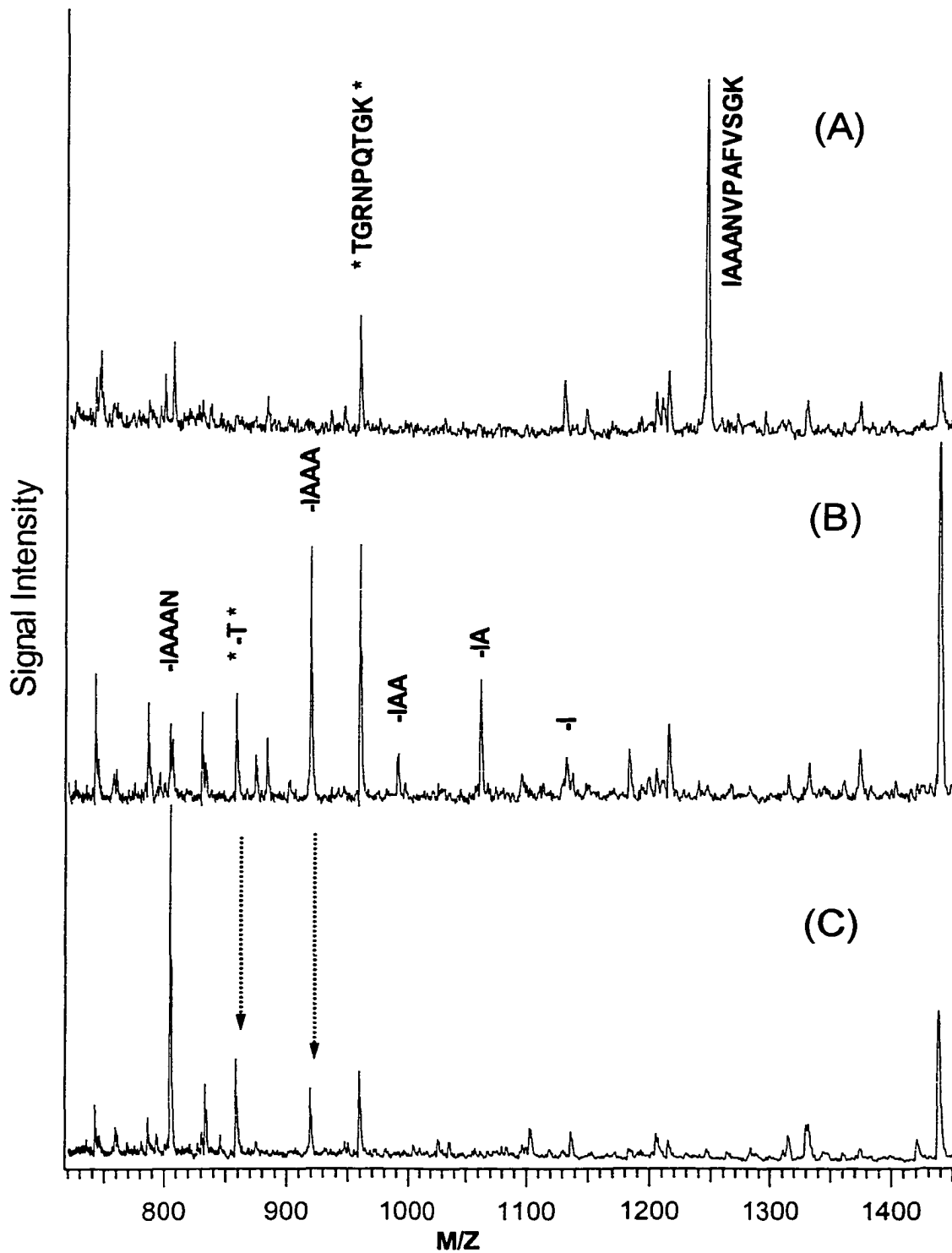
Figure 5.9 Sections of MALDI mass spectra from in-capillary digests of fraction containing DNA Binding Protein HU Alpha. (A) Only trypsin digest (B) Trypsin digest followed by LAP for 5 min. (C) Trypsin digest followed by LAP for 15 min.

85

Figures 5.9B and 5.9C. The appearance of the intermediate peptides as well as the N-terminally-blocked peptide that remained, confirmed the initially proposed sequence extracted from the database and therefore allowed for unambiguous identification of this protein. Table 5.1 summarizes the results for data base searching with the additional sequence information. Note that only the tryptic peptide at m/z 1244.7 and its N-terminal ladder products were taken for this database search using MS-FIT from the ProteinProspector software package[27] combined with the database from the National Center for Biotechnology Information (NCBI).[28] Even if the molecular weight information we have from Figure 5.6 is ignored we are able to identify the protein from

Table 5.1 Comparison of database search results with additional sequence information.

	M.W. range 7000 – 12,000 Da	Total M.W. range
Number of *E.coli* proteins in NCBI database (Version form August, 2000)	1028	10200
Number of proteins containing a tryptic peptide with mass 1244.7 ± 0.5 Da[*)]	10	369
Number of tryptic peptides with mass 1244.7 ± 0.5 Da and starting with I or L[**)]	1	37
Number of tryptic peptides with mass 1244.7 ± 0.5 Da and starting with IA or LA	1	8
Number of tryptic peptides with mass 1244.7 ± 0.5 Da and starting with IAA or LAA	1	2
Number of tryptic peptides with mass 1244.7 ± 0.5 Da and starting with IAAA or LAAA	1	1
Number of tryptic peptides with mass 1244.7 ± 0.5 Da and starting with IAAAN or LAAAN	1	1

*)   oxidized methionine considered as possible modification and maximum number of missed cleavages by trypsin = 4
**)   since I and L have identical masses

86

the database, since only one protein fits the N-terminal pattern eluted from the N-terminal digestion experiment (see third column of Table 5.1). However, if the protein under investigation is not entered in the database, this approach alone will not be sufficient and further *de novo* sequencing techniques will be required.

In conclusion, we have demonstrated the feasibility of combining analytical HPLC column fractionation with nanoliter chemistry and microspot MALDI TOF analysis. This combination allows the performance of dozens of experiments with sample volumes of only a few microliters or less. Such experiments include molecular weight determination, optimization of digestion conditions and multiple chemical or enzymatic reactions. The sequential enzymatic digestion of nanoliter sample volumes yields additional sequence information that allows for a more confident protein identification. This technique is therefore an interesting alternative or a complementary technique to MS/MS fragmentation where more sample is required or where fragment spectra become complex. Current work focuses on the use of this technique to identify more proteins from bacteria extracts. Several proteins have already been successfully identified and a summary of these efforts will be reported elsewhere.[29]

5.4   Literature Cited.

(1)   Fenselau, C. In *Mass Spectrometry for Characterization of Microorganisms*, ACS Symposium Series, Vol. 541, C. Fenselau (Ed.), American Chemical Society, Washington, DC, 1993, pp 1-7.

(2)   Logan, N. A., *Bacterial Systematics*; Blackwell Scientific Publications: London, UK, 1994.

(3)   Goodfellow, M.; O'Donnell, A. G. Eds. *Handbook of New Bacterial Systematics*, Academic Press, San Diego, CA, 1993.

(4)   Dai, Y.; Whittal, R. M.; Li, L. *Anal. Chem.* **1999**, *71*, 1087-1091.

(5)   Wang, Z.; Russon, L.; Li, L.; Roser, D. C.; Long, S. R. *Rapid Commun. Mass Spectrom.* **1998**, *12*, 456-464.

(6)   X. Liang, Zheng, K.; Qian, M. G.; Lubman, D. M. *Rapid Commun. Mass Spectrom.* **1996**, *10*, 1219-1223.

(7)   Dai, Y.; Li, L.; Roser, D. C.; Long, S. R. *Rapid Commun. Mass Spectrom.* **1999**, *13*, 73-78.

(8)   Whittal, R. M.; Keller, B. O.; Li, L. *Anal. Chem.* **1998**, *70*, 5344-5347.

(9)   Dai, Y. Q.; Whittal, R. M.; Li, L. *Anal. Chem.* **1996**, *68*, 2494-2500.

(10)   Whittal, R. M.; Li, L. *Analytical Chemistry* **1995**, *67*, 1950-1954.

(11)   Gobom, J.; Nordhoff, E.; Mirgoroskaya, E.; Ekman, R.; Roepstorff, P. *J. Mass Spectrom.* **1999**, *34*, 105-116.

(12)   Technical information on ZipTip Pipette Tips, Millipore Corp., Waltham, MA, USA.

(13)   Keller, B. O.; Li, L. *J. Am. Soc. Mass Spectrom.* **2000**, *11*, 88-93.

(14)   Kellner, R.; Houthaeve, T. In *Microcharacterization of Proteins*; Kellner, R.; Lottspeich, Meyer, H. E., Eds., Wiley-VCH: Weinheim, Germany, 1999, pp. 97-116.

(15)   Perkins, D. N.; Pappin, D. J. C.; Creasy, D. M.; Cottrell, J. S. *Electrophoresis* **1999**, *20*, 3551-3567.

(16)   Wilkins, M. R.; Gasteiger, E.; Tonella, L.; Ou, K.; Tyler, M.; Sanchez, J.-C.; Gooley, A. A.; Walsh, B. J.; Bairoch, A.; Appel, R. D.; Williams, K. L.; Hochstrasser, D. F. *J. Mol. Biol.* **1998**, *278*, 599-608.

(17)   For a historical review on CID, see Cooks, R. G. *J. Mass Spectrom.* **1995**, *30*, 1215-1221.

(18)   For example, see Biemann, K., In *"Methods in Enzymology: Mass Spectrometry"* McCloskey, J. A., Ed., Vol. 193, Academic Press: San Diego, CA, USA, 1990, pp. 455-479.

(19)   Spengler, B. *J. Mass Spectrom.* **1997**, *32*, 1019-1036, and references therein.

88

(20)   Staudenmann, W.; Hatt, P. D.; Hoving, S.; Lehmann, A.; Kertesz, M.; James, P. *Electrophoresis* **1998**, *19*, 901-908.

(21)   Korostensky, C.; Staudenmann, W.; Dainese, P.; Gonnet, G.; James, P. *Electrophoresis* **1998**, *19*, 1933-1940.

(22)   Sweeney, P. J.; Walker, J. M., In "*Methods in Molecular Biology: Enzymes of Molecular Biology*" Burrell, M., Ed., Vol. 16, Humana Press Inc.: Totowa, NJ, USA, 1993, pp. 319-320.

(23)   Thiede, B.; Liebold-Wittman, B.; Bienert, M.; Krause, E. *FEBS Letters* **1995**, *357*,65.

(24)   Woods, A. S.; Huang, A. Y. C.; Cotter, R. J.; Pasternack, G. R.; Pardoll, D. M.; Jaffee, E. M. *Anal. Biochem.* **1995**, *226*, 15.

(25)   Schriemer, D. C.; Yalcin, T.; Li, L. *Anal. Chem.* **1998**, *70*, 1569-1575.

(26)   Hoving, S.; Münchbach, M.; Schmid, H.; Signor, L.; Lehmann, A.; Staudenmann, W.; Quadroni, M.; James, P. *Anal. Chem.* **2000**, *72*, 1006-1014.

(27)   http://prospector.ucsf.edu

(28)   http://www.ncbi.nlm.nih.gov

(29)   Wang, Z.; Li, L., manuscript in preparation.

89

Chapter 6

High Molecular Weight Protein Analysis with Attomole Sensitivity by Microspot MALDI-TOF MS[a]

6.1 Introduction

Before the introduction of matrix-assisted laser desorption/ionization (MALDI) by Karas and Hillenkamp, other techniques, like plasma desorption (PDMS) or fast atom bombardment (FAB-MS), were not very sensitive for the analysis of biomolecules in the mass range above 10,000 daltons. Extrapolating from their initial results in 1988, Karas and Hillenkamp predicted detection limits for their technique in the subnanogram range for high molecular weight proteins.[1] And indeed, advancements in detector technology, post-source acceleration features, and introduction of new matrix substances have led to more accurate and especially more sensitive MALDI methods for the analysis of high molecular weight proteins. For example, Beavis and Chait reported in 1990 the detection of proteins up to 150,000 Da with picomole sensitivity.[2] Nelson, *et al.* demonstrated the successful analysis of human immunoglobulin, IgM, in 1994.[3] Shortly thereafter, they were able to detect the singly-charged species of IgM. This was the first report of mass spectrometric detection of a biomolecule in excess of 1 megadalton.[4] Until recently the analysis of such extremely high molecular weight proteins has been the domain of MALDI-TOF MS, however Van Berkel, *et al.* reported recently the detection of a multiply-charged intact 1.5 megadalton protein assembly using nanoflow electrospray quadrupole-time-of-flight mass spectrometry.[5]

---

[a] A form of this chapter is in preparation for publication: B. O. Keller, Li, L. "*High Molecular Weight Protein Analysis with Attomole Sensitivity by Microspot MALDI –TOF MS*".

90

Initial limitations such as low detection efficiencies due to poor ion transmission, inefficient detectors, and slow signal processing capabilities, have been improved dramatically in current state-of-the-art instrumentation and are still of some significance in ultrasensitive analysis as described in Chapter 2. Another area of research on improving sensitivity focuses on sample preparation techniques and sample introduction into the mass spectrometer. Especially in bioanalytical projects, detection sensitivity has become an important aspect because of rapidly increasing interest in proteome research.[6] For example, if a change in a proteome is to be correlated with spatial and/or temporal biological events in an organism, the number of cells or amount of tissue taken from a specific locale can be very limited. In addition to the challenge of dealing with a limited supply of sample, there are thousands of different proteins with varying abundances in a cell.[7] Multidimensional separation methods such, as HPLC-fractionation combined with gel electrophoresis, are often required to achieve separation of such a large number of diverse proteins.[8,9] Thus, after sample handling and separation, we are confronted with the reality of performing characterization with a very small amount of purified protein. Furthermore, from the protein analysis and characterization point of view, there are a number of experiments needed to be performed to maximize the information content on these proteins. The desired protein properties to be studied include molecular weight, protein identity, high-order structures, and post-translational modifications.[8]

There are several techniques reported in the literature on sensitivity improvement of mass spectrometric techniques based on electrospray ionization[10-15] or MALDI.[16-23] MALDI MS has also been applied for direct analysis of single cells or individual cell organelles.[20,22,24-26]

In this work, a multiple matrix/sample-layer preparation method is presented. This technique allows analysis of large proteins in low nanomolar concentrations, even in the presence of high amounts of salt contaminants. In previous chapters our nanoliter chemistry (nanochem) station has been introduced.[22] Using this nanochem station for deposition of subnanoliter volumes of protein samples combined with the multiple layer method allows the detection of high molecular weight proteins in the low attomole range, even under physiological conditions. Problems with sample spot location are addressed and a simple method is presented that allows for easy location of sample spots. This

method should be generally applicable to many commercially available and home-built instruments, even if video-observation of the matrix spots is poor in quality or not available at all. In addition, the possibility of using the nanochem station in conjunction with MALDI-TOF MS for monitoring the progression of reactions is demonstrated. A time study on partial and complete reduction of human α_2-macroglobulin confirms its high-order structure.

6.2 Experimental

6.2.1 Chemicals and Reagents. Human α_2-macroglobulin (α_2M, M.W. ~720 kDa), anti-bovine IgG (M.W. ~150 kDa), bovine lactoferrin (M.W. ~80 kDa), bacteriorhodopsin (M.W. ~27 kDa), trifluoroacetic and formic acid, dithiothreitol (DTT), iodoacetamide, sinapinic acid, 2,5-dihydroxybenzoic acid (DHB), 5-methoxybenzoic acid, 2-(4-hydroxy-phenylazo) benzoic acid (HABA) and α-cyano-4-hydroxycinnamic acid (4-HCCA) were purchased from Sigma-Aldrich-Fluka Canada (Oakville, Ontario, Canada). 4-HCCA was recrystallized from ethanol (95%) at 50C before use. Glassclad 18, used to deactivate the fused-silica capillaries used for sub-nanoliter volume deposition, was from United Chemical Technologies (Bristol, PA, USA). Polishing cloth and 1 & 0.3 micron alumina for target polishing were from Buehler (Lake Bluff, IL, USA). Protein stock solutions were made up in distilled water at a concentration of 1 mg/mL. Final protein concentrations and mixing ratios with matrix substances are mentioned for each spectrum in the following sections. All protein solutions were prepared in siliconized polypropylene vials (Rose Scientific, Edmonton, Alberta, Canada) to minimize sample loss by container wall adsorption.

6.2.2 Matrix and Sample Preparation. For the method comparison study, matrix and sample preparation are briefly described and referenced in the Result and Discussion section. Probe tips for the MALDI mass spectrometer were initially polished using a slurry of 1 µm and finally 0.3 µm alumina on a polishing cloth. Before use, the probe was sonicated in a 1:1 mixture of ethanol/10% formic acid for 15 minutes. The multilayer method used is a modified version of a previously reported double layer method.[27,28] As a very thin first layer a ~1 µL volume of a 20 mg/mL solution of 4-

92

HCCA in 40% methanol in acetone was deposited onto a MALDI target spot. The drop spreads over the whole target spot and evaporates quickly, leaving a very thin layer of tiny matrix crystals. The layer was visually checked over with a 30x magnification handheld microscope for cavities and if necessary the first layer formation was redone. As a second layer a 0.4 μL volume of saturated 4-HCCA in 40% methanol in water was then deposited onto the first layer. The third and last layer was a ~0.3 μL volume of the protein sample solution. Basic protein solution had to be acidified before deposition (e.g. with 0.1% TFA), otherwise the matrix layers would dissolve. As a washing step, a ~0.5 μL volume of dist. water was deposited on top of the third layer and blown off with pressurized air after approx. 30 seconds. However, it was found that for larger proteins (>30 kDa) washing steps were often not necessary (and sometimes not advantageous because of sample loss) even in the presence of high amounts of salt.

6.2.3 Microspot Sample Deposition and In-Capillary Reduction Reaction. The employed nanoliter chemistry station, and the sub-nanoliter handling procedures have been described in more detail elsewhere.[19,20,22,29] Briefly, a 20-μm-ID capillary tube connected to a syringe was used to draw a sub-nanoliter volume of protein sample from a small pipette tip. This small volume was then directly deposited onto the second matrix layer. For the α_2-macroglobulin reduction study, a ~150 pL volume of loaded sample was allowed to dry close to the entrance of the capillary, then an ~200 pL volume of 45 mM DDT solution was drawn into the capillary and allowed to react for 1 or 5 minutes before the mixture was directly deposited as described above.

The resulting sample spots were only approx. 150 μm in diameter and would be very hard to find for laser desorption, especially since our commercial instrument was not equipped with video cameras. We therefore developed the following strategy, which should be applicable to other commercial or home-built instruments with no video visualization capability or if the resulting microspot is hardly or not at all visible on the MALDI target. In this method, the matrix-covered probe tip was first placed into the mass spectrometer. Using software control, the probe tip can be moved in the plane parallel to the extraction plate. Scanning a cross section of the whole sample spot area can be easily done. Three laser marks were then created by firing high laser-power pulses (~16 μJ) onto three different regions (see Figure 6.1). This creates two corridors

93

into which subsequently two microspot samples can be accurately deposited, after removing the tip from the mass spectrometer and returning it to the nanochem station. Since the software-controlled mechanics of the probe tip positioning is very accurate and reproducible it is therefore easy to find the sample spot by scanning within a corridor, after placing the probe tip back into the mass spectrometer.
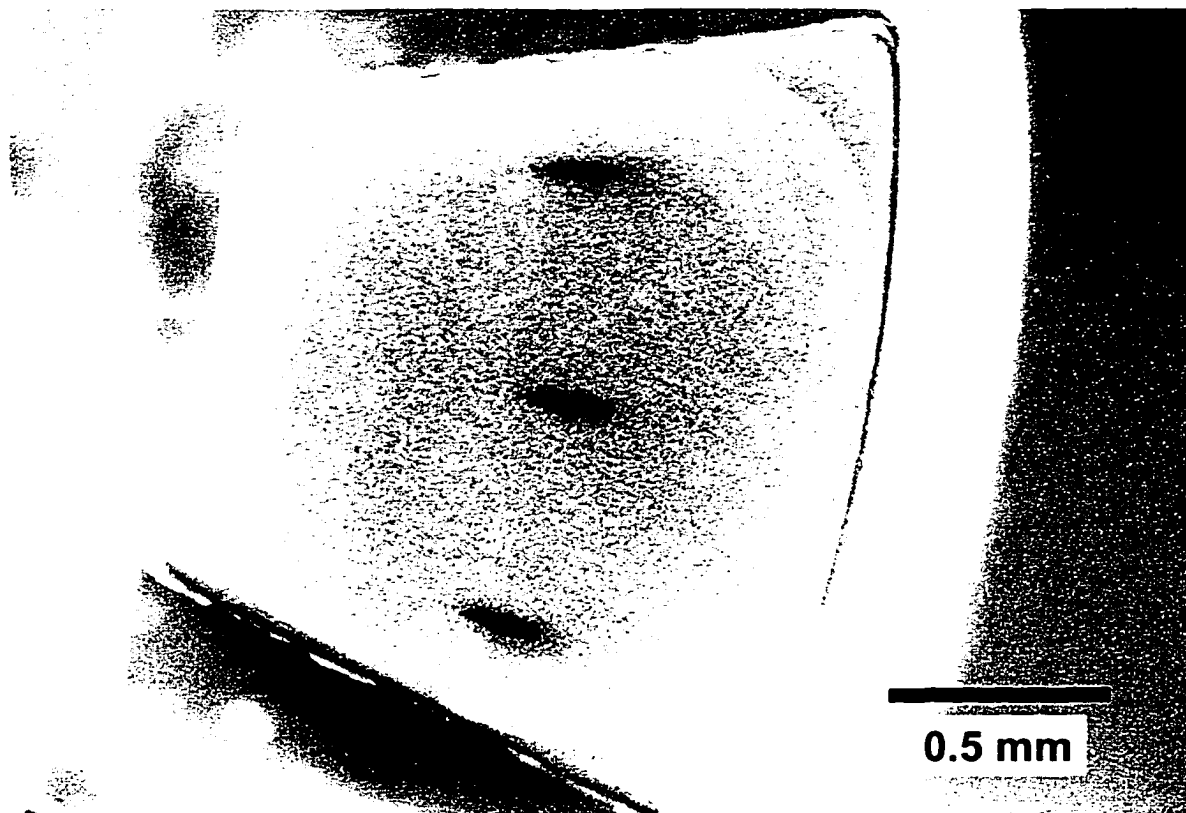
Figure 6.1   Microscopic image (40x) of the sample probe tip after 4-HCCA matrix deposition and formation of three laser marks.

6.2.4   MALDI-TOF MS and Data Processing. Mass spectral data of proteins were collected on a model G2025A LD-TOF continuous extraction system (Hewlett-Packard, Reno, NV, USA). This instrument was operated in positive ion mode at high acceleration voltage (28 kV) with an additional post-source acceleration voltage (-5 kV). The instrument was equipped with a pulsed nitrogen laser (337 nm radiation, 3 ns pulse width, model VSL 337ND, Laser Sciences Inc., Newton, MA, USA). In general, 50-100 laser

94

shots were averaged to produce a mass spectrum. Spectra were acquired and processed with Hewlett-Packard supporting software and reprocessed with the Igor Pro software package (WaveMetrics Inc., Lake Oswego, OR, USA).

6.3 Results and Discussion

6.3.1 Comparison of Different Matrix/Sample Preparation Methods. In MALDI-TOF analysis, there is a subtle difference in sample handling for detection of high molecular weight analytes (i.e., M.W. > 30 kDa in our TOF instruments), compared to low molecular weight species.[30] On the one hand, the large analyte needs to be isolated with a relatively larger number of matrix molecules in the co-crystals (or a greater matrix to analyte ratio), causing the reduction of analyte concentration in the solid phase. On the other hand, detection sensitivity of TOF instruments generally start to degrade for the detection of ions with m/z above 30,000, likely due to the reduction of detection efficiency of conventional detectors such as the multi-channel plate detector.[4,30] In addition, the possibility of sample loss in the sample handling procedure is greater for larger proteins than for small proteins or peptides, most likely due to their size and the related higher abundance of non-specific binding sites, such as hydrophobic patches, charged groups, and hydrogen bonding sites.[31] We paid particular attention to these factors during the process of optimizing the performance of our method. The goal of method development for protein mass spectrometry is to obtain an optimal resolution and detection sensitivity for the analytes under investigation. However, the method that gives the best resolution might not necessarily be the most sensitive. Because even a low-resolution mass spectrometry technique will provide much better mass accuracy than methods such as gel electrophoresis or gel permeation techniques, sensitivity improvement seems to play a more important role in mass spectrometric method development for large protein analysis than improvement of resolution. We compared several reported methods for matrix/sample preparation using as analyte bovine lactoferrin, an iron binding protein, which is commonly found in milk and other external secretions. Figure 6.2 shows the mass spectra for these methods at different
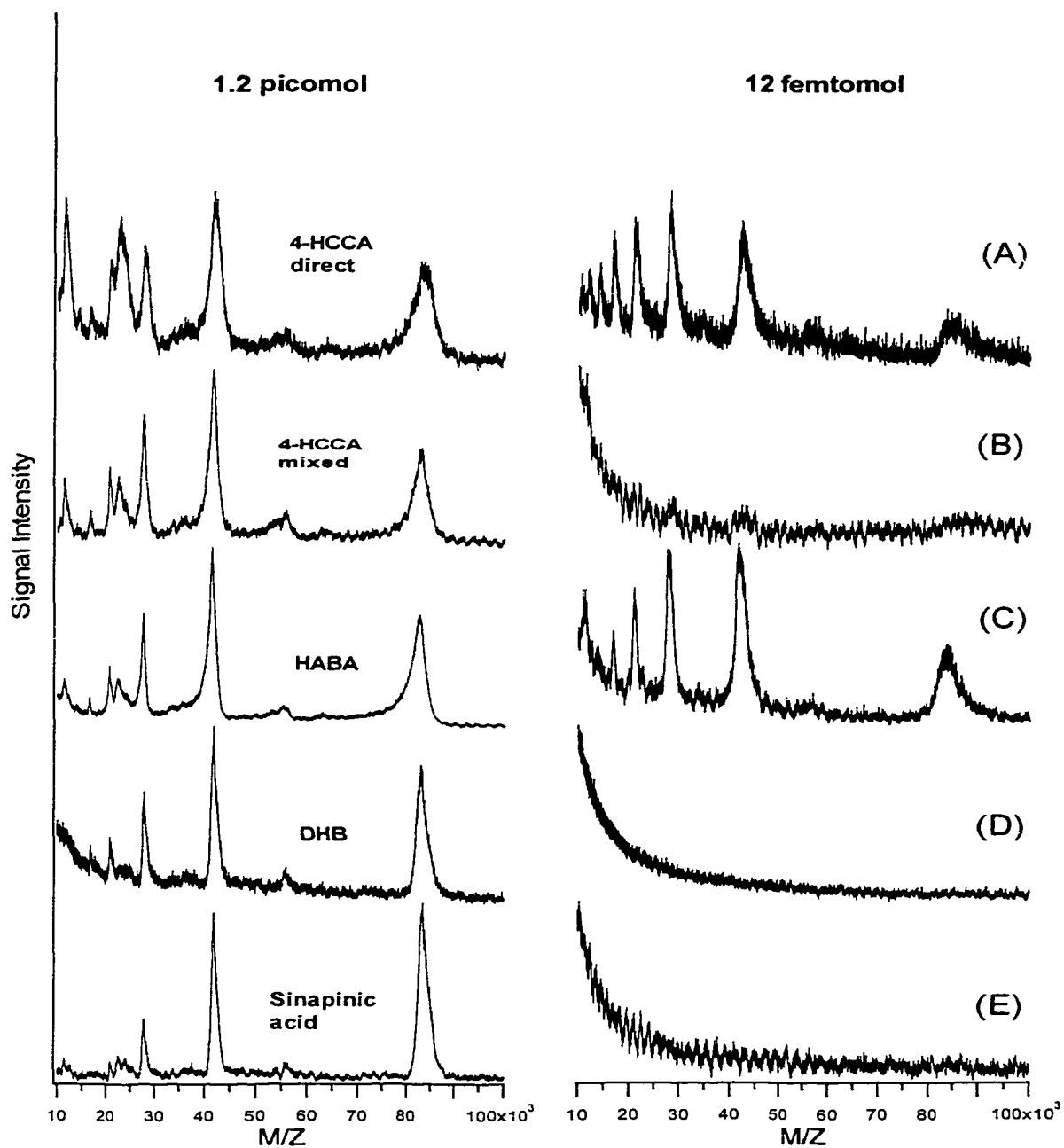
Figure 6.2 Comparison of different matrix/sample preparation methods with
lactoferrin (Lf, M.W. ~80 kDa) as sample analyte (A) Direct deposition
onto 4-HCCA covered target as described in the text. (B) Deposition of
aqueous Lf solution mixed with sat. HCCA onto first 4-HCCA matrix
layer. (C) Method according to Juhasz, *et al.* using HABA as matrix. (D)
Method according to Spengler, *et al.* using DHB as matrix. (E) Method
using sinapinic acid as matrix according to Dai, *et al.*

96

Table 6.1   Resolution comparison of singly charged species of bovine lactoferrin for different sample/matrix preparations.

Label in Fig. 6.2.	Matrix & Method	Resolution (FWHM) 1.2 picomole	Resolution (FWHM) 12 femtomole
(A)	4-HCCA (direct deposition)	~18	~7
(B)	4-HCCA (mixed)	~25	Not detectable
(C)	HABA[33]	~27	~21
(D)	DHB[32]	~36	Not detectable
(E)	Sinapinic acid[27,28]	~38	Not detectable

levels of analyte amount present. In Table 6.1 the obtained resolution values for the singly charged molecular ion of lactoferrin are listed for the individual experiments. The two-layer method of Dai, *et al.* using sinapinic acid[27,28] and the method of Spengler and coworkers using DHB as matrix substance,[32] give the best resolution for this analyte at high concentration. However, it becomes clear that at low analyte abundance only the method of Juhasz, *et al.* using HABA as matrix,[33] and our direct deposition method onto 4-HCCA are suitable for protein detection. The HABA method gives a slightly better resolution and for aqueous standard protein solution, and a similar sensitivity can be achieved as for our multiple layer method (see Figure 6.3A). However, there are several disadvantages using HABA as a matrix substance. Direct deposition onto a HABA covered MALDI target did not yield any signals and premixing of the analyte solution is therefore a necessity. The direct deposition option of our method is however quite advantageous, since it allows the employment of lower concentrations and smaller volumes, as is shown later in the microspot section. Direct deposition is also advantageous for future implementation into automated sample preparation. Another disadvantage of HABA is its low salt tolerance. As is shown in Figure 6.3B even at a salt

97
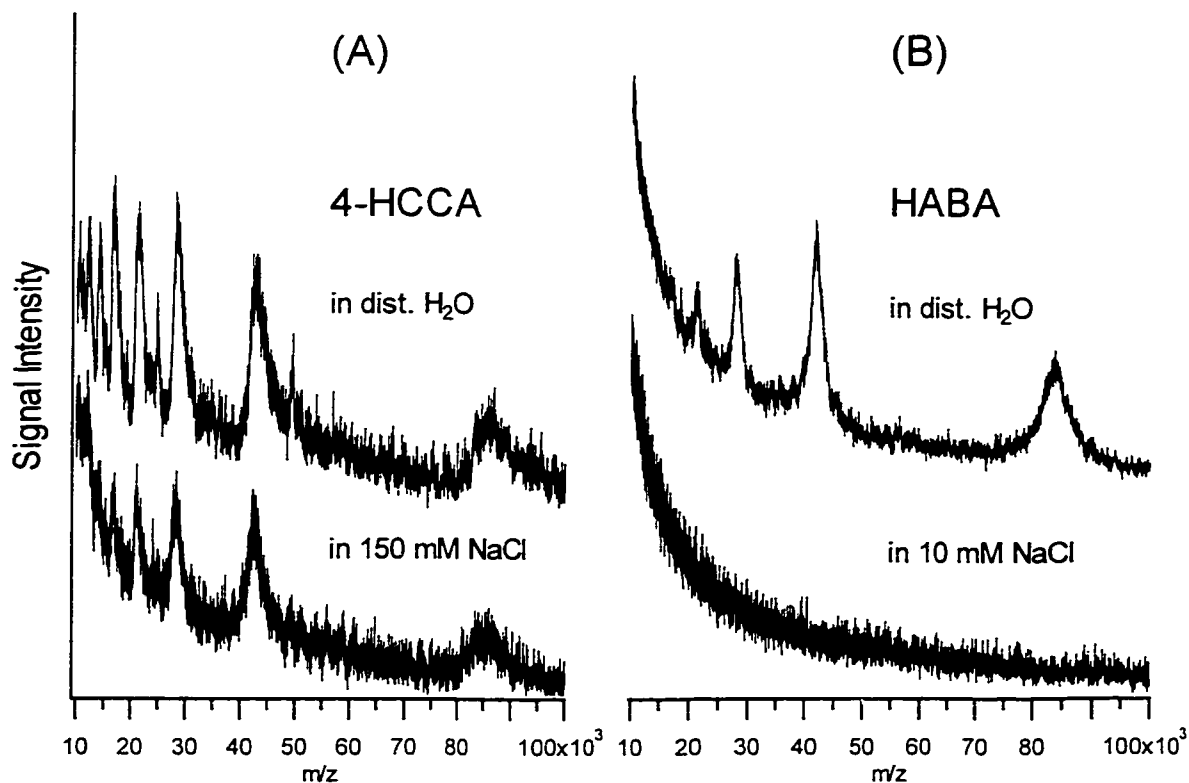
Figure 6.3. Comparison of 4-HCCA versus HABA. For each experiment a total protein amount of ~2 femtomole was used. (A) Direct depositions of 0.2 μL 10 nM lactoferrin solutions (top: in dist. water, bottom: in 150 mM NaCl) onto 4-HCCA covered targets. (B) 0.2 μL of 10 nM lactoferrin solutions (top: in dist. Water, bottom in 10 mM NaCl mixed 1:2 with HABA, 1.5 mg in acetonitrile:methanol:water [40:40:20]).

concentration of 150 mM our method still gives strong signal at the 2 femtomole level without using a washing step. HABA however, does not give any signal for the same analyte amount in the presence of only 10 mM salt. The double layer of 4-HCCA withstands several washing steps if necessary but HABA crystals are too soluble in water and many matrix crystals that contain analyte are easily washed off. It should be noted that we also deposited protein samples directly onto our first matrix layer, which resembles the method as reported by Vorm, *et al.* for peptides.[34] We found that the same low detection limits can be achieved for standard proteins in aqueous solutions as with the two-layer matrix preparation method (data not shown); however, the method is not as

98

rugged. The single layer is much more easily washed off when washing steps are applied or in cases where the sample solution contains slightly basic buffers (pH 7-8) or organic modifiers, the single layer dissolves easily, thus ruining the experiment. The lowest concentration of lactoferrin, which could be directly analyzed, was approx. 10 nanomolar. However, when multiple depositions are done with lower concentrated solutions, protein signals can still be obtained as demonstrated in Figure 6.4. In this case, the ruggedness provided by the second matrix layer is a benefit, since multiple depositions onto only the first matrix layer easily wash parts of the layer off. It should be noted however, that on-target concentration by multiple deposition is generally only of limited use, especially if samples are high in salt and/or buffer contents.
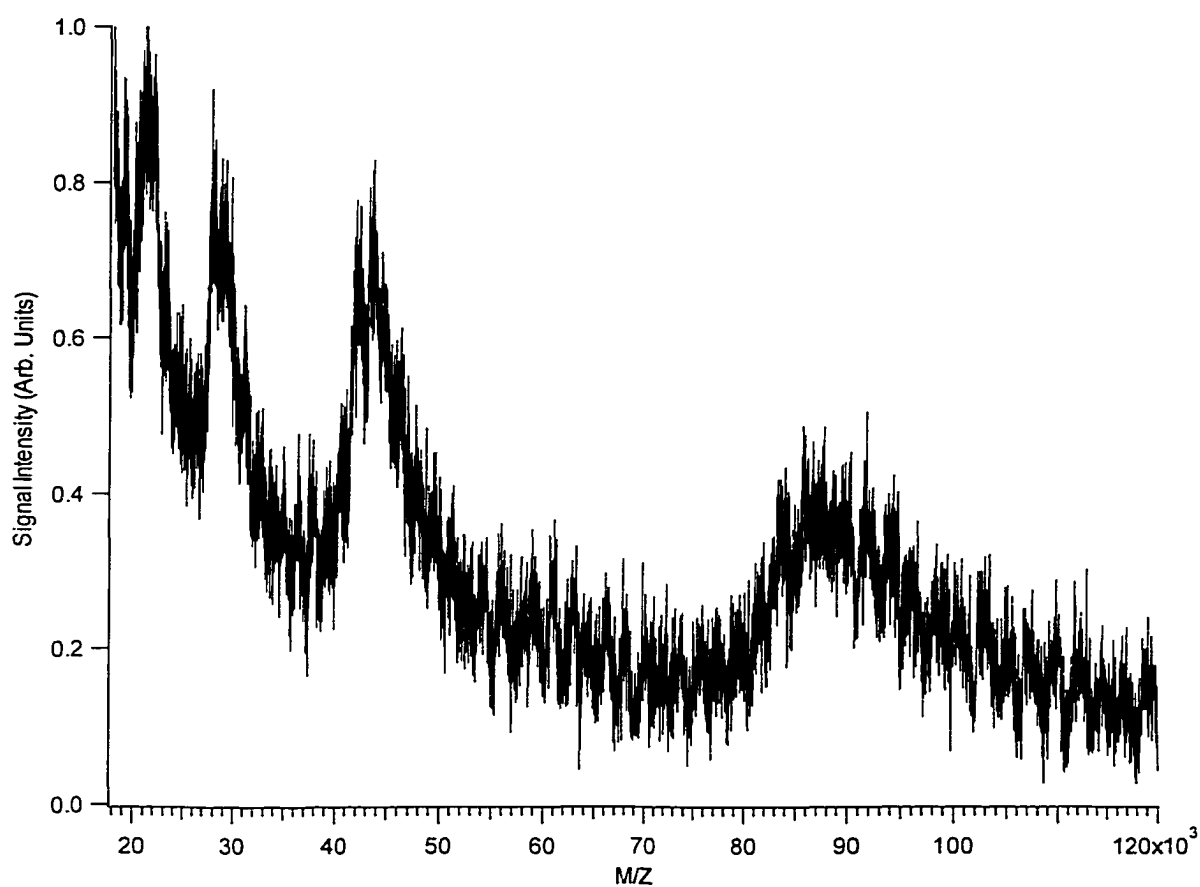
Figure 6.4   MALDI mass spectrum of a dilute Lf solution. Fifteen 0.2 μL aliquots of a 1 nM aqueous solution were spotted onto the same matrix-covered target (Total protein loading: ~3 femtomole).

99

To test our method, we analyzed several samples from different sources, which could not be analyzed previously without extensive purification and/or concentration procedures. The results are combined in Figure 6.5. Despite the high amounts of buffers and salts, all three samples are detectable without applying any washing steps. The attempt to analyze these samples by depositing them only onto the first matrix layer was unsuccessful; the layer dissolved. The slightly thicker matrix layer achieved by the double deposition technique is again an advantage since the layer is able to neutralize slightly basic buffers (pH 7.5-8) right on target and better withstands dissolvation. Of course, for samples at higher pH, neutralization will still be necessary prior to sample deposition. Our technique has quickly become a routine method in our laboratory because of its simplicity and high sensitivity. This method is very useful, especially as a preliminary fast screening method for unknown protein samples.

6.3.2 Microspot MALDI-TOF Analysis. The deposition of sub-nanoliter volumes of samples onto the double layer matrix using our nanoliter chemistry station allows the analysis of low attomole amounts of protein. This is demonstrated in Figure 6.6. Even at a level of 4 attomoles the molecular ion and the doubly-charged ion for lactoferrin are still detectable. Several aspects of instrumentation and sample preparation are responsible for the success of such a low-level protein analysis. For both macro- and microspot analysis the post-source acceleration feature in the commercial instrument, which enhances the sensitivity for high molecular weight analytes and the careful matrix layer preparation are crucial. In addition, for the microspot technique the described exact laser beam and probe tip control is essential. Figure 6.7 demonstrates that the microspot technique also works with sinapinic acid as matrix substance, but of course only with higher analyte amounts. In this case an additional fourth layer of matrix solution on top of the sample layer has to be deposited to achieve analyte desorption and ionization (i.e. using the sandwich method).[27,28] The reason for this is most likely the reduced solubility of sinapinic acid in aqueous media compared to 4-HCCA. The very short time span of sample deposition and sample drying could lead to insufficient mixing and co-crystallization of sinapinic acid and proteins. Compared to sinapinic acid, 4-HCCA enhances the formation of multiply-charged ions. (for example, see Figures 6.1, 6.6, or

100
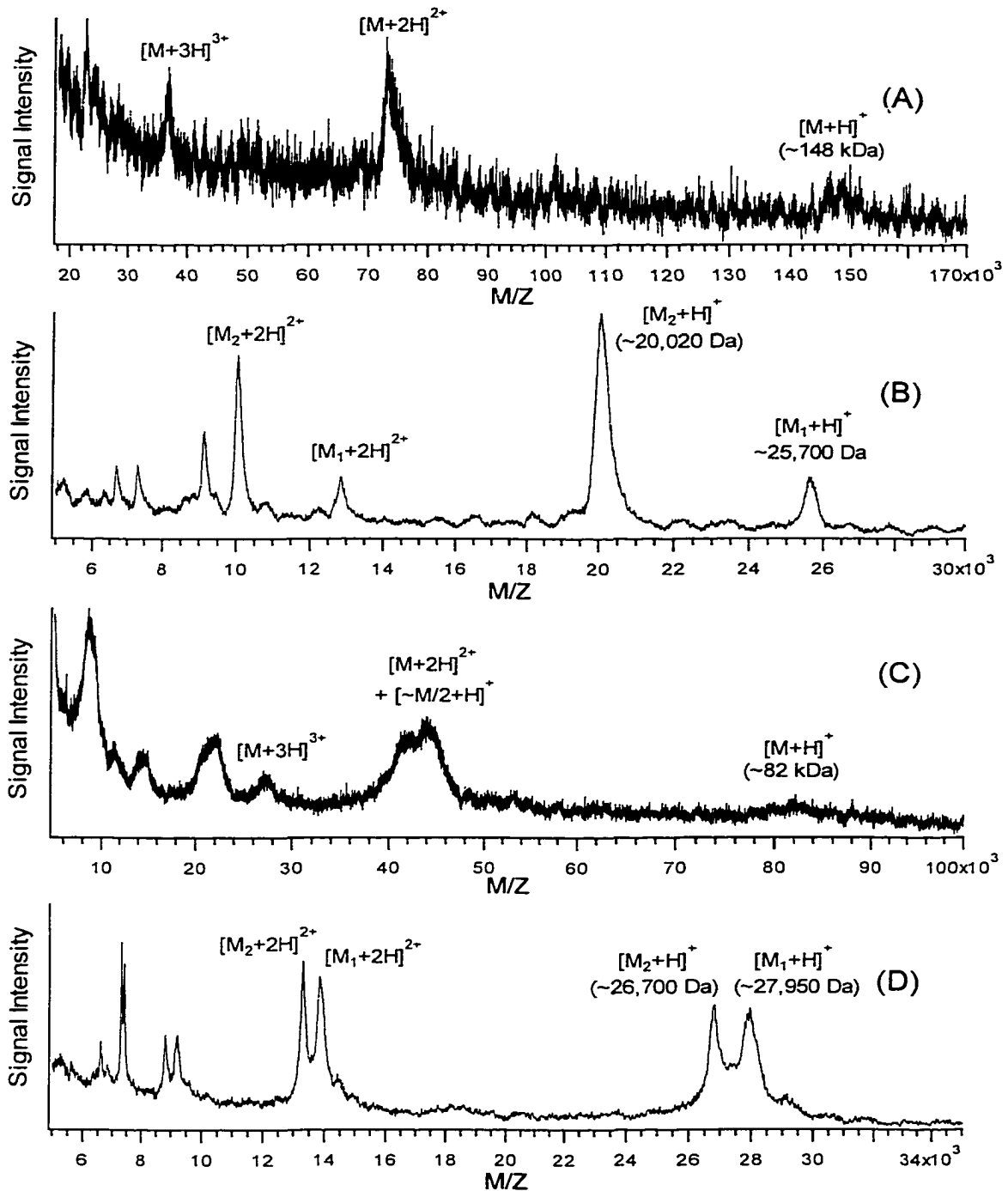
Figure 6.5 MALDI mass spectra of 'difficult' protein samples using the multilayer matrix/sample preparation. (A) Cleaved anti-gal IgG sample in PBS buffer (100 mM phosphate, 150 mM NaCl) (B) HRV protein mixture in 300 mM NaCl, 20 mM Imidazol and 0.2 % EDTA (pH ~7.5) (C) Natural secreted form of human P97 protein (M.W. of deglycosylated form ~82 kDa, gift from Dr. Luis Sojo, ABR Vancouver) in unknown solution conditions. (D) Bacteriorhodopsin, a very hydrophobic membrane protein, in aqueous solution.

101
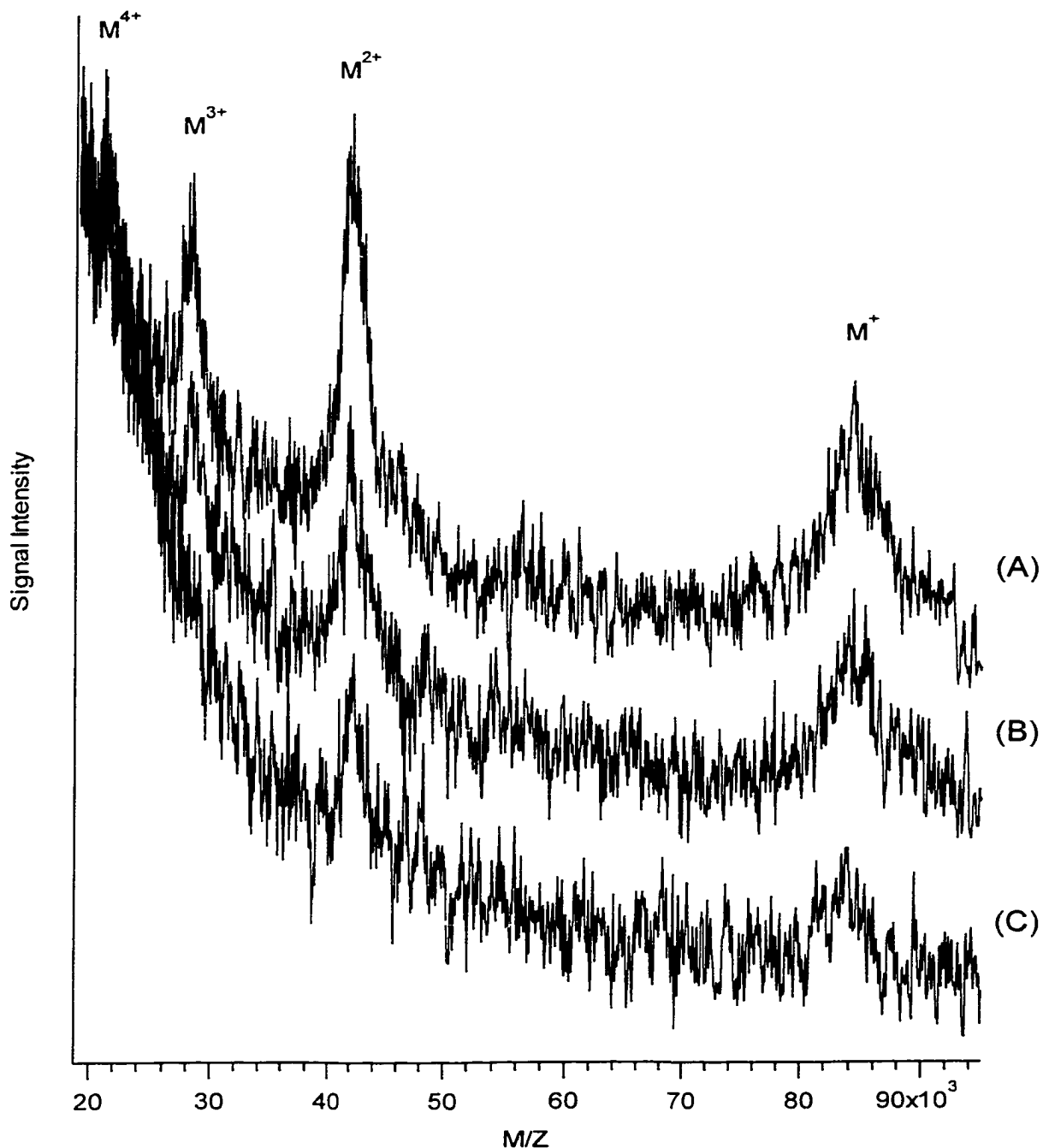
Figure 6.6 MALDI mass spectra of bovine lactoferrin in aqueous solution using 4-HCCA as the matrix: (A) 570 pL of 2 ng/μL lactoferrin loaded (14 amol) (B) 270 pL of 2 ng/μL lactoferrin loaded (7 amol) and (C) 170 pL of 2 ng/μL loaded (4 amol). Samples were loaded with a freshly prepared capillary in reverse order (C), (B), (A) and the capillary was rinsed with 50% acetonitrile/0.1% TFA in between sample loadings to minimize carryover.

102

6.7). This can be a disadvantage when analyzing protein mixtures due to the added complexity; but in case of reduction studies of single proteins this can also be advantageous, as is shown below.
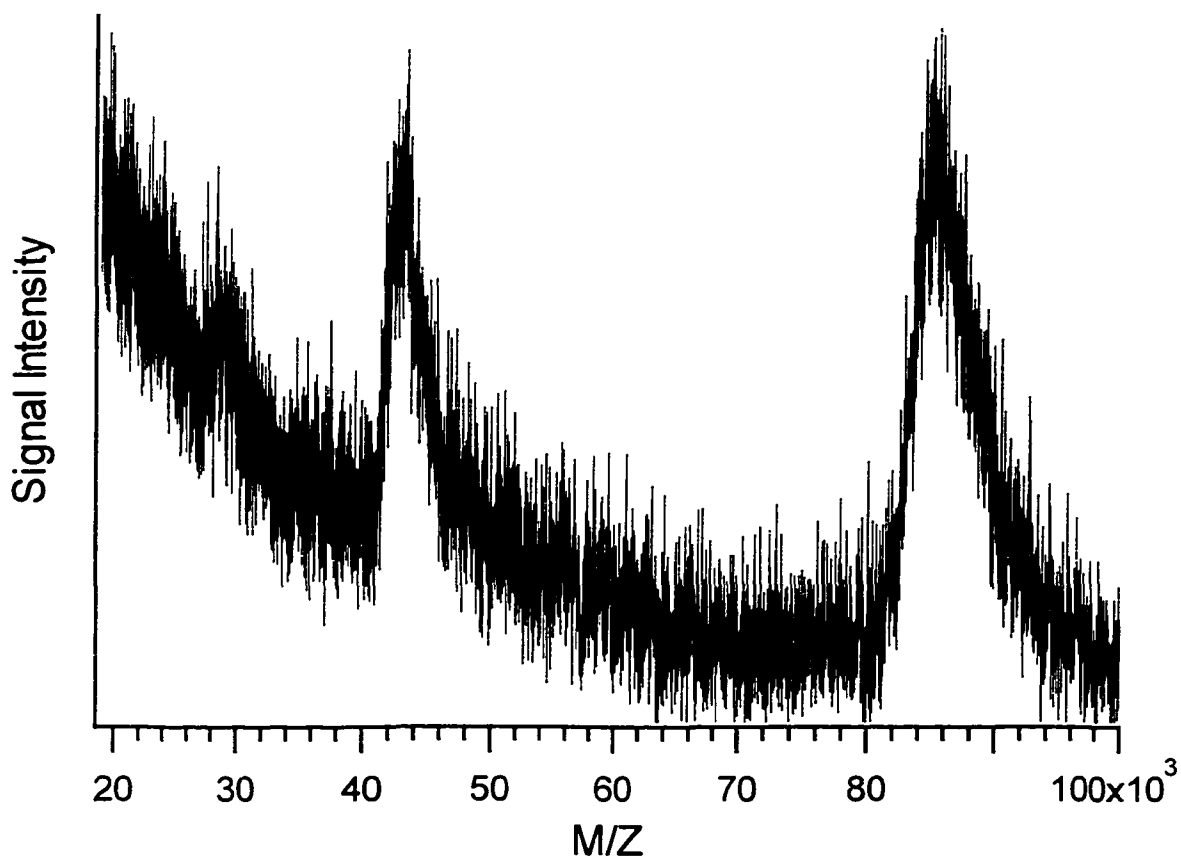
Figure 6.7   MALDI mass spectrum of lactoferrin in aqueous solution using sinapinic acid as the matrix. About 490 pL of 40 ng/μL lactoferrin (250 amol) were loaded.

As already shown above, the multilayer matrix/sample preparation is very tolerant to high salt concentrations. Figure 6.8 demonstrates the possibility of analyzing large proteins such as antibodies in physiological saline solution without a washing step at the attomole level by using the microspot MALDI technique. As plasma proteins, antibodies like IgG are very water-soluble. For many applications such as single cell analysis,[20,22] it is desirable to directly analyze salt-containing protein samples.

103
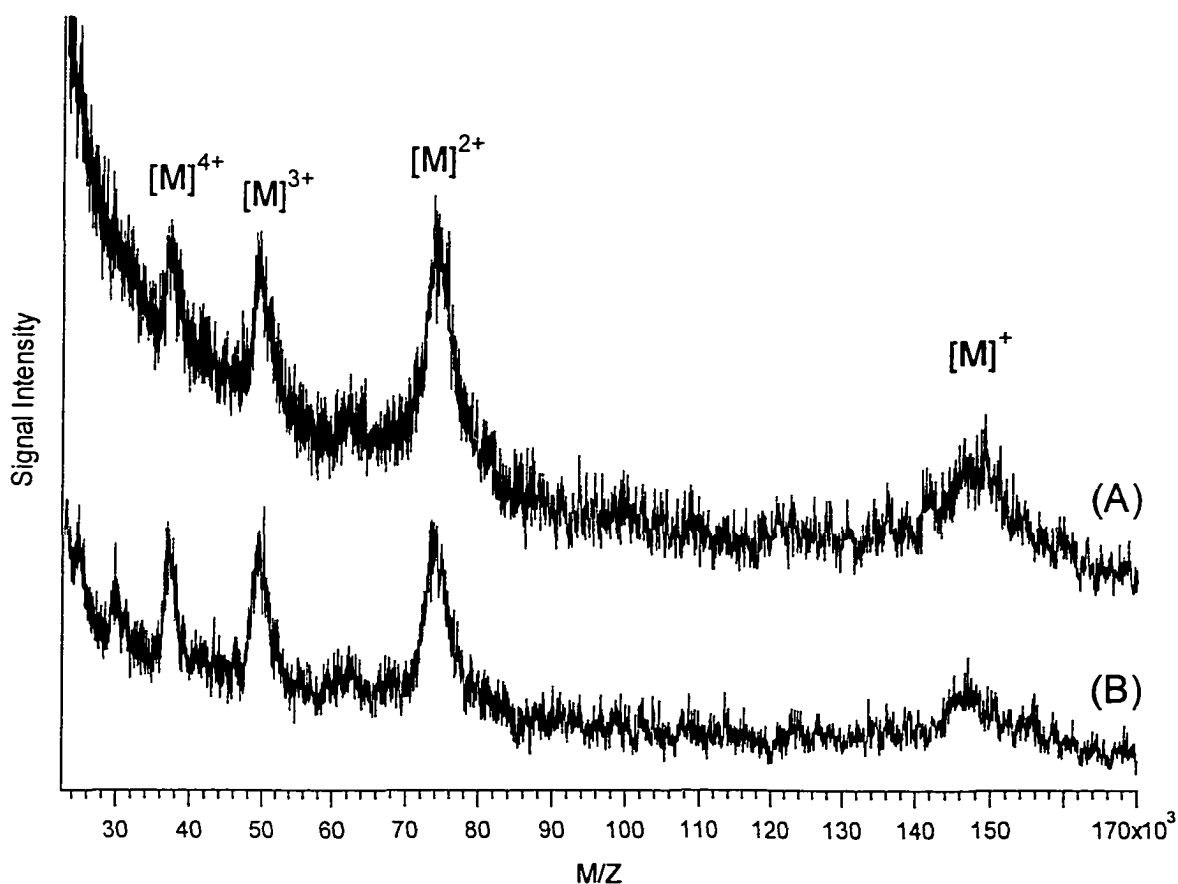
Figure 6.8   MALDI mass spectra of an antibody (IgG) obtained by (A) loading 420 pL of 0.01 μg/μL IgG in water (29 amol) and (B) loading of 310 pL of 0.01 μg/μL IgG in 150 mM NaCl (21 amol).

6.3.3 Reduction of Disulfide Linkages.

Many high molecular weight proteins such as antibodies or macroglobulins consist of multiple subunits, which are interlinked through disulfide linkages or non-covalent interactions. Reduction of the disulfide linkages leads to the free subunits and their analysis can provide valuable structural information. As an example, the protein α_2-macroglobulin (α_2-M) is a tetramer consisting of four identical 180 kDa subunits. Two subunits are assembled into a dimer through disulfide linkages, and the resulting two dimers are connected through non-covalent forces.[35,36] To deduce information on the presence of disulfide linkages, several

104

experiments to monitor the progression of the reduction process are often required. The advantage of combining nanoliter chemistry with microspot MALDI is the significant reduction of sample amount required for each experiment, thereby reducing the total amount of sample required for a set of experiments.

Figure 6.9 is a schematic illustration of the events happening during MALDI ionization and reduction with DTT.
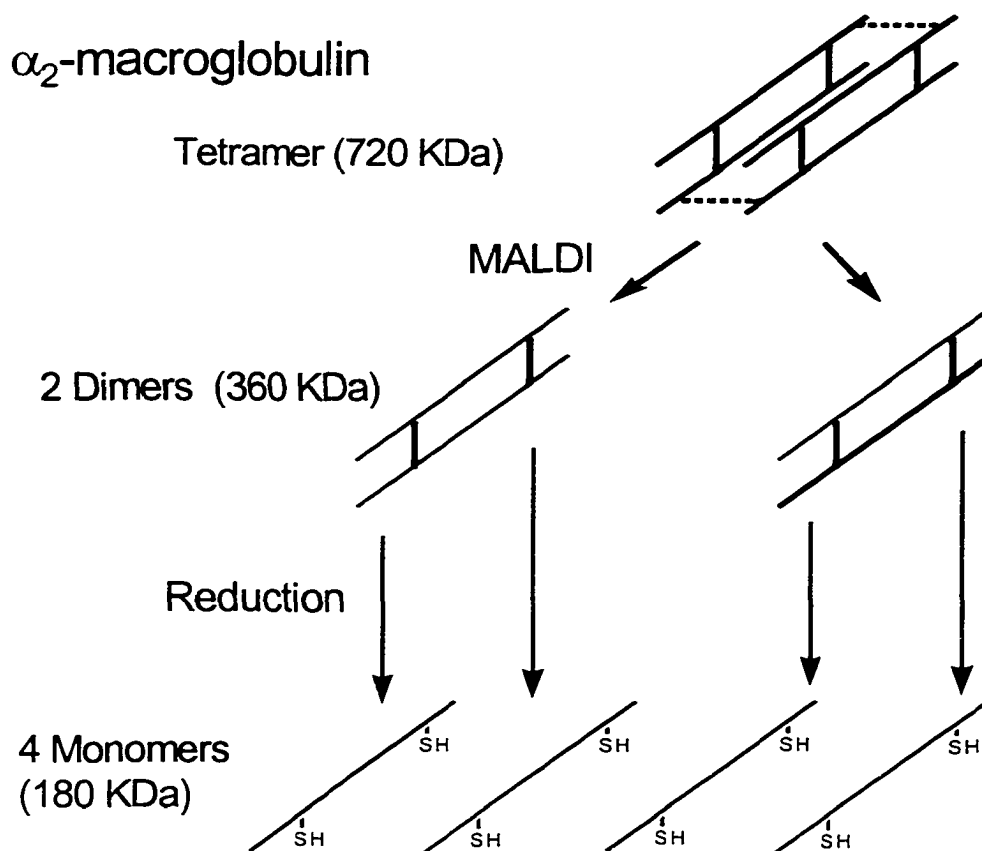
Figure 6.9   Schematic for cleavage of α_2-macroglobulin during MALDI and reduction processes. The diagonal bars represent the monomers and the vertical bars represent disulfide linkages. The dashed horizontal bars represent non-covalent linkages, which are broken during MALDI ionization.
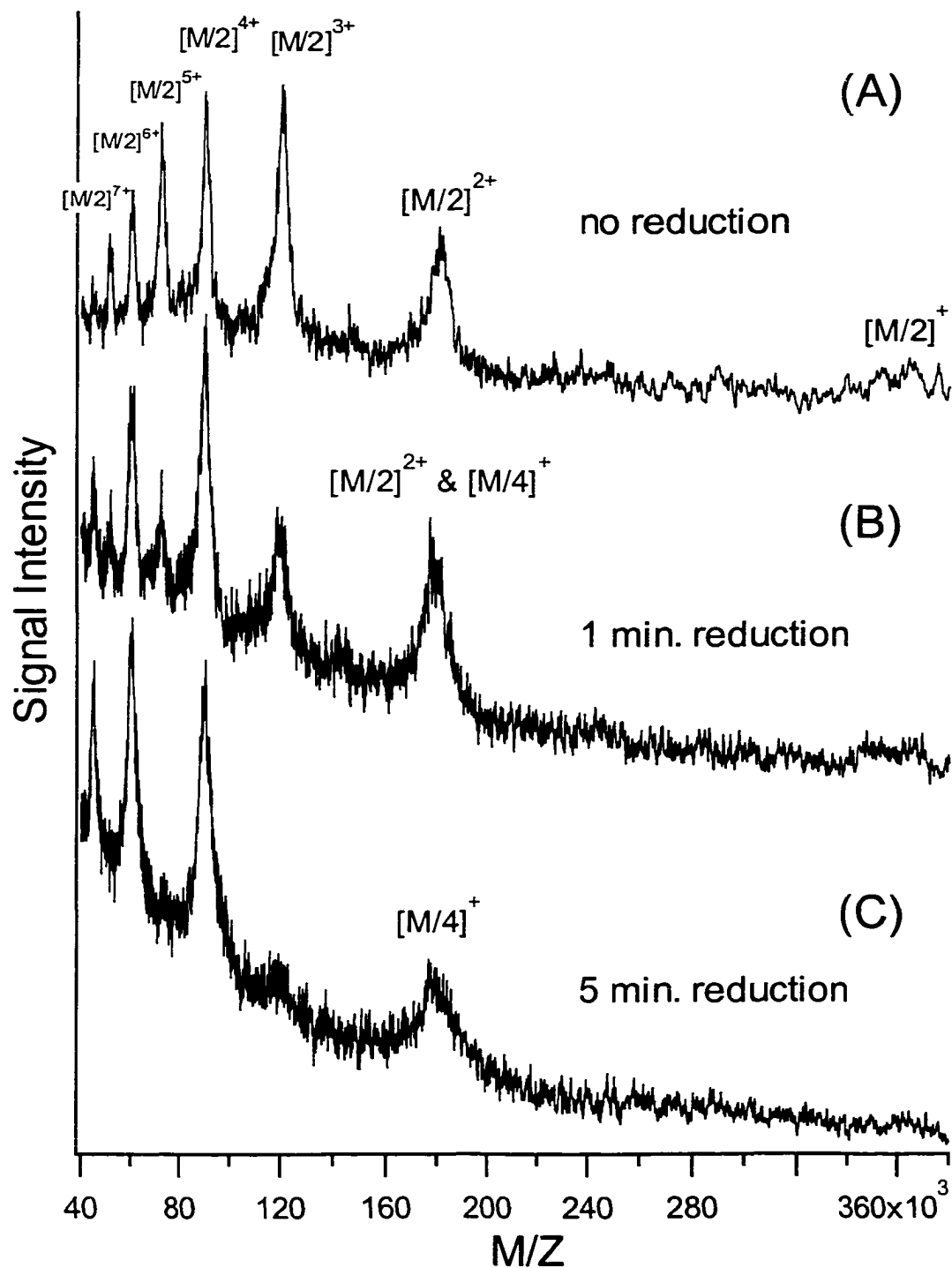
Figure 6.10 MALDI mass spectra of in-capillary reduction study of human α_2-macroglobulin. (A) Total loading of 20 amol, no reduction. (B) Total loading of 70 amol, 1 min. reduction with DTT. (C) Total loading of 75 amol, 5 min. reduction with DTT.

106

Figure 6.10A-C show mass spectra of non-reduced, partially-reduced and fully reduced α_2-M, respectively. The signal intensities of the ions with the odd charges of the non-reduced form (i.e. $[M/2]^{3+}$, $[M/2]^{5+}$, $[M/2]^{7+}$ in Figure 6.10A, where [M/2] stands for the dimer subunit of α_2-M) start to decline in the partially reduced form (Figure 6.10B) and finally disappear (Figure 6.10C). This follows the dissociation of the 360 kDa dimers by reduction, yielding the 180 kDa subunits or [M/4] as labeled in Figure 6.10A. This study benefits from the enhanced multiply-charged ion formation, which is a characteristic of the employed 4-HCCA matrix.[37] Note that the reduction steps require more protein than the simple molecular weight determination. This is most likely due to adsorption loss to the capillary wall during the drying step and/or due to the sensitivity loss resulted from introduced contaminants with the used reagents. Nevertheless, this structural study was performed with a total amount of less than 200 attomole of protein.

In conclusion, a method is presented which allows for very sensitive MALDI analysis of high molecular weight proteins. Simplicity, salt, and buffer tolerance make it an ideal screening method for difficult proteins, including very hydrophobic proteins. The combination of this technique with sub-nanoliter deposition techniques allows for low attomole detection sensitivity in commercial and home-built instruments. Introduction of reduction chemistry allows for high-order structural investigations at a sub-femtomole level.

6.4   Literature Cited

(1)   Karas, M.; Hillenkamp, F. *Anal. Chem.* **1988**, *60*, 2299-2301.

(2)   Beavis, R. C.; Chait, B. T. *Anal. Chem.* **1990**, *62*, 1836-1840.

(3)   Nelson, R. W.; Dogruel, D.; Williams, P. *Rapid Commun. Mass Spectrom.* **1994**, *8*, 627-631.

(4)   Nelson, R. W.; Dogruel, D.; Williams, P. *Rapid Commun. Mass Spectrom.* **1995**, *9*, 625.

(5)   Van Berkel, W. J. H.; Van Den Heuvel, R. H. H.; Versluis, C.; Heck, A. J. R. *Protein Sci.* **2000,** *9,* 435-439.

(6)   See for example, *Proteome Research: New Frontiers in Functional Genomics*; Wilkins, M. R.; Williams, K. L.; Appel, R. D.; Hochstrasser, D. F.; Eds.; Springer, Berlin, 1997.

(7)   Alberts, B.; Bray, D.; Lewis, J.; Raff, M.; Roberts, K.; Watson, J. D. *Molecular Biology of the Cell*; Garland: New York, 1994, 3rd Ed; Chapter 4.

(8)   Klose, J. *Electrophoresis,* **1989,** *10,* 140-152.

(9)   Rout, M. P.; Aitchison, J. D.; Suprapto, A.; Hjertaas, K.; Zhao, Y.; Chait, B. T. *J. Cell Biol.* **2000,** *148,* 635-651.

(10)   Andren, P. E.; Emmett, M. R.; Caprioli, R. M. *J. Am. Soc. Mass Spectrom.* **1994,** *5,* 867-869.

(11)   Wilm, M.; Shevchenko, A.; Houthaeve, T.; Breit, S.; L., S.; Fotsis, T.; Mann, M. *Nature* **1996,** *379,* 466-469.

(12)   Valaskovic, G. A.; Kelleher, N. L.; McLafferty, F. W. *Science* **1996,** *273,* 1199-1200.

(13)   Hofstadler, S. A.; Severs, J. C.; Smith, R. D.; Swanek, F. D.; Ewing, A. G. *Rapid Commun. Mass Spectrom.* **1996,** *10,* 919.

(14)   Lazar, I. M.; Ramsey, R. S.; Sundberg, S.; Ramsey, J. M. *Anal. Chem.* **1999,** *71,* 3627-3631.

(15)   Gucek, M.; Gaspari, M.; Walhagen, K.; Vreeken, R. J.; Verheij, E. R.; Van der Greef, J. *Rapid Commun. Mass Spectrom.* **2000,** *14,* 1448-1454.

(16)   Jespersen, S.; Niessen, W. M. A.; Tjaden, U. R.; Greef, v. d. J.; Litbom, E.; Lindberg, U.; Roeraade, J. *Rapid Commun. Mass Spectrom.* **1994,** *8,* 581-584.

(17)   Solouki, T.; Marto, J. A.; White, F. M.; Guan, S.; Marshall, A. G. *Anal. Chem.* **1995,** *67,* 4139-4144.

(18)   Zhang, H.; Caprioli, R. M. *J. Mass Spectrom.* **1996,** *31,* 690-692.

108

(19) Golding, R. E.; Whittal, R. M.; Li, L. In *Proceedings of the 43rd ASMS Conference on Mass Spectrometry and Allied Topics*; Atlanta, GA, May 21-26, 1995; p 1223.

(20) Li, L.; Golding, R. E.; Whittal, R. M. *J. Am. Chem. Soc.* **1996**, *118*, 11662-11663.

(21 Little, D. P.; Cornish, T. J.; O'Donnell, M. J.; Braun, A.; Cotter, R. J.; Köster, H. *Anal. Chem.* **1997**, *69*, 4540-4546.

(22) Whittal, R. M.; Keller, B. O.; Li, L. *Anal Chem.* **1998**, *70*, 5344-5347.

(23) Marko-Varga, G. *Chromatographia Suppl. I* **1999**, *49*, S95-S99.

(24) Li, L.; Garden, R. W.; Romanova, E. V.; Sweedler, J. V. *Anal. Chem.* **1999**, *71*, 5451-5458.

(25) Li, L.; Garden, R. W.; Sweedler, J. V. *Trends Biotechnol.* **2000**, *18*, 151-160.

(26) Rubakhin, S. S.; Garden, R. W.; Fuller, R. R.; Sweedler, J. V. *Nature Biotechnol.* **2000**, *18*, 172-175.

(27) Dai, Y. Q.; Whittal, R. M.; Li, L. *Anal. Chem.* **1996**, *68*, 2494-2500.

(28) Dai, Y.; Whittal, R. M.; Li, L. *Anal. Chem.* **1999**, *71*, 1087-1091.

(29) Keller, B. O.; Li, L. *J. Am. Soc. Mass Spectrom.* **2000**, *11*, 88-93.

(30) Schriemer, D. C.; Li, L. *Anal. Chem.* **1996**, *68*, 2721-2725.

(31) Liu, Q.; Lin, F.; Hartwick, R. A. *J. Liq. Chrom. & Rel. Technol.* **1997**, *20*, 707-718.

(32) Spengler, B.; Kirsch, D.; Kaufmann, R.; Karas, M.; Hillenkamp, F.; Giessmann, U. *Rapid Commun. Mass Spectrom.* **1990**, *4*, 301-305.

(33) Juhasz, P.; Costello, C. E.; Biemann, K. *J. Am. Soc. Mass Spectrom.* **1993**, *4*, 399-409.

(34) Vorm, O.; Roepstorff, P.; Mann, M. *Anal. Chem.* **1994**, *66*, 3281-3287.

(35) Bender, R. C.; Bayne, C. J. *Biochem. J.* **1996**, *316*, 893-900.

(36)   Gron, H.; Thogersen, I. B.; Enghild, J. J.; Pizzo, S. V. *Biochem. J.* **1996**, *318*, 539-545.

(37)   Beavis, R. C.; Chaudhary, T.; Chait, B. T. *Org. Mass Spectrom.* **1992**, *27*, 156-158.

110

Chapter 7

Nanoliter Solvent Extraction Combined with Microspot MALDI TOF Mass Spectrometry for the Analysis of Hydrophobic Biomolecules[a]

7.1   Introduction

Hydrophobic biomolecules are of great importance in many areas of life sciences. The analysis of hydrophobic components of a sample containing both hydrophilic and hydrophobic analytes of interest can sometimes be a challenging task.[1]   For example, detection of hydrophobic molecules by mass spectrometric methods such as electrospray-ionization (ESI) or matrix-assisted laser desorption ionization (MALDI) is often hindered by these methods' limited tolerance to surfactants or by signal suppression due to the presence of hydrophilic components that are generally easier to ionize than hydrophobic molecules.   Several discrimination effects have been described in the literature based on variations of sample preparation and analyte composition both for ESI [2] and MALDI.[3-5] One sample preparation method that was found to be compatible with mass spectrometric ionization techniques is the use of organic acids, such as formic acid,   in high concentrations.[6-9]   The major disadvantage of using strongly acidic solutions is the possibility of hydrolysis and degradation of the analytes.[10]   In the specific case of formic acid, formyl-adduct formation becomes an additional problem.[11]   In 1992, Juhasz and Costello   successfully   analyzed   water   insoluble   gangliosides   dissolved   in chloroform/methanol   mixtures   using   different   matrices   made   up   in   a   50% acetonitrile/water mixture by MALDI MS.[12]   Recently, Green-Church and Limbach developed a MALDI sample preparation method for hydrophobic peptides with acid-labile protecting groups by dissolving samples in chloroform and the matrix in a

---

111

chloroform/methanol mixture.[13] More recently, Limbach's group demonstrated that by addition of surfactants, mixtures of hydrophobic and hydrophilic substances can be analyzed simultaneously by MALDI MS.[14]

In this work, we present a small-scale solvent extraction technique combined with microspot MALDI MS for the analysis of hydrophobic analytes from mixtures that also contain hydrophilic peptides. Solvent extraction is one of the most widely used separation methods in chemistry and has been documented since the early thirteenth century.[15] The advancement of sensitive analytical instrumentation has lead to the development of a variety of miniaturized solvent extraction techniques. Solvent extraction into small droplets has been the subject of particular interest due to the unique features of liquid drops. Liquid drop-based systems have been used for windowless vessels for extraction experiments, renewable gas samplers, and simple sample introduction interfaces.[16,17] Jeannot and Cantwell described an analytical technique using microliter droplets for solvent extraction combined with gas chromatographic analysis for mass transfer measurements and speciation studies.[18] More recently, Liu and Lee demonstrated a continuous-flow microextraction setup using 1-5 μL organic phase droplets for analyte extraction from a passing sample solution combined with gas chromatographic analysis.[19]

Mass spectrometry is an exquisitely sensitive detection method whose sensitivity is often limited by chemical background noise. The introduction of a concentrated sample in a small volume into a mass spectrometer usually results in the improvement of the signal-to-noise ratios. The technique presented herein allows the extraction of hydrophobic analytes from microliter sample volumes into nanoliter-size droplets of organic phase. Subsequent deposition of the organic phase onto a matrix-covered MALDI target allows the analysis of hydrophobic peptides from mixtures also containing hydrophilic peptides. The applicability of this method is demonstrated for two very hydrophobic, cyclic peptides as well as a phospholipid in mixtures with a very basic peptide. Furthermore, with the ionophore valinomycin we show that this miniaturized solvent extraction system is a promising tool for investigating specific metal-peptide interactions in solution by MALDI.

112

7.2 Experimental

7.2.1 Chemicals and Materials. Alpha-cyano-4-hydroxycinnamic acid (4-HCCA), surfactin A from *Bacillus subtilis*, cyclosporin A, bovine sphingomyelin, valinomycin, Lys-[Ala^3]-bradykinin (M.W. 1163.4, amino acid sequence: KRPAGFSPFR) and des-Pro^2-bradykinin (M.W. 963.0, amino acid sequence: RPGFSPFR) were purchased from Sigma-Aldrich Canada (Markham, Ontario, Canada). Chloroform (CHCl$_3$), acetone, ethanol, methanol and copper(II)acetate were from Fisher Scientific (Fair Lawn, New Jersey, USA). Copper(I)chloride was from Anachema (Montreal, Quebec, Canada). Fused-silica capillaries (20-μm-ID, 90-μm-OD) were purchased from Polymicro Technologies (Phoenix, Arizona, USA). 4-HCCA was recrystallized from ethanol (95%) at 50°C before use.

7.2.2 Setup for Extraction Experiments. Figure 7.1 shows the experimental setup for nanoliter solvent extraction. The design of this system was based on a nanoliter chemistry station that has been described in more detail in Chapters 2 and 3.[20]
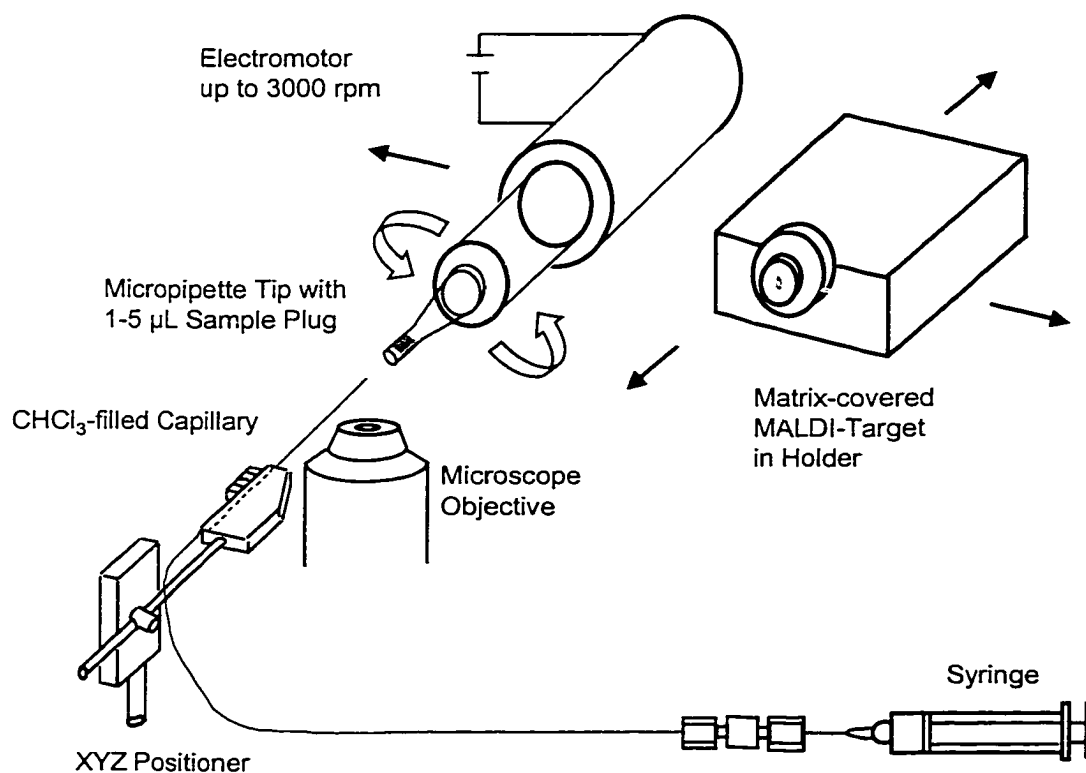
Figure 7.1 Modified nanoliter chemistry station for extraction experiments.

113

A horizontally positioned fused-silica 20-μm-ID capillary of ~20 cm in length was mounted onto a three-dimensional manipulator and positioned opposite to a plastic pipette tip containing the aqueous sample solution. The capillary's polyimide coating was removed from the tip, resulting in an outer diameter of about 70 μm. The pipette tip was connected to the rotating axis of a small electrical motor that was mounted onto another 3D manipulator. The setup was positioned on a microscope platform and manipulations of the capillary and the pipette tip could be observed through the microscope. For easier control and observation, two video cameras were set up so that manipulations could be followed on two monitors located beside the microscope.

Figure 7.2 shows a side view schematic of the extraction setup. Before the extraction, 1-3 μL of sample solution (i.e. the aqueous phase) were transferred into the pipette tip attached to an electrical motor. The capillary was then filled with a water-immiscible organic solvent such as chloroform. This was achieved by positioning the capillary into a chloroform-filled, horizontally mounted glass tube. By pulling the connected syringe, chloroform was drawn into the capillary. The chloroform-filled
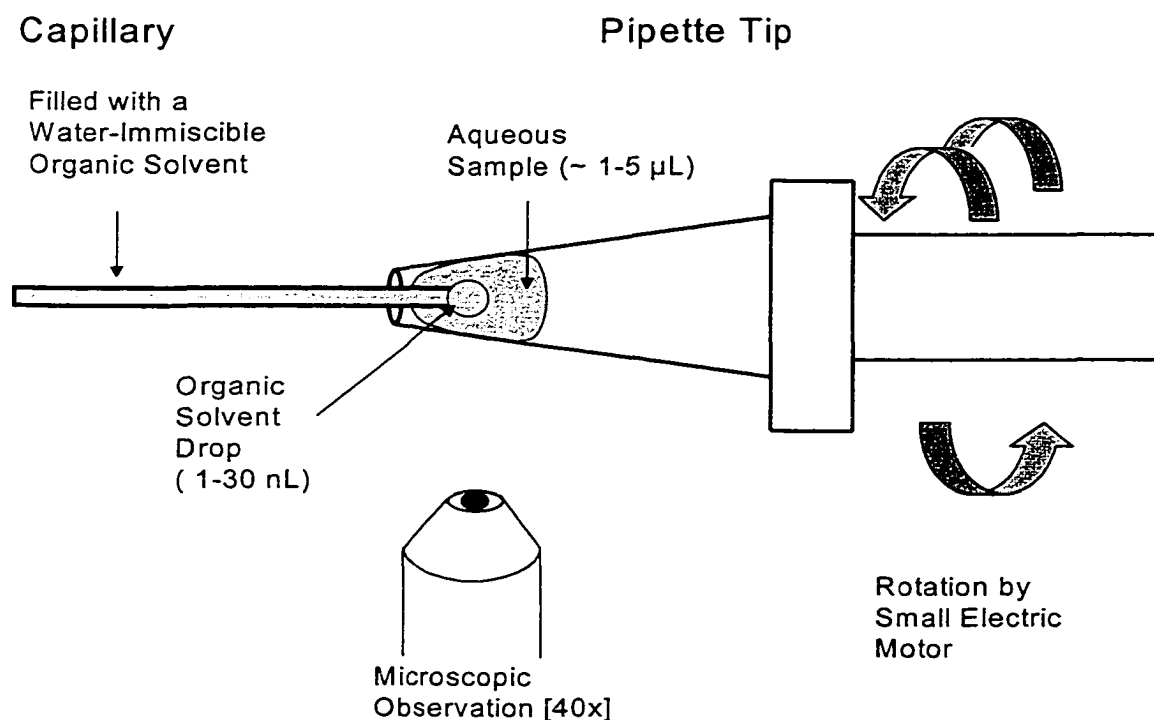
Figure 7.2 Schematic of extraction setup.

114

capillary was then positioned into the aqueous sample plug inside the pipette tip. Application of light pressure to the syringe forced the chloroform into the aqueous sample and resulted in a droplet. Figure 7.3 shows the microscopic images of different sized chloroform droplets formed inside water. The size of the organic phase droplets can be changed and well-controlled with the pressure applied to the syringe. For the purpose of taking these clear images of the droplets, the aqueous solution was presented in a horizontally mounted glass tube instead of a plastic pipette tip.

For the extraction experiments it was found that droplet sizes of up to ~30 nL are very stable even at pipette tip rotation rates of up to 3000 rpm. The rotation rates were measured using a digital tachometer ('Phototach', Model 8211, Cole-Parmer Instruments Co., Vernon Hills, Illinois, USA). The capillary with droplet can be moved in all directions inside the rotating pipette tip using the 3D manipulator. However caution must be exercised to not touch the pipette tip walls or the air/water interface with the organic phase, otherwise the droplet disintegrates. Since the chloroform phase inside the capillary is subject to very fast evaporation, it is necessary to hold a certain reservoir of organic phase in the capillary and the connected tubing. We estimate that with our current method and setup, several hundred nanoliters of organic phase are held in the capillary. This amount is sufficient to perform extractions up to more than half an hour (as long as the organic phase droplet stays in the aqueous phase). After the extraction the organic phase droplet was carefully withdrawn into the capillary. The capillary was removed from the pipette tip and immediately positioned in front of a matrix covered MALDI target (see Figure 7.1). By applying pressure to the connected syringe, the organic phase was then pushed out of the capillary and deposited onto the matrix layer.

7.2.3 Microspot MALDI TOF MS and Data Processing. The matrix layer on the MALDI target was prepared according to a previously reported two-layer method.[21,22] Briefly, to produce a very thin first layer, about 1 µL of a 5 mg/mL solution of 4-HCCA in 80% (v/v) acetone/methanol was deposited on the probe. After drying, a second layer of 0.4 µL 4-HCCA saturated in 35% (v/v) methanol/water was deposited and allowed to dry. The deposited organic phase evaporates very rapidly and the extracted analytes remain on a small, invisible microspot. The MALDI target was then introduced into a

115
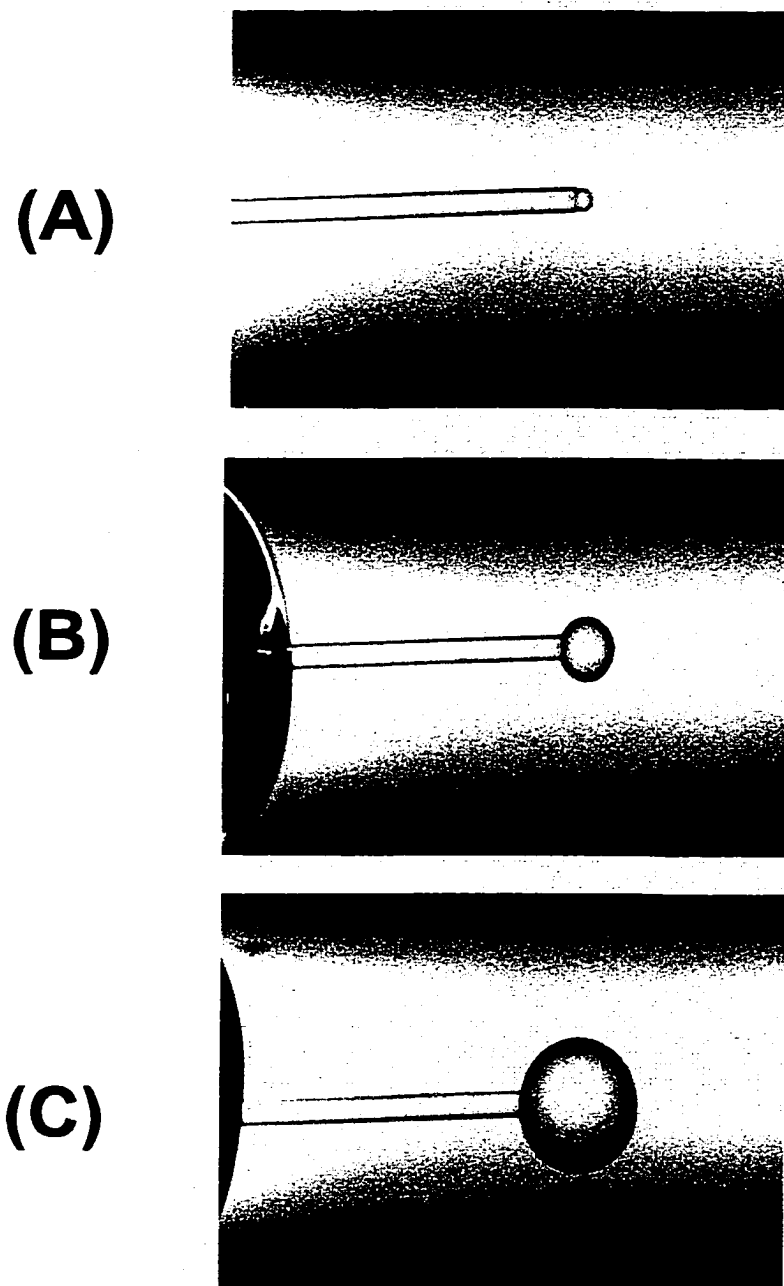
Figure 7.3 Microscope photographs (40x) of chloroform droplets at the tip of a 20-µm-ID and ~70-µm-OD capillary in an aqueous solution: (A) droplet volume ~1 nL (B) droplet volume ~30 nL (C) droplet volume ~ 250 nL.

116

homebuilt linear time-lag focusing MALDI time-of-flight instrument, equipped with a 337 nm nitrogen laser with a 3 ns pulse (model VSL 337ND, Laser Sciences Inc., Newton, MA, USA). This instrument has been described in detail elsewhere.[23] The area where the organic phase was deposited was then scanned with the laser beam under video observation. Once the sample microspot was detected, several dozen single-shot spectra were acquired and averaged using the Hewlett Packard supporting software. The data were then reprocessed using the Igor Pro software package (WaveMetrics, Lake Oswego, Oregon, USA). Each spectrum was normalized to the most intense signal.

7.3 Results and Discussion

Biomolecule analysis often deals with small amounts of sample. The nanoliter droplet extraction method offers several advantages compared to a conventional method that requires a relatively large volume of solvent for extraction. In the nanoliter extraction, the organic phase never touches the sample container wall, thus minimizing any possible extraction of contaminants adsorbed onto the plastic or glassware. Furthermore, there is no need to concentrate the organic phase after the extraction which avoids any possible sample loss during the concentration step. The nanoliter volume can be readily deposited onto a MALDI target resulting in a high analyte concentration within a microspot. Combined with microspot MALDI, very sensitive analysis of the extracted analyte is achievable. In the following discussion, we present several examples of applications using samples of biological significance to illustrate the salient features and analytical performance of the nanoliter extraction/microspot MALDI method.

Chart 7.1   Structure of surfactin A from *Bacillus subtilis*.

(n=9 ➔ M.W. 1008.32, n=10 ➔ M.W. 1022.34, n=11➔ M.W. 1036.37)

$$CH_3\text{—}(CH_2)_n\text{—}CH\text{—}CH_2\text{—}\overset{\overset{O}{\|}}{C}\text{—}\text{L-Glu—L-Leu—D-Leu—L-Val—L-Asp—D-Leu—L-Leu}$$

117
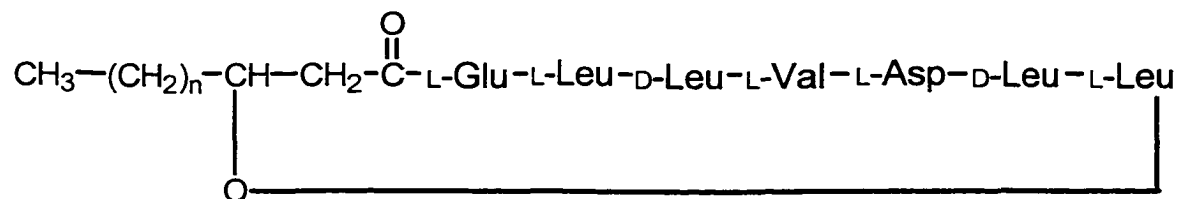
Figure 7.4 shows three MALDI spectra of a sample containing surfactin A and a more hydrophilic peptide Lys-[Ala^3]-Bradykinin obtained under different sample preparation conditions. Surfactin A is a cyclic lipoheptapeptide produced by *Bacillus subtilis* and its structure is shown in Chart 7.1.[24] This substance is a powerful biosurfactant and its diverse bioactivity is of great interest in biotechnological and pharmaceutical research.[25] Surfactins and other lipopeptides as well as their metabolites have been analyzed in typing studies of various strains of *Bacillus subtilis* using MALDI TOF MS.[26]

The spectrum obtained from the conventional sample/matrix preparation (Figure 7.4A) is dominated by the signal from the basic peptide Lys-[Ala^3]-Bradykinin while the signal from surfactin A is barely visible. This observation is not unusual since peptides containing arginine are known to give high signal intensities in MALDI analysis and suppress signals from other analytes.[5] When the analytes are prepared in a chloroform/methanol mixture (Figure 7.4B), signals from surfactin A improve somewhat however the spectrum is still dominated by the basic peptide. This result indicates that poor detectability of surfactin A is mainly due to the strong suppression effect of Lys-[Ala^3]-Bradykinin, not the reduced solubility of surfactin A in aqueous solution. A much improved detection of Surfactin A is observed, as shown in Figure 7.4C, when the sample is extracted by the nanoliter extraction technique followed by microspot MALDI. Obviously the lipopeptide was extracted into the chloroform phase and only a small amount of the basic peptide was transferred to the MALDI target. The appearance of the basic peptide could be due to two reasons: either a small portion of the aqueous phase was withdrawn into the capillary after the organic phase was withdrawn and then co-deposited onto the target with the organic phase, or the basic peptide was partially extracted into the chloroform phase.

Note that the observed signals of surfactin A at m/z 994, 980 and 966 do not correspond to the general structures of surfactin A shown in Chart 7.1. Since the mass difference between the adjacent peaks is 14 Da, one might think that these signals originate from isoforms with varying fatty acid chain lengths. However, this is not the case. Ziessow and coworkers demonstrated that these isoforms are due to amino acid substitutions, mainly valine instead of leucine at various positions.[25]

118
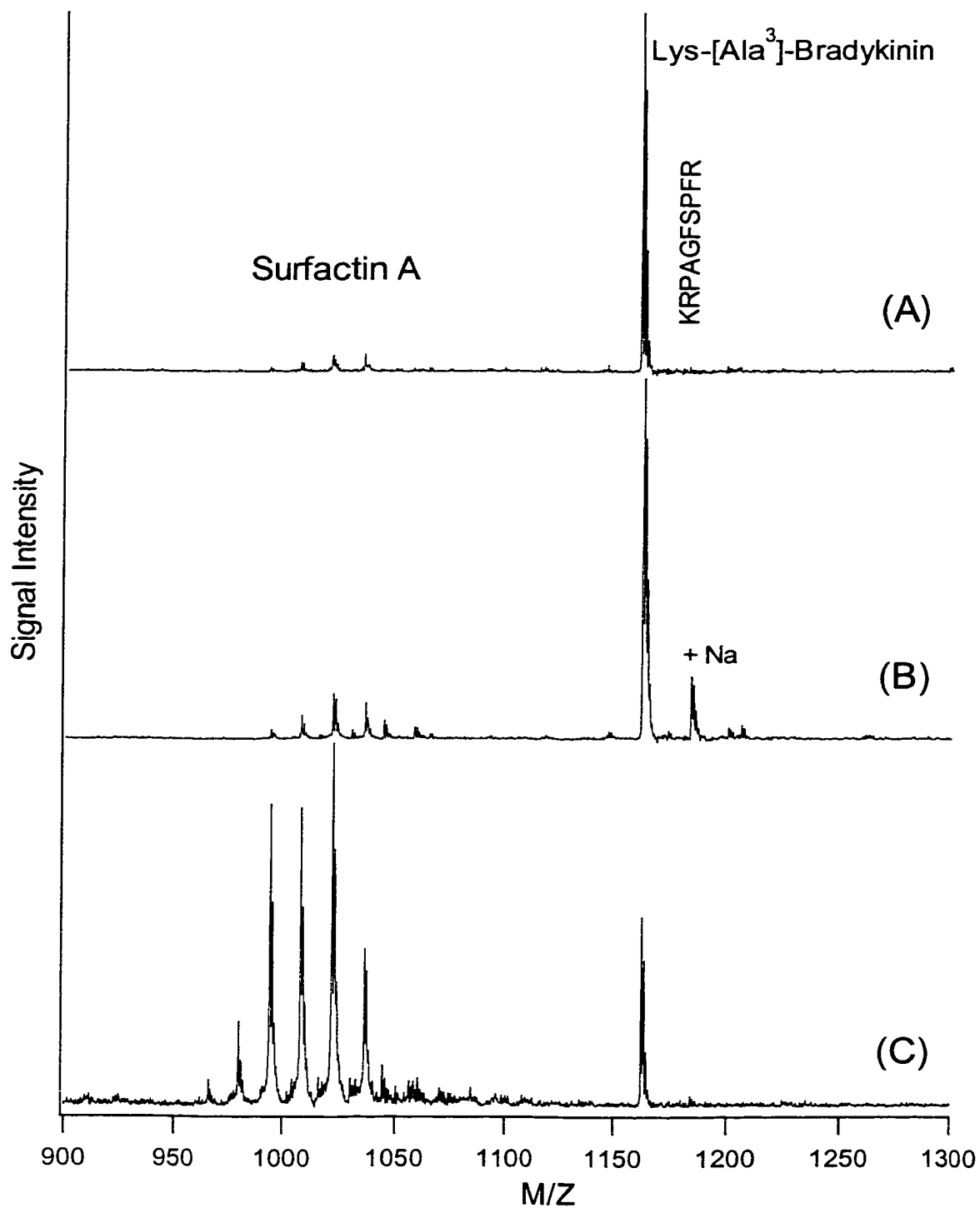
Figure 7.4   MALDI mass spectra of equimolar mixtures (~15 μM) of surfactin A and Lys-[Ala^3]-Bradykinin.   (A)   Conventional sample/matrix preparation from aqueous solution. (B) Sample/matrix preparation using chloroform/ methanol according to Green-Church *et al.*[13] (C) Sample preparation with the nanoliter extraction setup using the same sample solution as in (A).

119

Chart 7.2   Structure of bovine sphingomyelin

(R = stearic acid ➜ M.W. 730.66, R=nervonic acid ➜ M.W. 813.67
R = lignoceric acid ➜ M.W. 815.66)
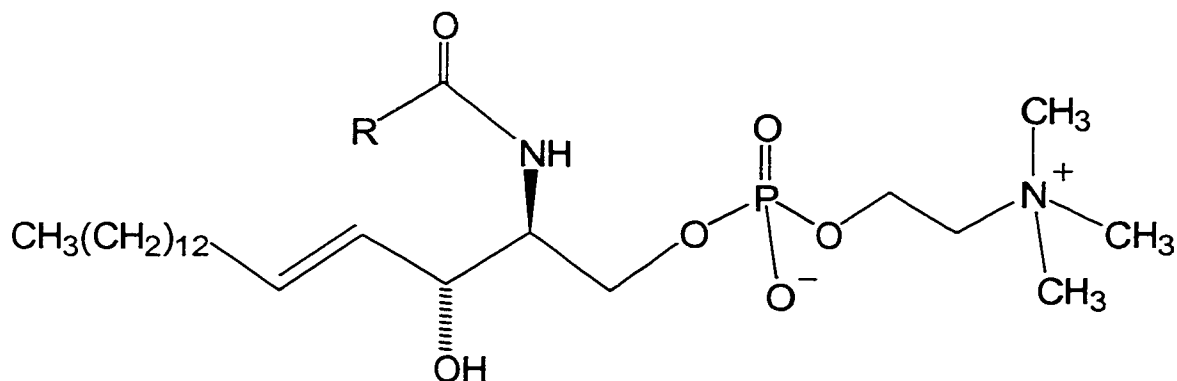
Figure 7.5 shows the analysis of sphingomyelin, which also demonstrates that, with the nanoliter extraction method, we can readily adjust the experimental conditions to detect hydrophobic and/or hydrophilic peptides. Sphingomyelin is a phospholipid found in plasma membranes of many mammalian cells and its structure is shown in Chart 7.2.[24] Sphingomyelin and three other phospholipids, namely phosphatidylcholine, phosphatidylserine and phosphatidylethanolamine constitute more than half the mass of lipid in most membranes.[27] Several recent reviews deal with the role of sphingomyelin, its relationship with cholesterol, and the resulting impact on cellular functions such as lipid and protein trafficking, signal transduction or membrane structure.[28-30] Determination of sphingomyelin structures has been reported using liquid chromatography combined with tandem mass spectrometry.[31,32]

As Figure 7.5A shows, the spectrum from the conventional MALDI sample preparation does not display signals from the phospholipid in a sample containing a hydrophilic peptide. Obviously the signal is suppressed by the basic peptide des-Pro[2]-bradykinin. In the nanoliter extraction experiments with the same sample solution (see panels B and C of Figure 7.5), we can fine-tune the experimental conditions so that both types of analyte can be detected with varying intensity. This was done by simultaneously depositing both organic phase and a small portion of the aqueous phase onto the MALDI

120
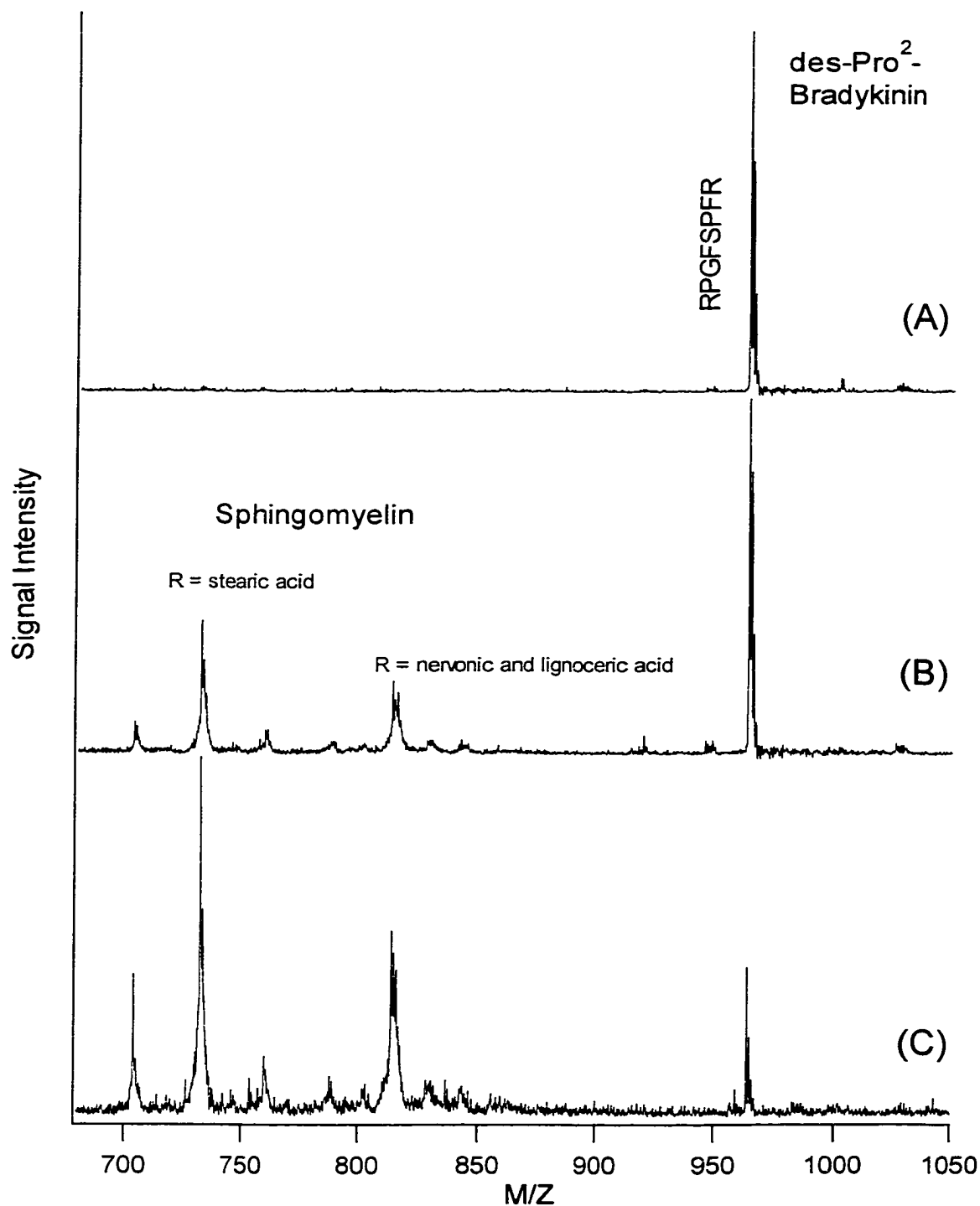
Figure 7.5 MALDI mass spectra of an aqueous mixture of sphingomyelin (~0.6 μM) and des-Pro²-Bradykinin (~1 μM). (A) Conventional sample/matrix preparation. (B) Chloroform extraction using the nanoliter technique. Simultaneous deposition of the organic phase and ~100 pL of the aqueous phase. (C) Same procedure as in (B) but simultaneous deposition of organic phase and only ~20 pL of aqueous phase.

121

target. After the extraction was completed, the organic phase was carefully withdrawn into the capillary with a small plug of aqueous solution. Since the phase borders are clearly visible under the microscope, it is trivial to adjust the amount of aqueous phase loaded in front of the organic phase. Using this simple approach, both hydrophilic and lipophilic compounds can be detected simultaneously, and the intensities for each analyte type can be varied by changing the amount of the loaded aqueous phase (Figure 7.5B,C). We note that loading a small amount of aqueous solution also has the benefit of inhibiting the otherwise very fast evaporation of the organic phase.

Chart 7.3   Structure of cyclosporin A (CsA).
(M.W. 1202.64, Abu = α-Aminobutyric acid residue, Me = methylation at N)
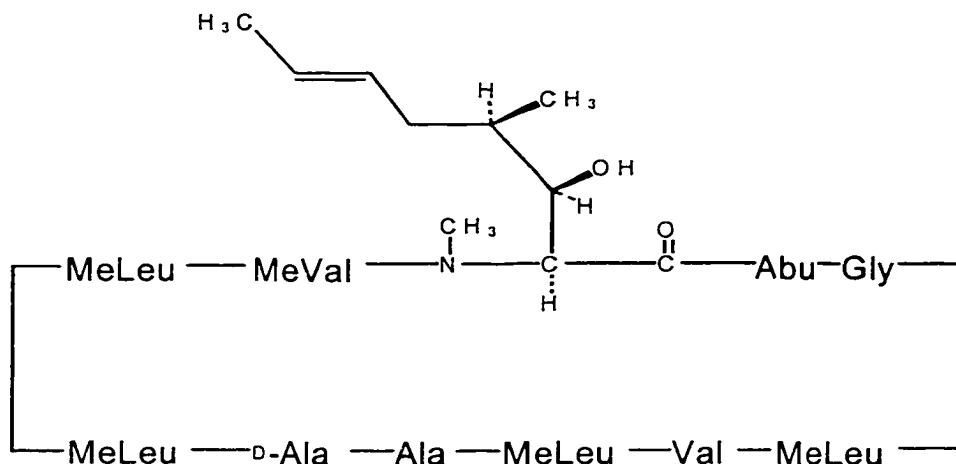
Nanoliter extraction can be very efficient and, combined with microspot MALDI, nanomolar concentration of hydrophobic analyte can be detected. This is shown in Figure 7.6 for the analysis of cyclosporin A (CsA). CsA is a cyclic peptide consisting of 11 primarily hydrophobic amino acid residues, as seen in Chart 3.[24] This peptide has immunosuppressant activity and is produced in nature by the fungus *Tolypocladium inflatum Gams*.[33]   It is used as a drug for organ transplant patients. Methods for monitoring the levels of CsA in blood by mass spectrometry, including MALDI TOF MS, have been developed.[34,35] In our study, an equimolar mixture (~0.6 μM) and a dilute

122
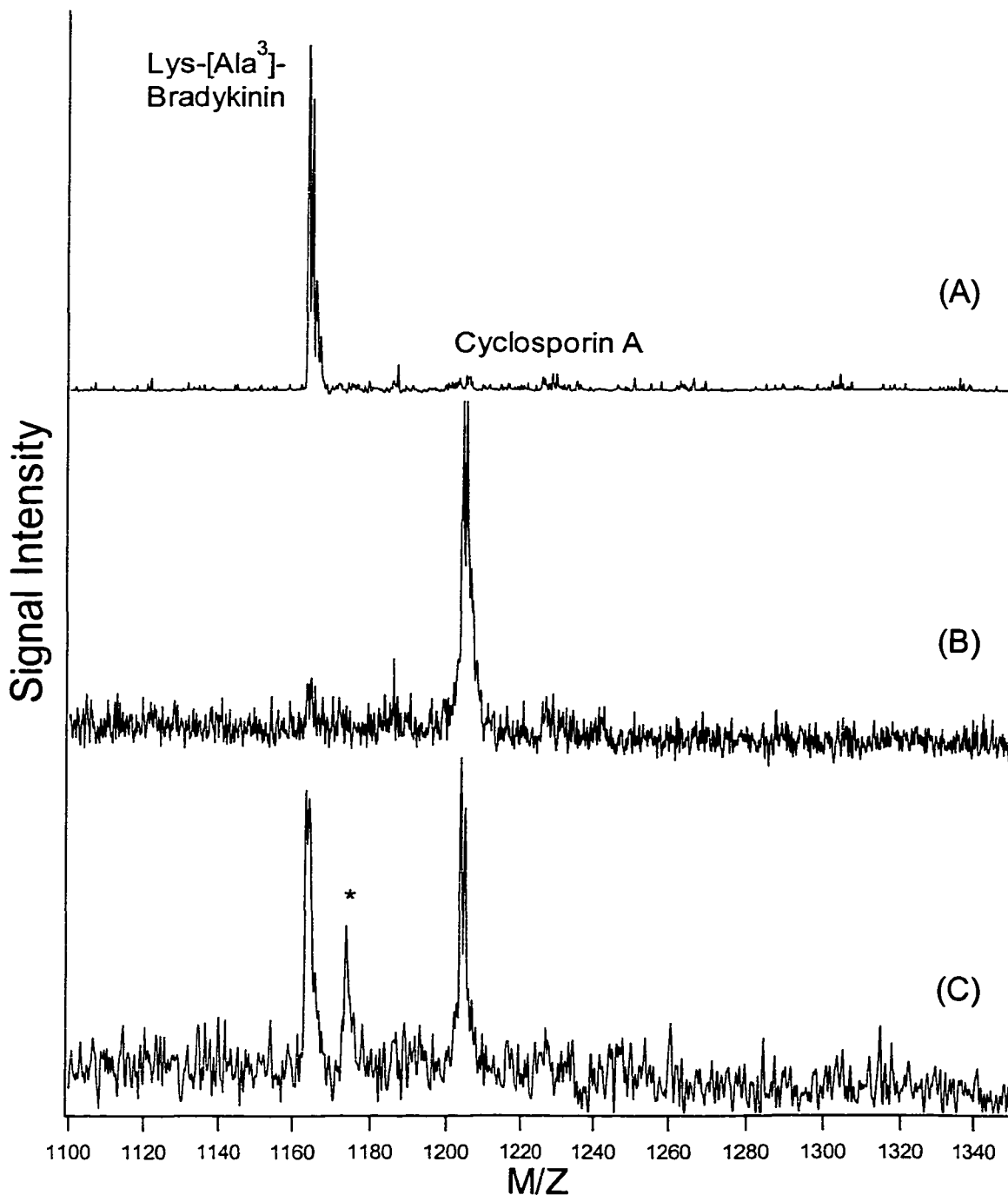
Figure 7.6 MALDI mass spectra of mixtures of Lys-[Ala^3]-bradykinin and cyclosporin A (CsA). (A) Conventional MALDI preparation of an equimolar mixture (~0.6 μM). (B) Analysis of the chloroform phase after nanoliter extraction using the same solution as in (A). (C) Analysis of the chloroform phase after nanoliter extraction of a solution containing 80 nM CsA and 1 μM Lys-[Ala^3]-bradykinin. The peak labeled '*' could be a degradation product of CsA.

123

analyte solution containing 80 nM cyclosporin A and 1 μM Lys-[Ala^3]-bradykinin were made. These dilute solutions were analyzed by a conventional MALDI method and then subjected to nanoliter extraction and the resulting extracts were analyzed by microspot MALDI. Figure 7.6A shows the mass spectrum of the conventional MALDI preparation. This result is similar to those observed for surfactin A and sphingomyelin; the signal of the hydrophobic CsA is suppressed by the basic peptide Lys-[Ala^3]-bradykinin. Analysis of the extract of the equimolar mixture demonstrates again the capability of the nanoliter technique to extract selectively the hydrophobic species (Figure 7.6B). The mass spectrum shown in Figure 7.6C demonstrates that it is possible to detect this hydrophobic peptide at 80 nM even in the presence of excess hydrophilic species. In conventional MALDI experiments, detection of CsA in the presence of Lys-[Ala^3]-bradykinin is only possible when the concentration of CsA is about 5-10 times higher than that of Lys-[Ala^3]-bradykinin (data not shown).

An interesting observation in dealing with samples containing an excess amount of hydrophilic species is worth noting. To obtain the spectrum in Figure 7.6C we guided the laser beam slightly off center of the microspot because a huge excess of Lys-[Ala^3]-bradykinin was found directly at the microspot's center. Obviously due to the excess of Lys-[Ala^3]-bradykinin in the sample, a considerable amount of this compound can be transferred to the MALDI target, even if the aqueous phase being withdrawn is very small. However the fact that CsA was detectable outside of the microspot's center indicates that the deposited chloroform phase acted as a mobile phase and transported CsA out of the center of the microspot, leaving Lys-[Ala^3]-bradykinin primarily in the microspot center. As a control, direct deposition of the same aqueous sample solution onto a MALDI target, followed by deposition of a chloroform droplet on top of the deposition site, did not show any CsA signal in the vicinity of the deposition site. This result indicates that for a successful analysis, analyte concentration by droplet extraction is crucial.

Nanoliter extraction combined with MALDI can be quite effective in reducing metal ion interferences. Figure 7.7 shows MALDI mass spectra of the samples containing CsA, sodium chloride, and copper(II) chloride. Regular MALDI sample preparation shows the protonated species of CsA, its sodium adduct, and the CsA-copper

124

complex, whereas the organic phase analysis only produces the protonated species. These results show that the nanoliter extraction method is an effective cleanup tool for hydrophobic analytes in solutions containing high amounts of salt. Even with two on-probe washes, the sodium adduct is still the dominant peak in regular MALDI sample preparation (Figure 7.7A). The analysis of the organic phase after extraction of the same solution was performed without any additional washing step (Figure 7.7B).
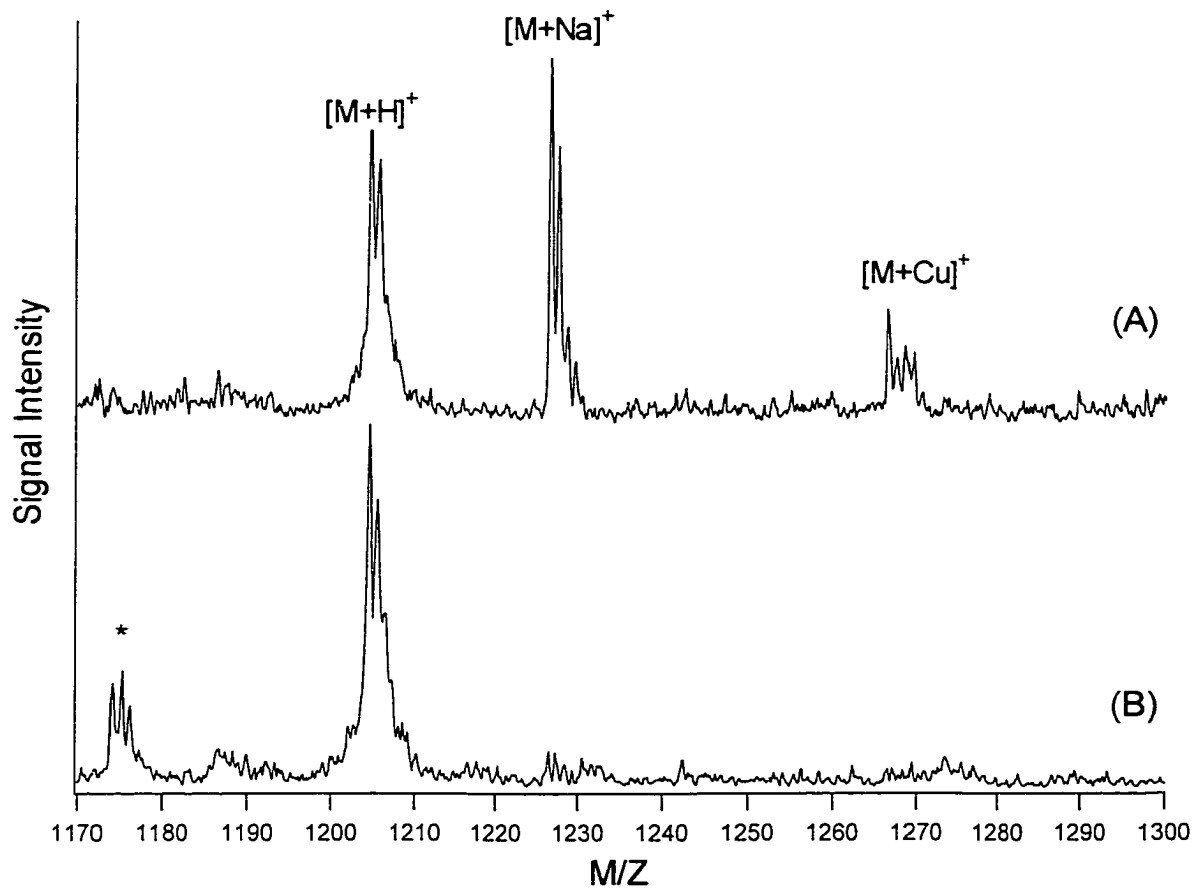
Figure 7.7   MALDI mass spectra of a ~3 μM CsA solution in 150 mM NaCl and ~3 mM Cu^{2+}. (A) Direct deposition of ~0.4 μL onto double-layer matrix and two washes with dist. H_2O. (B) Analysis of the chloroform phase after nanoliter extraction using the same sample solution as in (A). The signal at m/z 1174 is most likely a decomposition or fragmentation product of CsA (see also Figure 7.6C).

125

The addition of copper(II) chloride to the sample was intended to illustrate another important point. CsA is known to form complexes with certain metal ions in electrospray ionization MS. In binding studies of CsA with calcium, zinc, and copper by ESI MS, Dancer et al. found that copper and zinc produced singly-charged species by binding to deprotonated cyclosporin A, whereas calcium formed a doubly-charged species.[36] They found that the observed ESI signals were from covalently bonded metal-cyclosporin complexes, rather than the result of adduct formation.[36] Metal-ion interaction with CsA should affect its solubility in a solvent system. To examine if the CsA-copper complex can be extracted from an aqueous sample solution, several nanoliter extraction experiments were carried out from CsA solutions with added copper(II)acetate at pH ~3, ~7 and ~9. The matrix layer was thoroughly washed before organic extract deposition to minimize any copper contamination from the matrix. In all cases no CsA-copper complex could be detected. Similar experiments with CuCl did not show any CsA-copper complex; however it should be noted that Cu(I) can be easily converted into Cu and Cu(II) in aqueous solution.[37]

A close examination of the spectrum shown in Figure 7.7A indicates that the observed copper-cyclosporin complex is $[M+Cu]^+$ with monoisotopic m/z of 1264.8, not $[M-H+Cu]^+$ with monoisotopic m/z 1263.8 as was observed in the case of electrospray analysis.[36] In the MALDI experiment, it is apparent that copper(I) forms the adduct complex with CsA. It is known that copper(I) can be formed in gas phase from the reduction of copper(II) during the MALDI process. [38,39]

It is clear that CsA-copper complexes, if they are present in the aqueous solution, are not extracted into the organic phase. However, in systems where metal ion complexes can be extracted, the combination of nanoliter extraction and MALDI can be used to provide useful information on solution composition. This is illustrated in the study of ionophore valinomycin, which is known to bind strongly to potassium and serves as a potassium carrier through cell membranes.[27] When complexed with K^+, valinomycin's hydrophilic groups point towards the interior-situated potassium and are thus shielded by the exterior hydrophobic groups. Thus, passing of the complex through the phospholipid layers of membranes is facilitated.[40] The hydrophobic character of valinomycin-K^+ should therefore enable the extraction of this complex into a

126

hydrophobic organic phase. Valinomycin is a cyclic trimer of D-hydroxyisovaleric acid, L-valine and L-lactic acid residues and its structure is shown in Chart 7.4.[24]

Chart 7.4   Structure of valinomycin.

(L-Lac = L-Lactic acid residue, D-Hylva = D-Hydroxyisovaleric acid residue)

L-Val————D-Hylva—D-Val———L-Lac———L-Val———D-Hylva

L-Lac————D-Val———D-Hylva—L-Val———L-Lac———D-Val
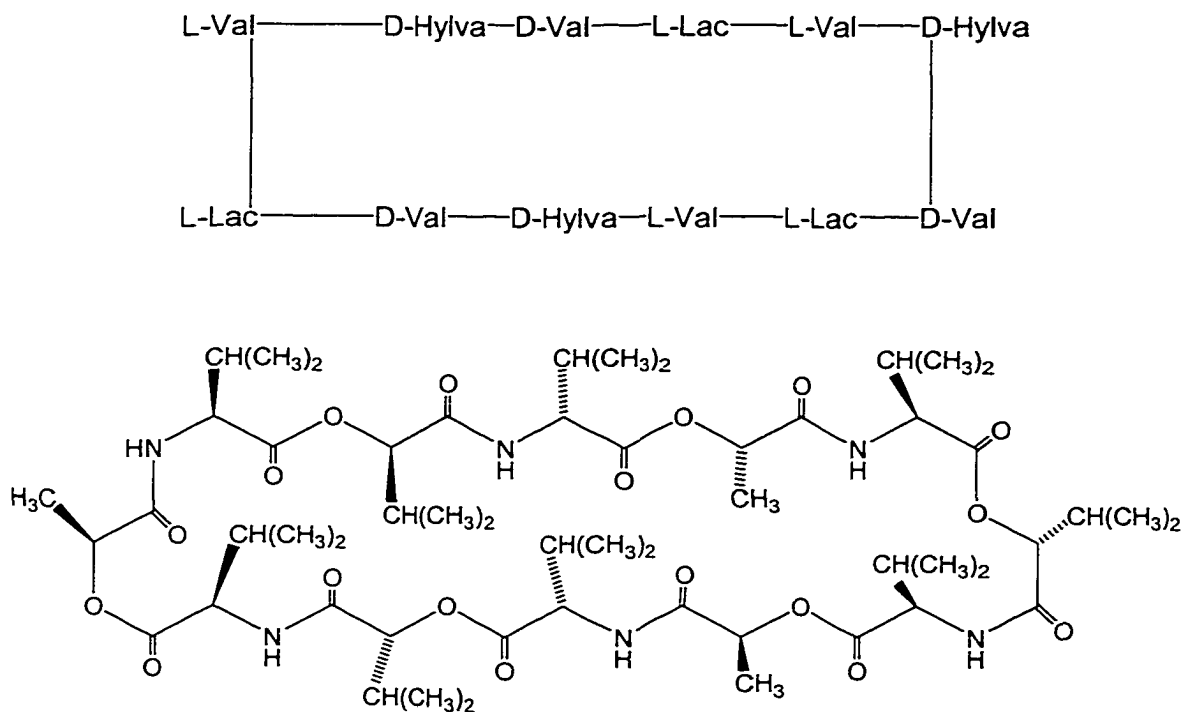
Sheil and coworkers studied valinomycin-alkali metal complexes and their stabilities by electrospray and MALDI mass spectrometry.[41,42] They concluded that MALDI can not be used as a reliable tool to probe metal ion selectivity for valinomycin due to varying intensities of valinomycin-alkali complexes depending on several experimental conditions.[42] This is confirmed in the results shown in Figure 7.8. Valinomycin has nearly 20,000 times higher affinity for potassium than for sodium.[43] Thus one would expect that a reliable analytical tool for metal ion specificity should show a dominant signal for the valinomycin-K$^+$ complex. This was true for only the nanoliter solvent extraction method (Figure 7.8B). Regular MALDI sample preparation techniques with and without washing steps do not reflect the actual sample composition

127

in solution. Figure 7.8A shows the mass spectrum obtained without on-probe washing. The sodium adduct peak is dominant, although the potassium peak is already much stronger than one would expect just taking into account the ratio of the salt concentrations (Na^+:K^+ = 150:1). This is an indication that potassium has a stronger affinity to valinomycin than sodium, but the high amount of sodium deposited onto the target still leads to a result that does not reflect the real conditions in the sample solution. Figure 7.8C shows the mass spectrum obtained with on-probe washing. The sodium-adduct signal decreased significantly but so did the valinomycin-K^+ signal. Obviously the washing step removed potassium and left the nearly salt-free analyte.
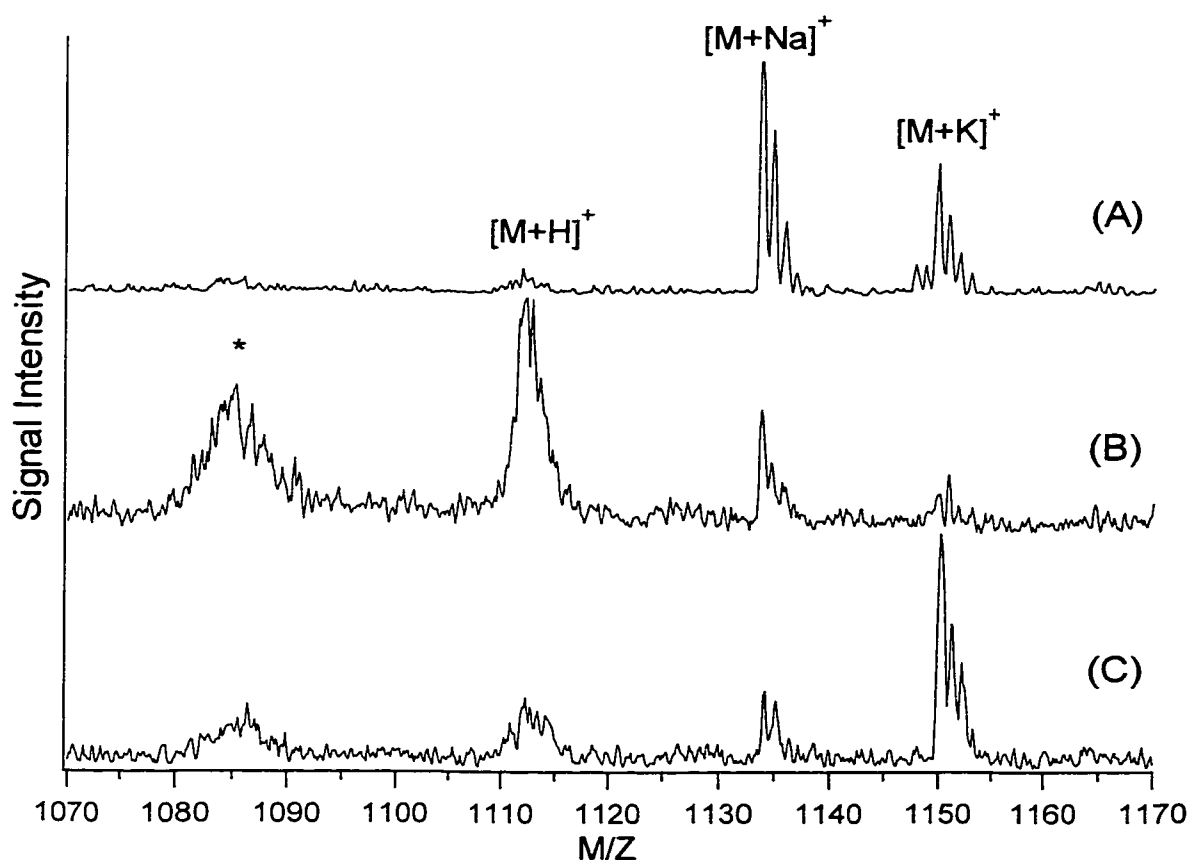
Figure 7.8   MALDI mass spectra of 2 μM valinomycin in 150 mM NaCl and 1 mM KCl. (A) Direct deposition of ~0.4 μL onto double matrix-layer. No washing steps were administered. (B) Analysis of the chloroform phase after nanoliter extraction using the same sample solution as in (A). (C) Repetition of the experiment done in (A) with three on-probe washing steps administered after sample deposition using dist. H_2O. The signal labeled '*' is a degradation or fragmentation product of valinomycin and is examined more closely later.

128

Another set of experiments was performed with varying potassium and sodium salt concentrations in the samples. The results are shown in Figure 7.9, which again demonstrate that the nanoliter extraction technique is superior to the regular MALDI preparation in reflecting actual composition of the analyte in solutions. Figure 7.9D shows that, even in the case where there is no potassium added intentionally to the sample, the valinomycin-K^+ complex shows a stronger signal than the sodium adduct in the extraction method. This is not surprising since potassium is a ubiquitous contaminant and can be present in the sample and/or containers used to prepare the sample. Only in the last case (Figure 7.9C, F) the obtained spectra are similar for both sample preparation methods since the potassium concentration is now dominant. The appearance of the sodium adduct in both cases shows that sodium is a ubiquitous contaminant as well.
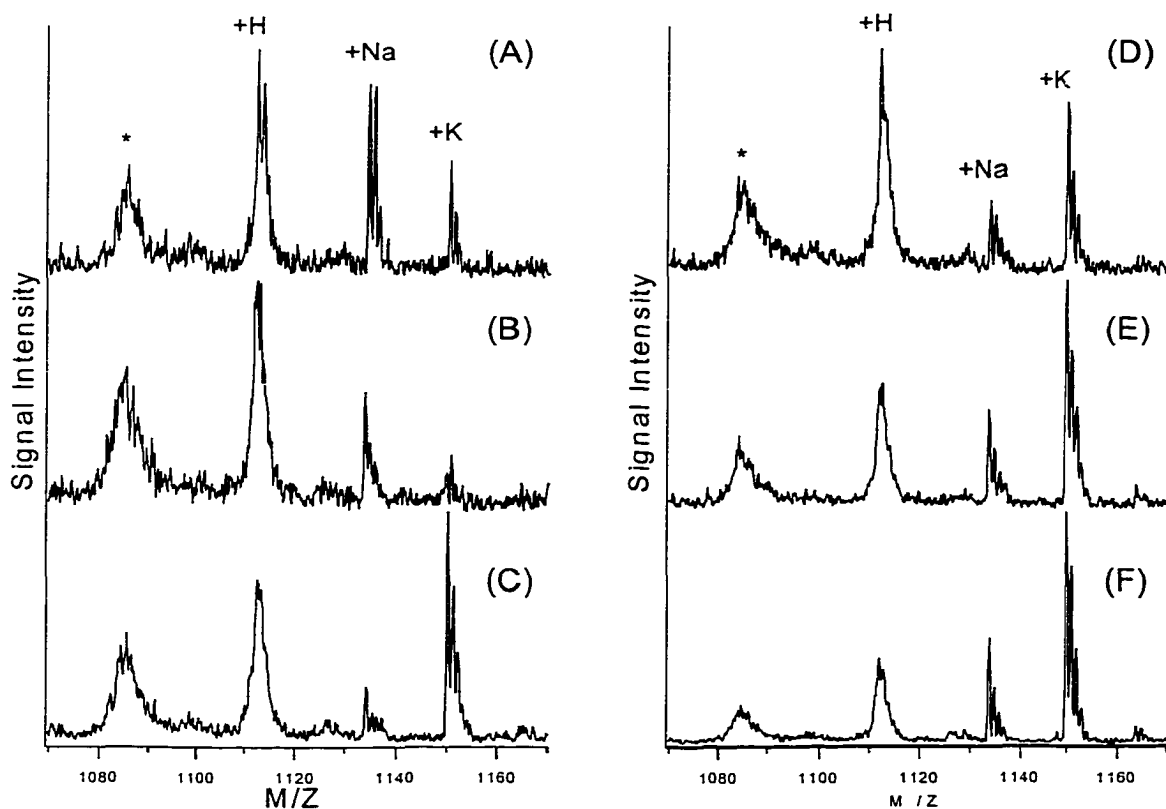
Figure 7.9   MALDI mass spectra of 2 µM valinomycin in varying sodium and potassium salt concentrations. (A+D) 150 mM NaCl. (B+E) 150 mM NaCl, 8 mM KCl. (C+F) 150 mM KCl. Sample preparation: (A+B+C) Direct deposition onto matrix covered target. Two on-probe washing steps were administered using dist. H₂O. (D+E+F) Analysis of the chloroform phase after nanoliter extraction. The signal labeled '*' is a fragmentation or degradation product of valinomycin (see Fig. 7.8).

129

Could the nanoliter extraction technique combined with microspot MALDI be employed to determine relative metal-peptide complexes stability rates? The above results indicate that this might be possible for specific metal-peptide complexes. For valinomycin this is very difficult due to sodium and potassium contamination of the matrix and sample and due to the extremely strong affinity of valinomycin for potassium. Another problem is the extraction of the neutral species which leads to the $[M+H]^+$ signal during MALDI analysis. It is unclear if this is due to an extraction of the neutral species already present in the sample, or due to a potassium loss of the valinomycin-K^+ complex during extraction, or both. An ideal system for further studies would therefore consist of a peptide that forms stable neutral complexes with metals that are not ubiquitous contaminants and are thus easy to extract.

An interesting observation for both the valinomycin and cyclosporin A studies (see Figure 7.9 and Figure 7.7) is that the metal-adduct species yield higher resolved signals than the protonated species. To investigate this issue an experiment was done on a MALDI instrument with linear and reflectron mode capabilities. As shown in Figure 7.10, we found that in the reflectron mode the $[M+H]^+$ signal has almost disappeared, indicating that the $[M+H]^+$ ions are unstable and fragment on their way to the detector. Detection of metastable ions that fragment in the field-free region is not possible in the linear mode since the fragments have the same velocity as their parent ion and thus arrive at the detector at the same time. However since some of the internal energy of the decomposing ion is released as kinetic energy the fragment ions have a range of velocities, thus leading to a broader signal.[44]

We have also obtained a post-source-decay (PSD) MALDI mass spectrum of the isolated $[M+H]^+$ ion of valinomycin (Figure 7.11). The $[M+H-28\text{ Da}]^+$ at m/z 1084.5 is the dominating signal, confirming that this species is a fragment of valinomycin most likely due to loss of CO. We already observe this signal in the spectra obtained in linear mode; this could have two reasons: the fragmentation occurs partially in the source region of the MALDI instrument before the acceleration region or valinomycin degrades in solution. The broad signal for $[M+H-28\text{ Da}]^+$ found in the linear mode indicates that valinomycin indeed undergoes in-source decay, however stock solutions which have been

130

stored for a time give higher signals for [M+H-28 Da]$^+$ than freshly made up solutions, indicating that degradation in solution occurs as well.
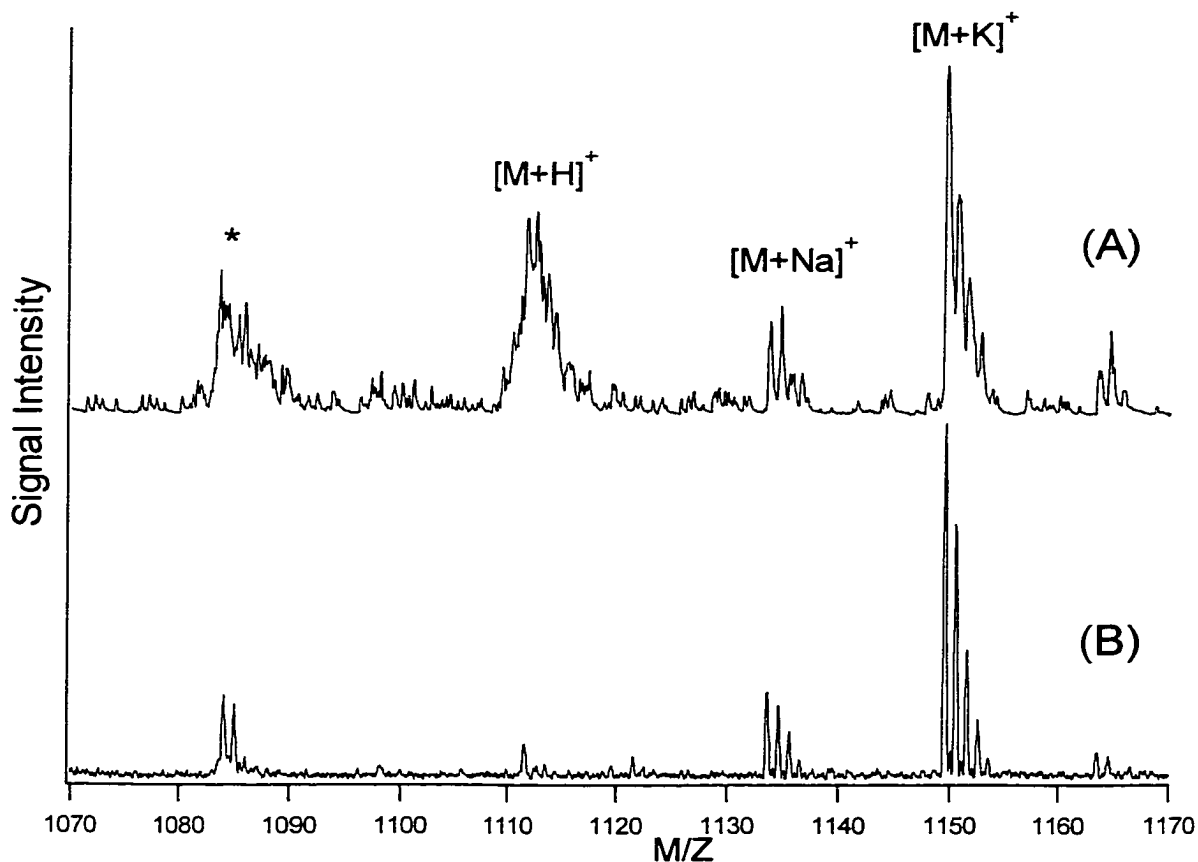
Figure 7.10 MALDI mass spectra of valinomycin. Spectra were obtained on a Voyager-DE Elite MALDI-TOF mass spectrometer (PE Biosystems, Framingham, MA, USA). (A) Linear mode. (B) Reflectron mode. Sampling was done on the same sample spot for both modes. The peak labeled '*' is a fragment or degradation product of valinomycin.

In conclusion, we have developed a nanoliter solvent extraction technique that allows the accumulation of hydrophobic analytes from small sample volumes with high salt contamination or with more hydrophilic analytes. The introduction of a nanoliter-sized organic phase droplet at the tip of a small capillary into a microliter-sized sample volume has several advantages over conventional solvent extraction: the use of organic solvent is minimized, the organic phase never touches the sample container wall, thus possible extraction of contaminants, e.g. polymers from plastic materials, are minimized,

131

and there is no need to concentrate the organic phase after the extraction process. The combination with microspot MALDI allows for very sensitive analysis of the extracted analytes. Finally, we demonstrate that the technique is a more reliable tool for probing metal-peptide complexes than regular MALDI sample preparations.
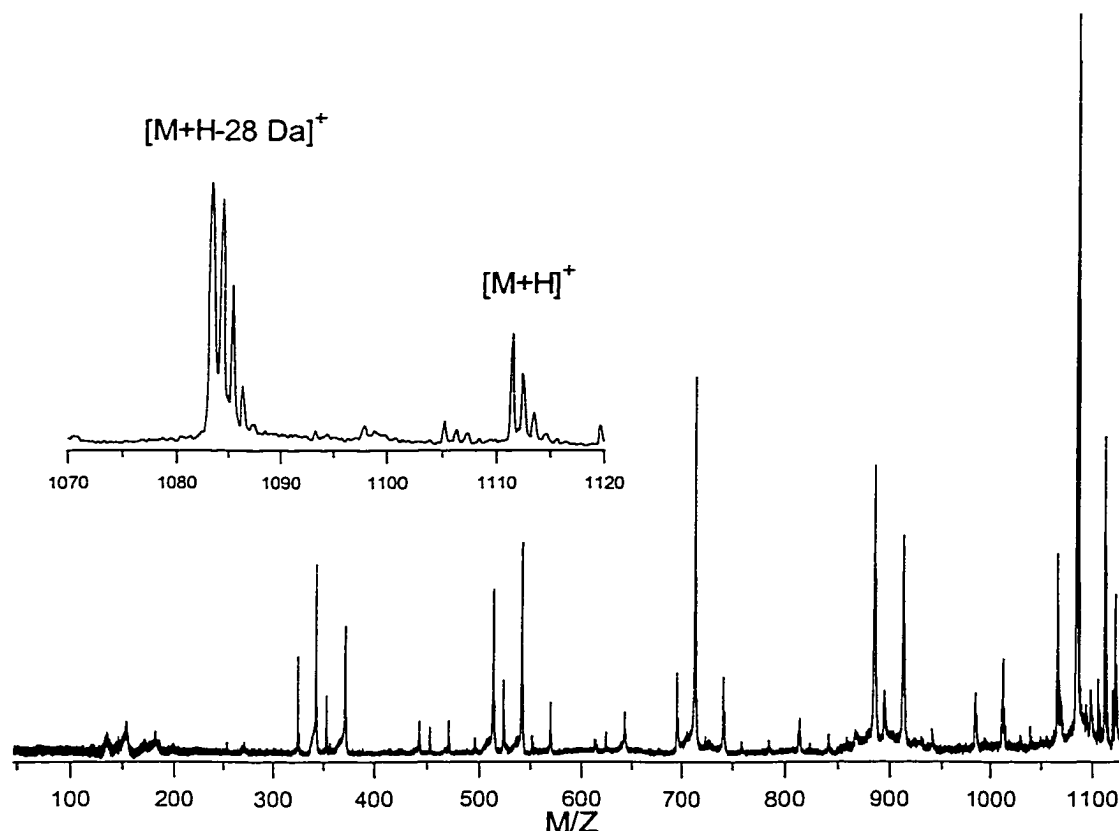
Figure 7.11 PSD-MALDI spectrum of a freshly prepared valinomycin sample obtained on a Voyager-DE Elite mass spectrometer (PE Biosystems, Framingham, MA, USA). The isolated m/z value was set at 1111.5 Da. The insert shows the expanded [M+H]$^+$ signal region.

7.4 Literature Cited

(1) Santoni,V.; Molloy, M.; Rabilloud, T. *Electrophoresis* **2000**, *21*, 1054-1070 and references therein.

132

(2)   (a) Tang, L.; Kebarle, P. *Anal. Chem.* **1991**, *63*, 2709-2715.   (b) Tang, L.; Kebarle, P. *Anal. Chem.* **1993**, *65*, 3654-3668.

(3)   Amado, F. M. L.; Domingues, P.; Santa-Marques, M. G.; Ferrer-Correia, A. J.; Tomer, K. B. *Rapid Commun. Mass Spectrom.* **1997**, *11*, 1347-1352 and references therein.

(4)   Kratzer, R.; Eckerskorn, C.; Karas, M.; Lottspeich, F. *Electrophoresis* **1998**, *19*, 1910-1919 and references therein.

(5)   Krause, E.; Wenschuh, H.; Jungblut, P. R. *Anal. Chem.* **1999**, *71*, 4160-4165.

(6)   Schaller, J.; Pellascio, B. C.; Schlunegger, U. P. *Rapid Commun. Mass Spectrom.* **1997**, *11*, 418-426.

(7)   Schindler, P. A.; Van Doresselaer, A.; Falick, A. M. *Anal. Biochem.* **1993**, *213*, 256-263.

(8)   Schey, K. L. *Protein and Peptide Analysis by Mass Spectrometry*; Methods in Molecular Biology 61; Humana Press: Totowa, NJ, 1996; pp 227-230.

(9)   Schaller, J. *Mass Spectrometry of Proteins and Peptides*; Methods in Molecular Biology 146; Humana Press: Totowa, NJ, 2000.

(10)   Schmidt, M.; Krause, E.; Beyermann, M.; Bienert, M. *Pept. Res.* **1995**, *8*, 238-242.

(11)   see for example Cadene, M.; Chait, B. T. *Anal. Chem.*, in press, or ABRF round table discussions at http://www.abrf.org/archives

(12)   Juhasz, P.; Costello, C. E. *J. Am. Soc. Mass Spectrom.* **1992**, *3*, 785-796.

(13)   Green-Church, K. B.; Limbach, P. A. *Anal. Chem.* **1998**, *70*, 5322-5325.

(14)   Breaux, G. A.; Green-Church, K. B.; France, A.; Limbach, P. A. *Anal. Chem.* **2000**, *72*, 1169-1174.

(15)   Francis, A. W. *Handbook for Components in Solvent Extraction*; Gordon and Breach: New York, 1972, references 1184,1203 and 1875.

(16)   Liu, H.; Dasgupta, P. K. *Anal. Chem.* **1996**, *68*, 1817-1821.

(17)   Liu, H.; Dasgupta, P. K. *Microchem. J.* **1997**, *57*, 127-136.

(18)   (a) Jeannot, M. A.; Cantwell, F. F. *Anal. Chem.* **1996**, *68*, 2236-2240.   (b) Jeannot, M. A.; Cantwell, F. F. *Anal. Chem.* **1997**, *69*, 235-239.   (c) Jeannot, M. A.; Cantwell, F. F. *Anal. Chem.* **1997**, *69*, 2935-2940.

(19)   Liu, W.; Lee, H. K. *Anal. Chem.* **2000**, *72*, 4462-4467.

(20)   Whittal, R. M.; Keller, B. O.; Li, L. *Anal. Chem.* **1998**, *70*, 5344-5347.

(21)   Dai, Y. Q.; Whittal, R. M.; Li, L. *Anal. Chem.* **1996**, *68*, 2494-2500.

(22)   Dai, Y.; Whittal, R. M.; Li, L. *Anal. Chem.* **1999**, *71*, 1087-1091.

(23)   Whittal, R. M.; Li, L. *Anal. Chem.* **1995**, *67*, 1950-1954.

(24)   Structures adopted from the Sigma 2000/2001 catalogue (Sigma-Aldrich, Oakville, Ontario, Canada) and their website: http://www.sigma-aldrich.com.

(25)   Kowall, M.; Vater, J.; Kluge, B.; Stein, T.; Franke, P.; Ziessow, D. *J. Colloid. Interface Sci.* **1998**, *204*, 1-8.

(26)   Leenders, F.; Stein, T. H.; Kablitz, B.; Franke, P.; Vater, J. *Rapid Commun. Mass Spectrom.* **1999**, *13*, 943-949.

(27)   Alberts, B.; Bray, D.; Lewis, J.; Raff, M.; Roberts, K.; Watson, J. D. *Molecular Biology of the Cell* 3rd ed., 1994, Garland Publishing: New York, p. 511.

(28)   Ridgway, N. D. *Biochim. Biophys. Acta* **2000**, *1484*, 129-141.

(29)   van Meer, G.; Holthuis, J. C. M. *Biochim. Biophys. Acta* **2000**, *1486*, 145-170.

(30)   Goswami, R.; Dawson, G. *J. Neurosci. Res.* **2000**, *60*, 141-149.

(31)   Karlsson, A. A.; Michelsen, P.; Odham, G. *J. Mass Spectrom.* **1998**, *33*, 1192-1198.

(32)   Hsu, F.-F.; Turk, J. *J. Am. Soc. Mass Spectrom.* **2000**, *11*, 437-449.

(33)   Merck Index, 11th Ed., 1989, Merck & Co: Rahway, NJ, USA.

134

(34)   Muddiman, D. C.; Gusev, A. I.; Stoppek-Langner, K.; Proctor, A.; Hercules, D. M.; Tata, P.; Venkataramanan, R.; Diven, W. *J. Mass Spectrom.* **1995**, *30*, 1469-1479.

(35)   Wu, J.; Chatman, K.; Harris, K.; Siuzdak, G. *Anal. Chem.* **1997**, *69*, 3767-3771.

(36)   Dancer, R. J.; Jones, A.; Fairlie, D. P. *Aust. J. Chem.* **1995**, *48*, 1835-1841.

(37)   Jander,   G.;   Blasius,   E.   *Lehrbuch   der   analytischen   und   präparativen anorganischen Chemie*, 12. Aufl., 1985, Stuttgart, Germany.

(38)   Lavanant, H.; Hoppilliard, Y. *J. Mass Spectrom.* **1997**, *32*, 1037-1049.

(39)   Wong, C. K. L.; Chan, T.-W. D. *Rapid Commun. Mass Spectrom.* **1997**, *11*, 513-519.

(40)   Zubay, G. *Biochemistry* 3rd ed., 1993, Wm. C. Brown Pub. 1993,

(41)   Ralph, S. F.; Iannitti, P.; Kanitz, R.; Sheil, M. M. *Eur. Mass Spectrom.* **1996**, *2*, 173-179.

(42)   Ralph, S. F.; Sheil, M. M.; Scrivener, E.; Derrick, P. J. *Eur. Mass Spectrom.* **1997**, *3*, 229-232.

(43)   Mathews, C.K.; van Holde, K. E. *Biochemistry* 1st ed., 1990, The Benjamin/Cummings Publ. Comp., Redwood City, California.

(44)   Rose, M. E.; Johnstone, R. A. W. *Mass Spectrometry for Chemists and Biochemists;* Cambridge Texts in Chemistry and Biochemistry; Cambridge University Press: Cambridge, UK, 1982; p 152.

135

Chapter 8

Conclusions and Future Work

This thesis focuses on two approaches to improve the sensitivity for protein and peptide characterization by MALDI TOF MS. The direct deposition of samples onto very thin matrix layers and the handling of nanoliter and subnanoliter sample amounts employing small-ID fused-silica capillaries achieve the goal mentioned above.

In Chapter 2 it is shown that by prudent sample/matrix preparations and spotting of subnanoliter sample volumes, zeptomole sensitivity for peptides can be achieved. This result was used to estimate the ionization efficiency for the basic peptide Substance P. In addition, Chapter 2 discusses the theoretical and practical limitations for further sensitivity improvement. It is apparent that for positive identification of peptides at such low levels the statistical isotopic distribution of an analyte becomes the limiting factor of the current technology to distinguish analyte signal from random background noise. Several hundreds of ions must reach the detector to create a reproducible signal with an acceptable isotopic distribution. New evolving technologies, which would allow the fragmentation and detection of a small number of ions might be a feasible way to lower the detection limits maybe even down to single molecules.

Chapter 3 is devoted to the identification of hemoglobin variants from single erythrocytes by peptide mass mapping. The major challenge to perform in-capillary chemistry in subnanoliter volumes is the mixing of sample and reagents on such a small scale. Evaporation of sample solvents in the capillary and reintroduction of reagents results in resolvation of the sample in the reagent's solvent. This methodology is a simple and effective solution to the mixing problem. Single erythrocytes from both a patient with sickle cell disease and a healthy individual were separately introduced into a capillary, enzymatically digested with trypsin, and the resulting digestion mixtures analysed by microspot MALDI TOF MS. Examination of the obtained peptide maps revealed the 1 amino acid difference in the primary sequence of normal hemoglobin compared to hemoglobin from blood with sickle cell disease.

136

Formation of matrix-clusters has been a well-known characteristic of several matrix substances, especially of 4-HCCA and DHB. Little attention has been paid to this phenomenon in the literature since matrix-clusters do not usually interfere with analyte signals when samples are clean and sufficiently concentrated. However in the analysis of very dilute and possibly salt-contaminated samples, matrix-cluster interferences can become so severe that distinction between analyte and matrix-cluster signals is impossible. As described in Chapter 4, matrix-cluster appearance follows specific formation schemes, i.e. they are aggregations of matrix molecules and predominantly sodium and potassium ions. Knowledge of the formation scheme and the characteristic assembly distribution allows for discerning real analyte signals from matrix-cluster peaks. The ability to distinguish matrix-cluster signals from analyte signals is particularly useful in microspot MALDI analysis since at the edges of the small sample spot analyte abundance decreases and thus matrix-cluster interference increases. Based on the described algorithms, an internet-based software was developed that allows the user to check if an observed signal matches with a theoretically possible matrix-cluster mass. However for correct interpretation the described characteristics of matrix-clusters and their assemblies must be considered carefully before a decision is made on whether or not a signal results from an analyte or from a matrix-cluster. Direct implementation of the algorithms and schemes into the mass spectrometer's software will lead to an effective tool for quality control of spectra acquisition, e.g. in high-throughput scenarios.

Mass spectrometric detection, characterization, and identification of as many bacterial proteins as possible, and subsequent establishment of a database are effective means to lay a foundation for a reliable tool of future bacteria investigations. One of the challenging tasks in this regard is the detection of low abundance proteins. In Chapter 5, HPLC-fractionation, nanoliter chemistry and subsequent microspot MALDI TOF MS are combined to enable low-abundance protein analysis from bacterial samples. The original method developed in Chapter 3 was expanded to include in-capillary concentration and cleanup methods. Sequential enzymatic and chemical in-capillary reactions for more complicated protein species were successfully performed and this allowed for unambiguous protein identification. Protein separation by capillary electrophoresis has recently evolved into a very powerful and sensitive technique. Based on the encouraging

137

results from the HPLC-fractionation combined with nanoliter chemistry and mass spectrometry it should be feasible to combine capillary electrophoresis with the nanoliter-chemistry technique. Such a combination could become an ultrasensitive technique since the sample loading requirements for capillary electrophoresis are considerably smaller than for HPLC.

An attractive feature of MALDI MS is its capability to analyze high molecular weight proteins yielding signals from species with relatively low charge states. The preferred matrix substance for large proteins is sinapinic acid since it yields mostly singly-charged analyte signals with high resolution. As discussed in Chapter 6 however, analysis of protein solutions with high salt content or concentrations below 10^{-6} M using sinapinic acid or other common matrix substances like HABA or DHB is generally very difficult or not possible. The direct deposition of dilute samples onto a double-layer of HCCA creates signals of protein species with higher charge states and lower resolution than from sinapinic acid. Nevertheless this is a small price to pay considering that highly salt-contaminated sample solutions with protein concentrations of 10^{-8} M are easily detectable. Combined with the nanoliter deposition technique, the 80 kDa protein lactoferrin could be detected with a total sample loading of 4 attomoles. High molecular weight proteins often consist of disulfide-linked subunits. An in-capillary reduction study consuming a total amount of 200 attomoles α_2-macroglobulin revealed part of its high-order structure. The formation of higher charged species with 4-HCCA was beneficial in this case. The described direct deposition technique has become a sensitive screening technique for high molecular weight proteins in highly contaminated solutions.

Detection of very hydrophobic analytes in the presence of more hydrophilic species by MALDI TOF MS is problematic due to suppression effects. This issue is addressed in Chapter 7. A newly developed solvent extraction technique employing a nanoliter droplet of organic phase within a few microliters of aqueous sample solution proved to be an effective and sensitive tool to circumvent suppression problems. The technique could be tuned so that both hydrophobic and hydrophilic analytes could be simultaneously analyzed. Probing valinomycin-alkali-metal complexes with this technique proved to produce more reliable results than regular MALDI preparations. This work can be extended to other ionophores and peptide-metal complexes. For

138

specific peptide-metal complexes it might be possible to use this technique for determining relative stability rates.

MALDI TOF MS has become an indispensable tool in the newly evolving field of proteome research. The combination of prudent sample/matrix preparations and nanoliter sample handling has made it one of the most sensitive mass spectrometric tools available for protein and peptide characterization. Further advancements in microfluidic technology might soon lead to automated systems which, combined with mass spectrometry, should play a major role in meeting future high-throughput requirements. Multidimensional microseparation techniques, e.g. combinations of different capillary electrophoresis systems might one day replace conventional gel electrophoresis technology and thus overcome current sensitivity limitations. Mass spectrometry will then certainly remain the detection method of choice.

139

Appendix A

Matrix-Cluster Identification Software

A Quickbasic program for identification of matrix-clusters was created utilizing the algorithms presented in Chapter 4.[1] This program allows the user to enter the mass of a questionable signal with a user-specified tolerance and the program searches for theoretically possible matrix-clusters in the entered mass range. Recently, Helmut Keller (Tengen-Watterdingen, Germany) transformed this program into JavaScript Code and included H_2O and CN loss options for 4-HCCA and included DHB as a matrix substance. This program is now accessible at http://www.chem.ualberta.ca/~liweb/MaClust.htm. A sample screen printout for a cluster at m/z 1060 is given below:

The following pages include the JavaScript Code and the original Quickbasic program.

JavaScript Code for the Matrix-Cluster Identification Software: (4-HCCA)

```
<!DOCTYPE HTML PUBLIC "-//IETF//DTD HTML 2.0//EN">
<HTML>
<HEAD>
<SCRIPT LANGUAGE="JAVASCRIPT">
function mass() {
      var h, j, f, d;
      h = document.form1.text1.value - 0;
      j = document.form1.text2.value - 0;
      f = document.form1.text3.value - 0;
      d = document.form1.text4.value - 0;
      if(h<0 || h>5 || j<0 || j>5 || f<0 || f>2500 || d<0 || d>500)
             alert('allowed values:\n\n for H2O losses:  0 - 5\n for CN losses:    0 - 5\n for mass:    max. 2500\n for tolerance:  0 - 500');
      else
             masse();
}
function masse() {
      var h, j, f,d, m, n, p, k, y, z, o, x, s, res, n1, p1, k1, x1, y1, z1, a, ma;
      ar = new Array();
      arr = new Array(3);
      h = document.form1.text1.value - 0;
      if(h<0 || h>5)
             alert("allowed value for H2O losses: 0 - 5");
      j = document.form1.text2.value - 0;
      f = document.form1.text3.value - 0;
      d = document.form1.text4.value - 0;
      o = 0;
      res = " ";
      m = 189.0426;
      ma = 189.17;
      for(n = 0 ; n < 11 ; n++){
      for(p = 0 ; p < (h+1) ; p++){
      for(k = 0 ; k < (j+1) ; k++){
      if ((n + p + k) < 1)
          continue;
      for(y = 0 ; y < 7 ; y++){
      for(z = 0 ; z < 7 ; z++){
      if ((y+z) > (n+p+k+1))
             x = 0;
       else {
             x = y + z - 1 + k;
             s = (n*m) + (p*(m-18.01057)) + (k*(m-26.0031)) - (x*1.0078) + (y*38.9637) + (z*22.9898);
             s = (Math.round(1000*s))/1000;
             a = (n*ma) + (p*(ma-18.02)) + (k*(ma-26.02)) - (x*1.0078) + (y*39.1) + (z*22.99);
             a = (Math.round(10*a))/10;
       }
       if( ((f-d)<s)  && ((f+d)>s) ){
             o = o + 1;
             n1 = n + "* M";
             if(n == 0)
                    n1 = " ";
             p1 = " + " + p + "* [M-H<sub>2</sub>O]";
             if(p == 0)
```

141

```javascript
                pl = " ";
        kl = " " + " + k + "* [M-CN]<sup>-</sup>";
        if(k == 0)
                kl = " ";
        xl = " -" + x + "* H";
        if(x == 0)
                xl = " ";
        if(x == (-1))
                xl = " " + " + (-x) + "* H";
        yl = " " + " + y + "* K";
        if(y == 0)
                yl = " ";
        zl = " " + " + z + "* Na";
        if(z == 0)
                zl = " ";
        arr[3] = "Mass Origin: " + nl + pl + kl + xl + yl + zl + "<br><br>";
        arr[1] = "Exact cluster mass (monoisotopic): " + s + " Da <br>";
        arr[2] = "Average mass: " + a + " Da <br>";
        ar[o] = arr[1] + arr[2] + arr[3];
        s = 0;
        a = 0;

                }
            }
          }
         }
        }
    }
    if (o < 1)
            res = "No Match Found";
    ar.sort();
    res = res + ar.join("");
    res = res + "<br> End of Search";
    args = "width=550,height=300,scrollbars";
    browser = window.open("","Result",args);
    browser.focus();
    browser.document.open("text/html","replace");
    browser.document.writeln("<HTML><HEAD><TITLE>Result</TITLE></HEAD>");
    browser.document.writeln("<BODY link=FFFFF vlink=FFFFF>");
    browser.document.writeln("<h3>Result:</h3><ul>");
    browser.document.writeln(res);
    browser.document.writeln("</ul></BODY></HTML>");
    browser.document.close();
    return false;
}
</SCRIPT>
</HEAD>
<body bgcolor="#FFFFFF">
<FORM name="form1">
<p><b>Singly Charged Matrix Cluster Peaks from 4-HCCA:</b></p>
<p>(Javascript must be enabled)</p>
 <table border="1" width="500" bordercolor="#FFFFFF" bordercolorlight="#FFFFFF" bordercolordark="#FFFFFF">
  <tr>
   <td width="370">
    <div align="right">How many H<sub>2</sub>O losses allowed?</div>
```

142

```html
      </td>
      <td width="120">
        <div align="center">
          <input type="text" size= "10" name="text1" value="0">
        </div>
      </td>
    </tr>
    <tr>
      <td width="380">
        <div align="right">How many CN losses allowed?</div>
      </td>
      <td width="120">
        <div align="center">
          <input type="text" size= "10" name="text2" value="0">
        </div>
      </td>
    </tr>
    <tr>
      <td width="380">
        <div align="right">Which mass did you observe (monoisotopic, in Da)?</div>
      </td>
      <td width="120">
        <div align="center">
          <input type="text" size= "10" name="text3">
        </div>
      </td>
    </tr>
    <tr>
      <td width="380">
        <div align="right">Which tolerance do you want to check (+/- in Da)?</div>
      </td>
      <td width="120">
        <div align="center"> ±
          <input type="text" size= "8" name="text4">
        </div>
      </td>
    </tr>
    <tr>
      <td width="380"> </td>
      <td width="120">
        <div align="center">
          <input type="button" size="10" value="calculate" onClick="mass()" name="button">
        </div>
      </td>
    </tr>
  </table>
</FORM>
<br>
<br>
<br>
<br>
<a href="d-vers03.htm">Go to 2,5-dihydroxybenzoic acid (2,5-DHB)
</BODY>
</HTML>
```

143

Original Quickbasic program:

```
2 CLS : REM Author: Bernd Oskar Keller, September 25, 1998
3 REM Modified: March 2, 1999
4 REM Modified: July 13, 1999
5 PRINT "Matrix Cluster Peaks from 4-HCCA ?"
6 PRINT
10 INPUT "Found Mass in Da = "; m
20 PRINT : INPUT "Max. Deviation in Da = "; d
30 FOR n = 1 TO 15
40 FOR x = -1 TO 13
50 FOR y = 0 TO 14
60 FOR z = 0 TO 14
65 IF z > n + 2 OR y > n + 2 OR x > n + 2 OR (y + z) > n + 2 THEN 100
70 s = n * 189.0424 - x * 1.0078 + y * 38.9637 + z * 22.9898
80 IF y + z <> x + 1 THEN 100
90 IF (m - d) < s AND (m + d) > s THEN 140
100 NEXT z
110 NEXT y
120 NEXT x
130 NEXT n
132 IF p = 0 THEN PRINT "No Match Found": GOTO 135
133 PRINT "No Further Match Found"
135 GOTO 160
140 PRINT "Mass Origin = "; n; "* M - "; x; "* H + "; y; "* K + "; z; "* Na"
145 PRINT "Exact M.W. (monoisotopic): "; s; "Da"
146 a = n * 189.17 - x * 1.0078 + y * 38.9637 + z * 22.9898
148 PRINT "Average M.W.: "; a; "Da"
150 p = p + 1: GOTO 100
160 PRINT : PRINT "End of Search": END
```

Reference:

(1)   Keller, B. O.; Li, L. *J. Am. Soc. Mass Spectrom.* **2000,** *11,* 88-93.